Preparation and evaluation of multiple-unit solid oral dosage forms containing chemical permeation enhancing agents

E Kleynhans

20682115

Dissertation submitted in fulfilment of the requirements for the degree *Magister Scientiae* in Pharmaceutics at the Potchefstroom Campus of the North-West University

Supervisor: Prof JH Hamman

Co-Supervisor: Dr JM Viljoen

November 2014

DECLARATION BY CANDIDATE

"I hereby declare that the dissertation submitted in partial fulfilment of the requirements for the degree Magister Scientiae in Pharmaceutics at the Potchefstroom Campus of the North-West University, is my own original work and has not previously been submitted to any other institution of higher education. I further declare that all sources cited or quoted are indicated and acknowledged by means of a comprehensive list of references"

E. KLEYNHANS

20682115

ACKNOWLEDGEMENTS

1 Corinthians 1; "[4]I thank my God always on your behalf, for the grace of God which is given you by Jesus Christ; [5] that in everything ye are enriched by him, in all utterance, and in all knowledge;"

I would like to express my gratitude and appreciation to several sources which contributed to the completion of this study and to those who also greatly impacted my life:

My supervisor Prof Sias Hamman - thank you for all your support. Thank you for an open door when there were days when all other doors in life were shut. You were not only an excellent supervisor and academic tutor, but also became my life coach and someone I am glad to call a friend. Thank you for challenging me and bringing out the best in me.

Dr Joe Viljoen – thank you for your guidance and care and always being there to support me emotionally through the studies.

Dr Crisna Gouws - thank you for your guidance and training in cell culture techniques, as well as the assistance with the growth and seeding out of caco-2 cells and with the TEER and transport studies.

Prof Jan Du Preez (Analytical Technology Laboratory) – thank you for the help during the validation of insulin. Thank you for the willingness to support and train me with HPLC analysis of my dissolution and transport samples.

Dr R. Lemmer – thank you for the assistance with the data analysis and statistics.

Dr. L.R. Tiedt, Head of Lab. for Electron Microscopy, Chemical Resource Beneficiation (CRB) – thank you for your assistance with the Electron Microscopy and providing me with extraordinary images of my formulations.

Organic Aloe (Pty) Ltd – thank you kindly for donating *Aloe ferox* for without this product my study would not have been possible.

National Research Foundation (NRF) of South Africa – the financial support towards conducting this research is acknowledged.

Lastly, I would like to thank my family and friends who loved and cared for me during the last two years. Tannie Anna, Oom Peter and Oom Colin, Dewald Louw, Liezel Minnaar, Ruan Joubert, Elizca Pretorius, Monique van Aarde, Heinrich Mattheus and my parents in heaven.

ARTICLE AND CONFERENCE PROCEEDINGS

Kleynhans, E., Hamman, J.H., Viljoen, J.M. & Tiedt, L. Multiple-unit solid oral dosage forms for effective peptide drug delivery. 17th World Congress of Basic and Clinical Pharmacology (WCP2014). Cape Town, South Africa. 2014. (Poster presentation: ANNEXURE A1)

Kleynhans, E., Hamman, J.H., Viljoen, J.M. Aloe gel materials as absorption enhancers in multiple-unit solid oral dosage forms for effective peptide drug delivery. 35th annual conference of the Academy of Pharmaceutical Sciences. Nelson Mandela Metropolitan University, Port-Elizabeth, South Africa. 2014. (Presentation: ANNEXURE A2)

Wallis, L., Kleynhans, E., Du Toit, T., Gouws, C., Steyn, D., Steenekamp, J. Viljoen, J. & Hamman, J. Novel non-invasive protein and peptide drug delivery approaches. *Protein and Peptide Letters*, 2014, Vol. 21, No. 11 (Article: ANNEXURE A3)

TABLE OF CONTENT

LIST OF ABBREVIATIONS

ACE-inhibitor	Angiotensin-converting-enzyme inhibitor
Ac-di-sol®	Croscarmellose sodium
A. ferox	*Aloe ferox*
A. marlothii	*Aloe marlothii*
ANOVA	One-way analysis of variance
A. vera	*Aloe vera*
CR	Controlled release
Caco-2	Caucasian colon adenocarcinoma
CAPIC	Cap-PEG-Insulin-Casein
CITES	Convention on the International Trade in Endangered Species of Wild Fauna and Flora
CYP3A4	Cytochrome P450, family 3, subfamily A, polypeptide 4 protein
CYP3A5	Cytochrome P450, family 3, subfamily A, polypeptide 5 protein
D_2O	Deuterium oxide
df	degrees of freedom
DoE	Design of experiments
DMEM	Dulbecco's Modified Eagle Medium
EDTA	Ethylene-diamine-tetra-acetic-acid
EGTA	Ethylene-glycol-tetra-acetic-acid
F	F ratio
FITC	Fluorescein isothiocyanate
HCl	Hydrochloric acid

HIM2	Hexyl-insulin monoconjugate-2
HEPES	*n*-(2-hydroxymethyl) piperazine-*N*-(2-ethanesulfonic acid)
HPLC	High performance liquid chromatography
KH_2PO_4	Potassium dihydrogen orthophosphate
KRB	Krebs-Ringer bicarbonate buffer
LOD	Limit of detection
LOQ	Limit of quantification
LLC-PK1	Lewis lung carcinoma-porcine kidney 1 cells
MCC	Microcrystalline cellulose or Avicel®
MSCK	Madin-Darby canine kidney
MS	Mean squares
NaOH	Sodium hydroxide
P_{app}	Apparent permeability coefficient
PBS	Phosphate buffer saline
PEG	Polyethylene glycol
PepT1	Peptide transporter 1
Pep T2	Peptide transporter 2
P-gp	P-glycoproteins
R^2	Correlation coefficient
RSD	Relative standard deviation
SA	Sustained action
SD	Standard deviation
SEM	Scanning electron microscope

SLN	Solid lipid nanoparticles
SS	Sum of squares
TPS	3-(Trimethylsilyl)-propionic acid-D4
TC-7	Caucasian colon adenocarcinoma cell subclone
TEER	Transepithelial electrical resistance
TMC	N-trimethyl chitosan chloride
ZO	Zonula occludens
ZOT	Zonula occludens toxins
2/4/A1 cells	Rat intestinal cells

LIST OF FIGURES

LIST OF TABLES

LIST OF EQUATIONS

CHAPTER 3: MATERIALS AND METHODS

ABSTRACT

The most popular and convenient route of drug administration remains the oral route, however, protein and peptide drugs such as insulin have poor membrane permeability and stability in the gastrointestinal tract. Absorption enhancers can be added to drug delivery systems to overcome the epithelial cell membrane permeability problem. Although previous studies have shown that aloe leaf materials improve the transport of drugs across intestinal epithelia, their performance in solid oral dosage forms has not yet been investigated.

Beads containing insulin and each of the selected absorption enhancers (i.e. *Aloe ferox, Aloe marlothii and Aloe vera* gel materials*)* were produced by extrusion-spheronisation, using a full factorial design to optimise the formulations based on transepithelial electrical resistance (TEER) reduction of Caco-2 cell monolayers as response. The optimum bead formulations were evaluated in terms of friability, mass variation, particle surface texture, shape, size and dissolution. The transport of insulin across excised pig intestinal tissue from the optimised bead formulations was determined over a 2 h period. The samples obtained from the transport studies were analysed for insulin content by means of high-performance liquid chromatography (HPLC).

The results showed that the TEER reduction, as an indication of tight junction modulation, obtained for the bead formulations containing aloe materials was concentration dependent. Furthermore, inclusion of croscarmellose sodium (Ac-di-sol®) as a disintegrant showed an enhanced TEER reduction effect in combination with the aloe gel materials. Dissolution profiles indicated that the beads containing aloe leaf materials in conjunction with insulin, released the insulin within an hour. In accordance with the TEER reduction results, the *A. marlothii* and *A. vera* materials containing beads showed similar increased insulin delivery across excised pig intestinal tissue, which was pronouncedly higher than that of the control group (insulin alone).

It can be concluded that beads containing aloe leaf materials have high potential as effective delivery systems for protein therapeutics such as insulin via the oral route of administration.

Keywords: Oral route, insulin, absorption enhancers*, Aloe ferox*, *Aloe marlothii*, *Aloe vera*, extrusion-spheronisation, transepithelial electrical resistance.

UITTREKSEL

Die mees populêre en gerieflikste roete van geneesmiddeltoediening bly steeds die orale roete, maar sommige proteïen en petiedgeneesmiddels soos insulien het ongewenste membraandeurlaatbaarheid en stabilitiet in die gastro-intestinale kanaal. Absorpsiebevorderaars kan by afleweringsisteme gevoeg word om die membraan-deurlaatbaarheidsprobleem aan te spreek. Alhoewel vorige studies getoon het dat aalwyn blaarmateriale die transport van geneesmiddels deur die dermepiteel bevorder, is hul werking in vaste orale doseervorm nog nie ondersoek nie.

Krale met insulien en geselekteerde absorpsiebevorderaars (d.i. *Aloe ferox, Aloe marlothii en Aloe vera* jel materiale) is vervaardig deur ekstrusie-sferonisasie en geoptimaliseer met behulp van 'n volle faktoriaalontwerp waartydens die transepiteel elektriese weerstand vermindering van Caco-2 selmonolaag gebruik was as respons. Die optimale formulerings is geëvalueer in terme van brosheid; massavariasie; deeltjie-oppervlak; tekstuur en vorm; grootte en dissolusie. Die transport van insulien oor varkderm weefsel vanaf die geoptimaliseerde kraalformulerings is bepaal oor 'n 2 uur tydperk. Die monsters verkry uit die transport studies is ontleed vir insulieninhoud deur middel van 'n hoë-druk vloeistof-kromatografiese analise.

Resultate het getoon dat die transepiteel elektriese weerstand vermindering as 'n aanduiding van hegte aansluiting modulering vir die kraalformulerings wat aalwyn jel materiale bevat, konsentrasie-afhanklik was. Verder het die insluiting van natriumkroskarmellose (Ac-di-sol®) as disintegrant, verbeterde transepiteel elektriese weerstand vermindering in kombinasie met die aalwyn jel materiale getoon. Dissolusie profiele toon dat die insulien binne die eerste uur vanuit die krale wat aalwyn jel materiale bevat, vrygestel word. In ooreenstemming met die transepiteel elektriese weerstand verminderingsresultate, het die krale wat *A. marlothii* en *A. vera* jel materiale bevat, soortgelyke insulien aflewering oor varkderm weefsel getoon wat aansienlik hoër as dié van die kontrole groep (insulien alleen) was.

Daar kan tot die gevolgtrekking gekom word dat krale wat aalwyn jel materiale bevat hoë potensiaal het om as orale afleweringsisteme vir terapeutiese proteïne, soos insulien, te dien.

Sleutelwoorde: Orale toedieningsroete, insulien, absorpsie bevorderaars, *Aloe ferox, Aloe marlothii, Aloe vera,* ekstrusie-sferonisasie, transepiteel elektriese weerstand.

CHAPTER 1: INTRODUCTION, AIM AND OBJECTIVES

1.1 Background and motivation

1.1.1 The oral route of drug administration

The oral route of administration is one of the most popular routes of drug administration, because it is simple, convenient and safe (York, 2007:7-8). This route of drug administration is known for high patient acceptability and compliance, having the benefit of providing a large surface area for systemic drug absorption. It also enables the use of immediate and sustained release dosage forms and avoids discomfort, pain and possible infections which occur by administration of parental dosage forms (Hamman, 2007:58).

The oral route of drug administration has some disadvantages such as a relative slow onset of action; certain drugs undergo enzymatic degradation and are instable in secretions of the gastrointestinal tract and potentially variable absorption (Rekha & Sharma, 2013:49).

Most therapeutic proteins and peptides are administered by means of the parenteral route of drug administration due to degradation in the gastrointestinal tract and poor membrane permeability. Parenteral delivery (e.g. injection) suffers from certain disadvantages such as discomfort, pain and risk of infections. This clearly indicates the need for sophisticated oral dosage forms which are capable of enhancing protein drug delivery from the gastrointestinal tract (Hamman, Enslin & Kotzé, 2005:166; Hamman & Steenekamp, 2012:220). Formulating a solid oral dosage form for protein and peptide drugs requires addressing several challenges such as manufacturing cost, poor bioavailability as well as overcoming physiological and biochemical barriers. Formulation strategies which can be used to address some of these challenges include the use of particulate carrier drug delivery systems, inclusion of enzyme inhibitors, developing bioadhesive systems, site-specific delivery and inclusion of absorption enhancers (Rekha & Sharma, 2013:53).

1.1.2 Absorption enhancing agents

Absorption enhancers are compounds used in pharmaceutical preparations to increase drug absorption across the intestinal epithelium, thereby improving bioavailability. These permeation enhancing compounds improve drug movement across the intestinal epithelium through different mechanisms of action. One type of chemical absorption enhancing agent acts by modulating tight junctions between adjacent epithelial cells and has shown promise for improving bioavailability due to enhanced paracellular movement of macromolecular drugs across the intestinal epithelium. It was shown that cationic polymers, such as

chitosan, are able to open the tight junctions in a reversible way (Crowley & Martini, 2004:537; Deli, 2009:892; Rosenthal *et al.*, 2012).

It was found that when *Aloe vera* gel and whole leaf extract are co-administered with certain vitamins to humans, the bioavailability of the vitamins are increased (Vinson, *et al.,* 2005:760). Solutions of aloe leaf materials also showed *in vitro* drug absorption enhancement properties with the potential to improve oral protein and peptide drug delivery (Chen *et al*., 2009:587; Lebitsa *et al*., 2012:297; Beneke *et al*., 2012:475). Furthermore, *A. vera* gel material indicated the potential to enhance delivery of drugs across the buccal mucosa (Ojewole *et al*., 2012:354) as well as the skin (Fox *et al*., 2014:96-106).

1.1.3 Solid oral dosage forms containing absorption enhancers

The formulation of aloe leaf gel and whole leaf materials in solid oral dosage forms as functional excipients intended for effective protein drug delivery via the gastrointestinal tract has not yet been investigated. Proof of concept is therefore needed to show that aloe leaf materials can be used as functional excipients in solid oral dosage forms for peptide drug delivery.

1.2 Problem statement

Protein and peptide drugs exhibit poor membrane permeability and stability after oral administration and currently are almost exclusively administered by injection. To overcome the poor intestinal epithelial permeability of peptide drugs, absorption enhancers can be added to the drug delivery system. Although drug absorption enhancing agents have been discovered, most are not efficient enough or exhibited cell damaging and toxic effects. Previous studies have shown that aloe leaf materials, applied in the form of aqueous solutions, improve the *in vitro* transport of drugs across intestinal epithelia through opening of tight junctions in a reversible manner without destroying the integrity of the epithelial layer (Chen *et al.,* 2009:587). Furthermore, *A. vera* leaf materials showed relatively low toxicity and cell damaging effects in different cell lines (Du Plessis & Hamman, 2014:169).

The research problem, which will be investigated in this study, is to determine if aloe leaf materials are effective as functional excipients in solid oral dosage forms to enhance protein drug transport across the intestinal epithelium. A multiple unit dosage form (beads filled into a hard gelatine capsule) was chosen due to its advantages over conventional single unit dosage forms, such as more uniform absorption with lower inter-subject variability and higher surface area of the dosage form in contact with the gastrointestinal mucosal surface for interaction by the chemical permeation enhancer.

1.3 Aims and objectives

1.3.1 General aim

The aim of this study is to investigate the *in vitro* drug permeation enhancing effect of *Aloe ferox*, *Aloe marlothii* and *Aloe vera* leaf gel materials as functional excipients, when formulated into spherical beads, across excised pig intestinal tissue.

1.3.2 Specific objectives

- To chemically fingerprint *A. ferox, A. marlothii* and *A. vera* gel materials by means of proton nuclear magnetic resonance (^{1}H-NMR) spectroscopy.
- To use a design of experiments (i.e. a 2^3 full factorial design with MODDE 9.0^{TM} software) to optimise bead formulations containing *A. ferox, A. marlothii* and *A. vera* gel materials produced by extrusion-spheronisation.
- To evaluate and characterise the bead formulations in terms of friability, mass variation, particle surface texture, shape, size, dissolution profiles and to determine their effects on the transepithelial electrical resistance (TEER) of Caco-2 cell monolayers as the "response" for the formulation optimisation, employing a design of experiments.
- To determine the effect of the optimised *A. ferox*, *A. marlothii* and *A. vera* gel containing beads on the transport of insulin by using the Sweetana-Grass Diffusion Chamber method with excised pig intestinal tissue.

1.4 Ethical aspects of research

The excised pig intestinal tissue was obtained from a local abattoir (Potchefstroom Abattoir, Potchefstroom, South Africa) immediately after the pigs was slaughtered and the tissue disposed of by the Vivarium at the North-West University, Potchefstroom. There was no ethical approval needed as the pigs were slaughtered for meat production and not research purposes.

CHAPTER 2: ORAL DELIVERY OF PROTEIN AND PEPTIDE DRUGS

2.1 Introduction

The oral route of drug administration remains the most popular route due to high patient compliance and acceptability, ease of use and convenience of administration (Hamman, 2007:58). The oral route of drug administration also provides a large surface area for systemic absorption and many drugs are well absorbed from the gastro-intestinal tract. This, however, does not apply to protein and peptide drugs due to several hurdles that prevent intact absorption of these macromolecular compounds. The effective delivery of proteins and peptides via the oral route still remains unfulfilled (Renukuntla *et al*., 2013:76).

Formation of protein and peptide molecules occurs through the polymerisation of amino acids when covalent bonds are formed between carboxyl and amino groups. A relatively short polymer chain of amino acids is known as a peptide and when the chain contains more than 20 amino acids, it is classified as a polypeptide. Linking two or more polypeptides result in the formation of a protein (Garret *et al*., 2002:87). Advantages of proteins and peptides over conventional small molecular drugs include high activity, high specificity, low toxicity and minimal non-specific and drug to drug interactions (Renukuntla *et al*., 2013:76).

The complex macromolecular structure of proteins and peptides cause certain challenges to formulate a solid oral dosage form for effective systemic delivery. It is important to understand and overcome these challenges without altering the biological activity of the protein and peptide drugs in order to optimise treatment.

2.2 Challenges to oral delivery of protein and peptide drugs

In order to effectively formulate a solid oral dosage form containing protein and peptide drugs for systemic delivery, several challenges need to be overcome. These include protection of the drug from biochemical degradation, facilitation of drug permeation through the gastro-intestinal tract epithelium and optimisation of the biological half-life while maintaining the pharmacological effect (Shargel *et al*., 2012:514-515).

Endogenous biochemical and physical constraints exist in the gastro-intestinal tract to provide physiological protection against harmful toxins, antigens and pathogens from entering the systemic circulation. However, they also prevent effective oral delivery of

protein and peptide drugs as they counteract absorption of these macromolecular compounds in the gastro-intestinal tract (Hamman *et al*., 2005:166).

2.2.1 Physical Barriers

Physical barriers of the gastro-intestinal tract against protein absorption include the unstirred water layer, efflux systems, the intestinal epithelial cell membranes and tight junctions (Hamman *et al*., 2005:167).

Before the physical barriers to gastro-intestinal absorption of protein and peptide drugs are described, a brief overview of the pathways of drug absorption from the gastrointestinal tract will be given. Figure 2.1 illustrates the potential pathways and mechanisms of drug transport across the gastro-intestinal epithelial cells into the surrounding blood vessels after oral administration.

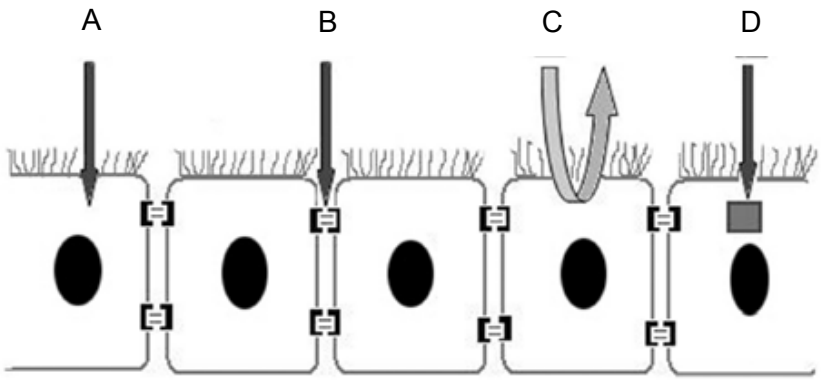

Figure 2.1: The potential pathways and mechanisms of drug transport across the gastro-intestinal epithelium: (a) transcellular pathway, (b) paracellular pathway,(c) carrier mediated efflux transport, (d) carrier mediated active transport (adapted from Beg *et al*., 2011:692)

Paracellular pathway

The paracellular pathway involves transport of molecules by means of passive diffusion through the aqueous pores between epithelial cells and is believed to be an important pathway of macromolecular absorption. The main barrier to this pathway is the presence of tight junctions, which act as a semi-permeable barrier controlling the paracellular passage of molecules (Pauletti *et al*., 1996:5; González-Mariscal *et al.,* 2005:56).

Transcellular pathway

The transcellular pathway includes transport of drug molecules across the apical cell membrane, through the cytosolic interior and across the basolateral membrane by means of simple passive diffusion, endocytosis, active transport or facilitated diffusion. Passage by simple passive diffusion of highly charged macromolecules, such as protein and peptide drugs, is prevented by the bilayer lipoprotein structure of the biological cell membrane (Hamman *et al*., 2005:167). M-cells in the Peyer's patches have the ability to transcytose large molecules in endosomes directly to the basolateral side of the cells and release the molecules into the extracellular space (Pauletti *et al*., 1996:6).

Carrier mediated efflux transport

Carrier mediated efflux transporters are energy dependent transporters using P-glycoproteins (P-gp) to transport drug molecules from within the epithelial cells to the apical side and therefore back into the lumen of the gastrointestinal tract (Beg *et al*., 2011:693).

Carrier mediated active transport

Carrier mediated transport or facilitated diffusion is an active process where a molecule is transported across the gastro-intestinal cell membrane via membrane proteins. Popular water soluble vitamins absorbed by means of carrier mediated transport include: folic acid, ascorbic acid and pyridoxine (Hamman, 2007:92).

2.2.1.1 Tight junctions

Tight junctions (Zonula occludens) are dynamic protein structures located above desmosomes (macula adherens) and gap junctions. They form a continuous network of interconnected parallel strands at the apical cell poles of adjacent gastro-intestinal epithelial cells (Rajasekaran *et al*., 2008:758). The core components of tight junctions are the scaffolding proteins which link the transmembrane and peripheral membrane proteins to the cytoskeleton, providing stability and serving as a matrix for signalling pathways (Van Itallie & Anderson, 2014:157). Freeze-fracture electron microscopic analysis of rat intestine epithelial cells was used to investigate the presence of integral membrane proteins which includes claudins, occludins, tricellulin and MarvelD2. Scaffolding proteins of the tight junctions were identified as Zonula Occludens (ZO-1, ZO-2, ZO-3) which functionally bind actin and actin-binding proteins to the cytosckelton (Lemmer & Hamman, 2013:104; Van Itallie & Anderson, 2014:157)

Tight junctions have gate and fence functions by controlling the passage of water, ions and molecules through the paracellular pathway (González-Mariscal *et al*., 2005:56). Endogenous and exogenous stimuli can reversibly or irreversibly open tight junctions and enhance the absorption of protein and peptide drugs (Lemmer & Hamman, 2013:103).

2.2.1.2 The unstirred water layer

The epithelial cells of the gastro-intestinal tract are covered by a stagnant aqueous layer consisting of water, mucus, electrolytes, glycoproteins and nucleic acids. Large molecules such as proteins and peptides may have restricted access to the epithelial membrane surface due to this stagnant aqueous layer. More specifically, high-molecular weight glycoproteins in this layer act as a barrier to drug absorption by facilitating the interaction between the diffusing molecules and components of the mucus layer or stabilising the unstirred water layer (Hamman *et al*., 2005:67; Hamman *et al*., 2011:73).

2.2.1.3 The intestinal epithelial cell membrane

The biological cell membrane is composed of a phospholipid bilayer. Molecules therefore need a certain degree of lipophilicity and must possess a molecular weight below a certain value to cross the phospholipid bilayer. The apical membrane of the epithelial cells acts as an absorption barrier to hydrophilic and high molecular weight molecules such as proteins and peptides. Conversely, the basolateral membrane differs in function, morphology and biochemical composition and might cause a less pronounced barrier function because of the higher fluidity in comparison to the apical membrane (Hamman *et al*., 2011:74).

2.2.1.4 Efflux systems

Some drugs are pumped by counter transport efflux proteins back into the lumen of the gastrointestinal tract after being taken up into the epithelial cells. One of the main active efflux transporter proteins is known as P-glycoprotein (P-gp). Energy is required for this active transport process and can occur against a concentration gradient. Efflux may cause a decrease in the bioavailability of drugs which are substrates for P-gp. Efflux can, however, competitively be inhibited by other substrates of P-gp (Ashford, 2007:283).

2.2.2 Biochemical barriers

For protein and peptide drugs to exert their pharmacological action it is imperative they are absorbed intact, without degradation, into the systemic circulation (Hamman *et al*., 2005:168). Proteins and peptides undergo degradation in the

gastrointestinal tract through various mechanisms, which include metabolism by digestive enzymes or microorganisms present in the lumen of the gastrointestinal tract as well as by chemical degradation reactions due to the acidic environment in the stomach (Pauletti *et al*., 1996:10).

The main proteolytic enzyme in the stomach is pepsin and lumenal degradation of orally administered proteins and peptides are initiated by trypsin, α-chymotrypsin, elastase and exopeptidases such as carboxypeptidase A and B, released by the pancreas into the intestine (Hamman *et al.,* 2005:168). This is followed by further degradation by enzymes such as aminopeptidase, di- and oligopeptidase and carboxypeptidase (Leuβen *et al*., 1996:117).

2.3 Approaches to overcome protein and peptide drug delivery challenges

There are various strategies to overcome bioavailability problems of protein and peptide drugs. In general, two categories of approaches can be distinguished, namely chemical modifications and formulation strategies. Chemical modifications can be made to protein therapeutics such as synthesising pro-drugs, preparation of peptidomimetics and structural modifications to target specific membrane transporters or receptors. Poor bioavailability can also be addressed by formulation of special dosage forms containing enzyme inhibitors and/or absorption enhancers.

2.3.1 Chemical modifications

2.3.1.1 Pro-drug approaches

A pro-drug is a pharmacologically inactive chemical derivative of a parent drug which requires biotransformation to become pharmacologically active (Pauletti *et al.*, 1996:10). The use of pro-drugs may be limited for proteins and peptides because of the structural complexity of these macromolecules therefore, most pro-drug strategies applied to these drugs usually focus on modifying a single functional group (Hamman *et al.*, 2005:169).

Pro-drugs targeted towards membrane transporters (Figure 2.2) are chemically modified to become substrates for membrane transporters and thereby can enhance the uptake of protein and peptide drugs. The pro-drug is transported across the intestinal epithelial membrane and may follow one of two pathways: it can reach the systemic circulation intact where it undergoes biotransformation and releases the free active drug, or the pro-drug may

undergo enzymatic hydrolysis whilst present in the intracellular environment and then be released as free active drug into the systemic circulation (Majumdar *et al.*, 2004:1438).

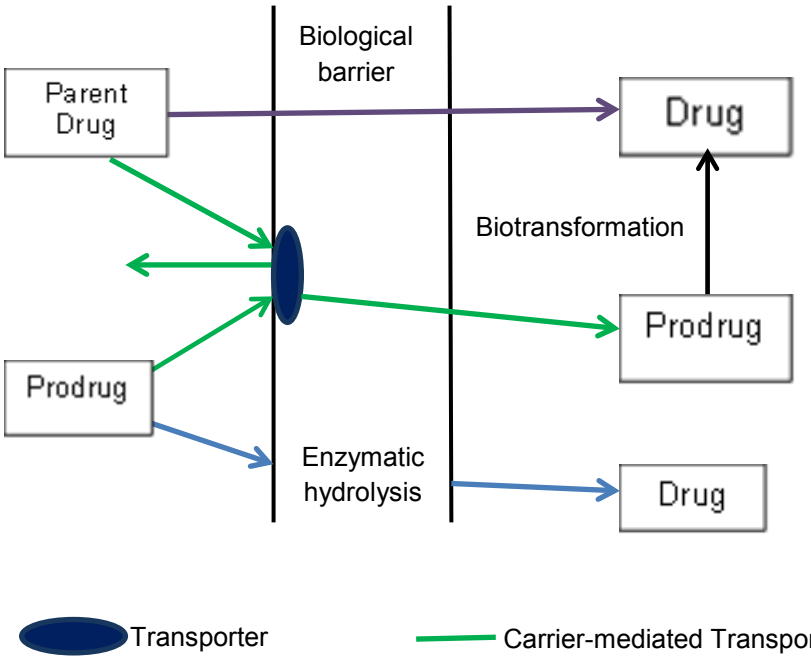

Figure 2.2: Schematic illustration of the pro-drug approach (adapted from Majumdar *et al*., 2004:1439)

2.3.1.2 Structural modification

Chemical modifications such as amino acid substitution, lipidisation and PEGylation have shown to be beneficial in terms of enzymatic stability as well as intestinal permeability for protein and peptide drugs (Pauletti *et al*., 1997:235-256; Renukuntla *et al*., 2013:75-93).

Amino acid substitution

Structural modification based on amino acid substitution, also known as analogue formation, can be achieved by the substitution of a specific amino acid with a different amino acid, or replacing an L-amino acid with a D-amino acid. The short half-life and enzymatic stability of the endogen hormone, somatostatin, was changed by replacing an L-amino acid with a D-amino acid and shortening the 14 to an 8 amino acid sequence (Werle *et al*., 2006:351).

Lipidisation

Lipidisation is known as the conjugation of a fatty acid to a protein or peptide molecule to improve the macromolecule's lipophilicity and thereby also its bioavailability

(Shen, 2003:607). These chemical modification techniques include non-reversible lipidisation, albumin binding as well as reversible lipidisation (Hackett *et al*., 2013:1335).

PEGylation

Polyethylene glycol (PEG) is known as a non-toxic and biocompatible polymer, which is soluble in organic and aqueous solvents. The pharmacokinetic properties of protein and peptide drugs can be improved by covalent linking of PEG to the macromolecule's structure and this process is known as PEGylation. PEGylation strategies include non-specific, site-specific, enzymatic and non-covalent PEGylation (Pfister & Morbidelli, 2014:135-142). PEGylation has been known for the advantages of increasing the *in vivo* circulating half-life of proteins and peptides, protecting them from *in vivo* degradation, decreasing their renal clearance and improving their physicochemical properties (Pfister & Morbidelli, 2014:135). PEGylation of α-interferon (PEG-INTRON®) is an example of a commercially available product on the market for the treatment of Hepatitis C (Hamman *et al.,* 2005:169). PEGylation has evolved into an advanced field with different complex strategies, as illustrated in Figure 2.3.

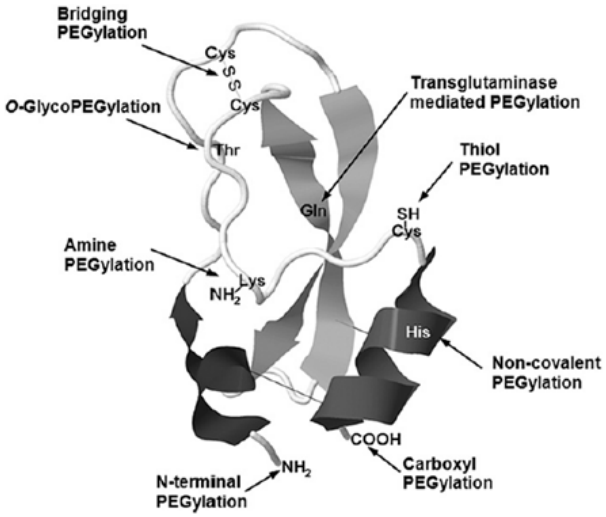

Figure 2.3: Illustration of different PEGylation strategies (Pfister & Morbidelli, 2014:137)

2.3.1.3 Peptidomimetics

Peptidomimetics are synthetic chemical entities that resemble the structure of certain peptides and mimic the biological activity of these peptides. Designing peptidomimetics can

be achieved by either replacing one atom to the design or secondary structural elements of peptides for more complex peptidomimetics (Hamman *et al*., 2005:170).

2.3.1.4 Targeting membrane transporters and receptors

Targeting membrane transporters

Due to a high concentration of peptide transporters in the small intestine, research has been focused on these transporters as potentially effective targets for protein and peptide drug delivery. These peptide transporters (i.e. PepT1 and PepT2) are proton-coupled and energy dependent, have extensive substrate specificities and are capable of transporting hydrophilic peptidomimetic drugs such as ACE-inhibitors, renin-inhibitors and β-lactam antibiotics (Hamman *et al*., 2005:170; Pauletti *et al*., 1997:247).

Intestinal protein and peptide absorption may be improved by conjugating these macromolecules to substrates of other carrier mediated transporters rather than peptide transporters. For example, targeting the bile acid transporter may improve drug delivery to the liver (Pauletti *et al*., 1997:248).

Receptor mediated endocytosis

Receptor mediated endocytosis has shown the ability to move macromolecules across the cell membranes. Combining these molecules, which are substrates for the receptors to protein or peptide drugs, may enhance their absorption after oral administration. Epidermal growth factor, immunogobulins, transferrin and cyanocobalamin are some of the molecules transported by means of receptor mediated endocytosis. Previous attempts were made to increase both the stability and the transport of molecules by coating drug-loaded nanoparticles with cyanocobalamin. During the *in vitro* studies the cyanocobalamin-coated nanoparticles showed a higher level of transport than the uncoated particles across the epithelial cell monolayers (Hamman *et al*., 2005:170; Chalasani *et al*., 2007:421).

2.3.2 Formulation technologies

2.3.2.1 Particulate systems

Multiple-unit dosage forms contain a number of subunits, each one containing a certain portion of the total drug dose. This type of dosage form is often compared to single unit dosage forms that contain only one dose of drug to be administered singularly (Gandi *et al*., 1999:160).

Multiple-unit dosage forms offer several advantages over single-unit drug delivery systems, which include a higher degree of homogenous dispersion in the gastrointestinal tract that causes optimised drug absorption. Furthermore, this dosage form is known to reduce peak plasma fluctuation, side effects and overall variation in transit times (Gandi *et al*., 1999:161; Ishida *et al*., 2008:46). Multiple-unit dosage forms also have technological advantages, which include better flow properties, low friability, narrow particle size distribution, ideal shape, higher suitability for film coating and ease of packaging (Vervaet *et al.,* 1995:131).

Beads are multiple-unit particulate drug delivery systems which can be manufactured by different methods, one of which is called extrusion spheronisation. This manufacturing technique has relatively short processing times with savings on production costs (Mallipeddi *et al*., 2010:53). It consists of a number of steps: firstly a homogenous powder mixture has to be obtained by mixing the dry ingredients; secondly wet massing takes place; then rod-shaped extrudates of uniform diameter are produced from the wetted powder mass by means of extrusion. Spheronisation is conducted to round off the rods into spherical particles/pellets or beads (Summers & Aulton, 2007:419).

Particulate carrier delivery systems have been developed to potentially enhance the oral delivery of protein and peptide drugs, using micro-emulsions, liposomes, nano- and microparticles. Solid lipid nanoparticles (SLN) were found to be a suitable particulate carrier system for the oral administration of insulin to diabetic rats. This carrier system improved blood glucose lowering effects significantly compared to an oral insulin solution and empty SLN for up to 24 h. The mechanism of improved glucose lowering effect was due to the solid matrix of the SLN protecting the insulin against chemical degradation and enhancing absorption (Sarmento *et al*., 2007:748).

Natural biopolymers have also been investigated for prospective particulate carrier delivery systems for insulin delivery, as they are biocompatible and non-toxic. Insulin was encapsulated into a hydrogel, which involved dispersion of a biopolymer solution (e.g. chitosan, gelatine or pectin) into liquid droplets and solidification of the droplets to form particles/beads ranging 40 nm to 1.8 mm. The aim of the study was to protect the insulin from chemical degradation. Furthermore, a hydrogel coated particle design containing alginate-coated zinc calcium phosphate nanoparticles showed sustained blood glucose reduction for 12 h during *in vivo* studies after oral administration of these particles to diabetic rats (Lim *et al*, 2014:16)

2.3.2.2 Enzyme inhibitors

Due to enzymatic breakdown of protein and peptides in the gastrointestinal tract, the inclusion of an enzyme inhibitor in the dosage form is an important formulation strategy to increase the bioavailability of protein and peptide drugs. Enzyme inhibitors have reversible or irreversible binding affinity to the target enzymes and the ability of decreasing the target enzyme's activity. A popular example of intestinal protease inhibitors which can be included into dosage forms includes aprotinin, an inhibitor of trypsin and chymotrypsin. By addition of a pH modifier to a dosage form, an indirect enzyme inhibition effect may be achieved due to the negative environmental influence for optimal enzyme activity (Choonara *et al*., 2014:1273).

2.3.2.3 Bioadhesive systems

Bioadhesive polymers have shown potential to improve bioavailability of protein and peptide drugs. This is achieved through the bioadhesive drug delivery system for which the gastrointestinal retention time is increased, leading to an increase in drug absorption. When these bioadhesive polymeric systems are orally administered and reach the mucosal layer, wetting and swelling of the polymer takes place and either van der Waal's forces interact between polymer chains and the mucin chains, or an ionic, covalent or hydrogen bond is formed (Rekha & Sharma, 2013:54).

The mucoadhesive and permeability enhancing effect of trimethyl chitosan-cysteine (TMC-Cys) nanoparticles was studied in Caco-2 cells and in rat follicular cells. The TMC-Cys/insulin nanoparticle showed increased mucoadhesion and permeation (Yin *et al*., 2009:5691).

2.3.2.4 Site specific delivery

Site specific delivery is a formulation strategy which targets specific regions in the gastrointestinal tract to reduce the enzymatic degradation of protein and peptide drugs. Enteric coating of encapsulated protein and peptide drugs in particles is a popular mechanism to delay drug release to the ileum and colon, where the pH is more suitable and proteolytic activity lower compared to that of the stomach and duodenum (Park *et al*., 2010:67).

Colon-specific delivery systems such as pressure-induced drug delivery, micro-activated systems, particulate drug delivery systems as well as pH and time dependent delivery systems are also considered to be attractive approaches for site specific delivery of proteins

and peptides (Wallis *et al*., 2014:1097). This delivery strategy has disadvantages for protein drugs with large therapeutic absorption windows because of the minimal water present in the colon as well as the fact that irregular drug release and absorption may occur (Park *et al*., 2010:67).

2.3.2.5 Absorption enhancers

Absorption enhancers allow drug transport into and across epithelial cells to enter the systemic circulation through numerous different mechanisms which may include decreasing mucus viscosity, changing membrane fluidity, disturbing cell membrane integrity and opening of tight junctions (Chin *et al.*, 2012:105). The main requirements for successful drug absorption enhancement include that the drug permeation be predictable, reproducible and reversible. The absorption enhancer should also increase the intestinal permeability without long term or toxic effects (Legen *et al*., 2005:184).

Types of absorption enhancers and their mechanisms of action

There are many types of drug absorption enhancers, which include salicylates, fatty acids, surfactants, chelating agents, toxins and venom extracts, as well as anionic and cationic polymers. These absorption enhancers are briefly described below with emphasis on aloe materials, which were investigated in this study.

Salicylates, such as sodium salicylate, act as absorption enhancers by increasing cell membrane fluidity, decreasing the concentration of non-protein thiols and preventing cell-association or protein aggregation. Medium chain glycerides or long chain fatty acids may act paracellular or transcellular by either dilating tight junctions, disrupting cell membranes or causing cell damage, while bile salts reduce mucus viscosity and disrupt membrane and tight junction integrity by cytotoxic effects as well as phospholipid solubilisation (Hamman, 2007:166).

Surfactants such as sodium dioctyl sulfosuccinate, sodium dodecyl sulfate and polyoxyethelene, cause epithelial membrane damage by removing membrane lipids and proteins, thereby enhancing drug absorption. Toxic and damaging effects are commonly experienced with this group of drug absorption enhancers (Hamman *et al*., 2005:172). The chelating agents, ethylene-diamine-tetra-acetic-acid (EDTA) and ethylene-glycol-tetra-acetic-acid (EGTA), have the ability to open tight junctions to allow for paracellular drug absorption. These chelating agents form complexes with calcium and magnesium and thereby cause Ca^{2+} depletion in cells which induce disruption of actin filaments and adherent junctions.

EDTA and EGTA also reduce cell adhesion and activate protein kinases (Raiman *et al*., 2003:130).

Zonula occludens toxins (ZOT) regulate tight junction opening in a reversible way by binding to zonulin receptors and thereby causing zonulin-mediated modulation of the paracellular transport pathway (Fasanoa *et al.,* 2004:803). The polypeptide component of *Apis mellifera* (European honey bee) venom extract, melittin, may enhance absorption of intestinal drugs by assuming an extended α-helical conformation in the cell membrane to form a voltage gated ion channel (Su *et al.,* 2001:64). Melittin is also known to induce bilayer micellisation and act as a membrane fusion peptide (Liu *et al.,* 1999:85). Anionic polymers, e.g. the polyacrylic acid derivative Carbopol ® 934P, affect epithelial tight junctions by depleting the extracellular calcium levels. Some of these polymers are also able to inhibit trypsin and carboxypeptidase A, both luminal enzymes. Opening of tight junctions can cause enhanced paracellular transport of peptide drugs (Borchard *et al*., 1996:132). Chitosan salts and N-trimethyl chitosan chloride (TMC) are polycationic polymers with mucoadhesive properties and the ability to regulate tight junction integrity through interaction with negatively charged sites on the cell membranes (Kotzé *et al.,* 1997:244).

2.3.2.6 Aloe plant derived materials as absorption enhancers

Botany and phytochemistry of the genus 'Aloe'

Aloe L. (Asphodelaceae) is a family of succulent plants consisting of nearly 420 species and 10 subdivided groups. Different parts of aloe plants are used for medicinal purposes in Africa, Western India and Arabia. One of the major threats to the aloe plant is unsustainable harvesting, therefore the trade in all species, except *Aloe vera,* is strictly regulated by the Convention on the International Trade in Endangered Species of Wild Fauna and Flora (CITES) (Grace *et al*., 2008:604).

Aloe plants are classified as xerophytes due to their capability of water storage in specialised leaves to adapt to dry environmental conditions. The plants range in physical size from a few centimetres to 2 to 3 m and their leaves are usually arranged in rosettes, with jagged edges (Rodriquez *et al*., 2010:306).

Differences in the composition of aloe materials arise due to various factors, i.e. environmental conditions such as differences in soil composition, climatic conditions, and exposure of the plant to light, the age of the plant and cultivating methods. It is also important to address the correct preservation after collection of plant parts due to aloe leaf gel material being unstable and hydrolysis of polysaccharides may occur

(Rodriquez *et al*., 2010:311). Depending on the medicinal use, different parts of the aloe leaf may be used, e.g. the exudate, gel or whole leaf (Chen *et al*., 2009:588).

Polysaccharides present in the gel of aloe leaves are thought to be one of the most important chemical components responsible for medicinal properties. Anthraqionones (e.g. aloin), vitamins (e.g. B1, B2, C, folic acid), enzymes (e.g. amylase, lipase) and low-molecular weight substances (e.g. salicylic acid, uric acid) are examples of other components present in different ratios in different aloe species (Choi *et al*., 2003:55).

Aloe ferox

Aloe ferox (Figure 2.4) is commercially known as "Cape Aloe" and the exudate from this aloe species is popularly used as a laxative (Van Wyk, 2008:343). The bitter exudate of *A. ferox* has been exported to Europe since 1761 (Van Wyk, 2008:347). *A. ferox* has been documented to treat conjunctivitis, ringworms, warts, herpes, shingles, eczema, dermatitis and acne. Accidental abortions have also occurred during high dosages of *A. ferox* exudate/laxative (Grace *et al*., 2008:604-612). In previous studies, *A. ferox* gel reduced blood glucose levels in normal mice and has been considered for anti-diabetic activity (Reynolds & Dweck, 1999:16).

Figure 2.4: Photograph of *Aloe ferox* plant (Kimpex Enterprises, 2014)

During previous ^{1}H-NMR spectroscopy, it was shown that *A. ferox* gel and whole leaf materials did not contain acemannan (aloverose) compared to *A. vera* gel (Beneke *et al*., 2012:477).

Aloe marlothii

Aloe marlothii (Figure 2.5) is a single stemmed aloe which can grow to a height of 6 m and is also known as Mountain Aloe. Tea made from chopped *A. marlothii* leaves has been reported to benefit stomach ailments (Grace *et al*., 2008:606). During an ethnobotanical survey of medicinal plants used by Bapedi traditional healers in the Limpopo Province of South Africa, it became evident that *A. marlothii* leaves and roots are used to treat Diabetes Mellitus by cooking these parts of the plant for 5 min before administration (Semenya *et al*., 2012:442). Other uses for *A. marlothii* include treatment of respiratory infections and round worm infestations (Amoo *et al.*, 2014:21).

Figure 2.5: Photograph of *Aloe marlothii* plant (Sias Hamman)

Aloe vera

Aloe vera (*Aloe Barbadensis Miller*) has yellow flowers and its leaves are arranged in a rosette configuration on a single stem (Figure 2.6). Anthraquinones are present in its exudate which is responsible for laxative properties (Vinson *et al*., 2003:761). Glycoproteins present in *A. vera* leaf gel are believed to assist in wound healing and to stimulate cell proliferation, whilst lectin-like substances promote growth of fibroblasts. A total of 70% of its glycoproteins consist of mannose (Choi *et al*., 2003:55-56). Acemannan (aloverose) is a characteristic polysaccharide found in *A. vera gel* with a distinct β-(1-4)-D-mannosyl backbone (Hamman, 2008:1603).

Figure 2.6: Photograph of *Aloe vera* plant (The Aloe Vera Site, 2014)

A. vera gel has been used for the treatment of Diabetes Mellitus in patients in India, Texas, Thailand and Arabia. Oral and topical administration of the aloe gel resulted in sustained lowering of blood glucose effects as well as promotion of diabetic wound healing (Reynolds & Dweck, 1999:16).

A. vera whole leaf and gel liquid preparations increased the bioavailability of both a water-soluble vitamin (i.e. vitamin C) and a fat-soluble vitamin (i.e. vitamin E) (Vinson *et al*., 2003:760). In previous *in vitro* studies, *A. vera* gel and whole leaf materials showed drug absorption enhancement properties, which was instigated by opening of tight junctions between epithelial cells, shown through experiments indicating a reduction in the TEER of excised rat intestinal tissue and cell culture monolayers. The presence of acemannan (aloverose) contributed to the enhanced transport of atenelol across excised intestinal tissue (Chen *et al.,* 2009:591; Beneke *et al*., 2012:481; Lebitsa *et al*., 2012:297).

2.4 *In vitro* techniques to investigate intestinal drug absorption

In vitro techniques have been developed to examine the delivery and absorption of drug molecules and to reduce the ethical aspects involved when using live animal models. These techniques showed to be cost effective and less invasive compared to *in vivo* pharmacokinetic studies within animal models. *In vitro* techniques have drawbacks, such as a lack of gastric emptying effects, gastrointestinal pH variations and gastrointestinal transit rate which cannot be incorporated into the data analysis (Westerhout *et al*., 2014:167).

2.4.1 Excised tissue techniques

Excised animal tissue techniques are useful to investigate the rate, extent and mechanism or pathway of drug absorption. Some animal tissues show physiological and anatomical similarities to that of humans. Popular excised tissue techniques are the everted sac technique and the Ussing type diffusion chamber technique (Le Ferrec *et al*., 2001:654).

Everted sac technique

This technique involves the everting of pieces of gastro-intestinal tissues, closing of the ends and exposure of these 'sacs' to drug solutions. Samples are withdrawn from within the sac at pre-determined intervals and analysed for drug content. The everted sac of pig or rat small intestine has been successfully used to study drug transport of macromolecules as well as the effect of absorption enhancers. Furthermore, the effects of active drug transporters (e.g. P–gp) on drug transport through the intestinal barrier can be studied using this technique. The transport of compounds, which have the affinity to bind to the muscularis mucosa and/or serosa, may be underestimated due to the fact that the serosa is not removed during tissue preparation for this technique (Le Ferrec *et al.,* 2001:6).

Ussing type diffusion chamber technique

The use of Ussing type diffusion chambers as an *in vitro* technique, were used to study drug transport across the intestinal epithelium requires delicate and precise tissue preparation. During this technique, animal intestinal tissue is isolated, the serosa and overlaying longitudinal and circular muscle layers are removed by blunt dissection. The tissue is then cut into smaller pieces and each piece is mounted between two half cells (Legen *et al*., 2005:185).

Advantages of this technique include the presence of an apical mucus layer and active transport proteins as well as metabolic enzymes. This technique allows measurement of drug absorption along different regions of the intestine using only small amounts of drug. Bi-directional transport studies can also be employed using this technique (Vervaet *et al*., 2010:290).

Disadvantages associated with this technique include the fact that the excised intestinal tissue is not supplied with blood and not connected to nerves and the excised tissue has limited viability after 120 min. Inter-laboratory variances are experienced due to the technique being dependent on experimental conditions (Vervaet *et al.,* 2010:291).

Grass and Sweetana (1988:372) developed and patented the Sweetana-Grass Diffusion Apparatus. This apparatus was derived from Ussing Chambers and is seen as an appropriate model to analyse drug transport across excised intestinal tissue. The Sweetana-Grass diffusion cell can be manufactured in different sizes to optimise the surface area to volume for different tissue and can also be used to evaluate enzymatic degradation, permeation enhancement and drug absorption in different tissue regions (Grass & Sweetana, 1988:372).

2.4.2 Cell culture techniques

There has been development of a wide variety of cell culture models that mimic the *in vivo* human intestinal epithelium. Examples of such cell lines include Caucasian colon adenocarcinoma (Caco-2) cell line, Madin-Darby canine kidney cells (MDCK), Lewis lung carcinoma-porcine kidney 1 cells (LLC-PK1), rat intestinal cells (2/4/A1) and Caco-2 cell subclone (TC-7), which are frequently used in drug permeation studies (Balimane & Chong, 2005:337).

Caco-2 cell line

The Caucasian colon adenocarcinoma (i.e. Caco-2) cell line remains the cell culture model of choice for high throughput prediction of human intestinal drug absorption (Westerhout *et al*., 2014:168). Caco-2 cells differentiate spontaneously into a monolayer of polarised epithelial cells and exhibit many functions of those resembling enterocytes in the human small intestine. Tight junctions are present between Caco-2 cells and they contain microvilli, enzymes and transporter proteins (Ashford, 2007:308).

Caco-2 cell monolayers can be used to determine drug transport via all the drug absorption pathways, e.g. passive transcellular, passive paracellular, carrier mediated transport and transcytocis. It was found that Caco-2 cells quantitatively under express active transporters and the tight junctions have a higher transepithelial electrical resistance (TEER) resembling the tight junctions present in the colon rather than that of the small intestine (Hamman, 2007:16).

This *in vitro* technique does have limitations, such as the absence of a mucus layer, a long differentiation period and low expression of transporters. It is a static model with inter- and intra-laboratory variability of permeation data (Deferme *et al*., 2008:188).

Studies have also shown that compounds with high permeability are well absorbed, whilst compounds with low permeability, especially those transported by carrier mediated

transporters, cannot be classified as poorly absorbed compounds in humans because of under expression of transporters in Caco-2 cells (Balimane *et al*., 2006:E7).

MDCK and LLC-PK1 cells

The Madin-Darby canine kidney (MDCK) and Lewis lung carcinoma-porcine kidney 1 cells (LLC-PK1) are both non-intestinal cell models used in drug permeation studies. MDCK differentiate into columnar epithelial cells with expression of tight junctions. A good correlation was reported for passive drug permeation in MDCK and Caco-2 cell lines, however, because of different origins of the cells, the expression levels of some transporters would be different (Balimane & Chong, 2005: 337; Hamman, 2007:21).

2/4/A1 cells

Rat intestinal cells (2/4/A1) mimic passive paracellular transport of the human small intestine due to the similar paracellular pore radius to the human small intestine, compared to the Caco-2 cell line pore size which is smaller. Previous studies indicated a three hundred-fold higher permeation of poorly permeable compounds in 2/4/A1 than Caco-2 cells, compared with human jejunum (Deferme *et al*., 2008:200).

TC-7 cells

The TC-7 cell line is a Caco-2 cell subclone with stronger metabolic capability because they express CYP3A4 and CYP3A5, whereas Caco-2 cells only express CYP3A5. This makes this cell model more suitable for transport combined with metabolic studies (Deferme *et al*., 2008:200).

2.5 Insulin delivery

2.5.1 Importance of oral delivery

Type 1 Diabetes Mellitus is a well-known chronic condition, where the pancreas produces too little or no insulin and Type 2 Diabetes Mellitus occurs when insulin cannot effectively be utilised by cells for the regulation of carbohydrate and fat metabolism (Rekha & Sharma, 2013:48). Physiologically, the human body is designed for the pancreas to release insulin into the hepatic portal vein when it detects an increase in blood glucose levels postprandial, where after it reaches its primary site of action, the liver and then the peripheral tissue. The goal of insulin therapy is to control the basal and postprandial glucose levels and to minimise the risk of hypoglycaemia. Insulin administered subcutaneously, pulmonary or by any other route of administration, excluding the oral route of administration,

has the disadvantage of excess insulin in the peripheral circulation. This may result in hypoglycaemia, immune response as well as insulin resistance in Type 2 diabetic patients. Oral delivery of insulin is of importance for different reasons, of which mimicking the natural physiological pathway of insulin is probably most important (Rekha & Sharma, 2013: 52).

2.5.2 Current studies based on oral delivery of insulin

2.5.2.1 Chemical modification

PEGylation

One of the first oral insulin products which achieved therapeutic levels after oral administration was the PEG-conjugated insulin, known as hexyl-insulin monoconjugate-2 (HIM2; NOBEX Corporation, North Carolina, USA). HIM2 was developed by linking a short chain of polyethylene glycol to an alkyl group in order to form an amphoteric oligomer. This oligomer then attached to lysine at position 29 in the β chain of recombinant human insulin. After oral administration of HIM2 to diabetic patients, in two consecutive dosages, it resulted in acceptable bioavailability and glucose-lowering effects (Hamman *et al*., 2005:169; Clement *et al.*; 2004:54).

2.5.2.2 Formulation strategies

Solid-oil-in-water micro-emulsions

Solid-oil-in-water micro-emulsions of insulin were formulated and administered to diabetic rats. This study showed increased hypoglycaemic activity in rats, as well as decreased enzymatic degradation of insulin and enhanced permeability. The oral administration of insulin in this dosage form however has disadvantages, such as reduced loading capacity and low physicochemical stability (Choonara *et al.,* 2014:1274).

Aracheosomes

A specialised lipid-based oral delivery system, called archeosomes composed of archaeobacterial membrane lipids containing diether and/or tetraether lipids, displayed increased stability against low pH, bile salts and pancreatic lipases and increased the hypoglycaemic effect in diabetic rats (Choonara *et al.,* 2014:1274).

Nanoparticle based systems

Nanoparticle based oral delivery systems of insulin have been utilised to increase the bioavailability of insulin because they can encapsulate the insulin and provide protection

against the biochemical barriers. An oral insulin formulation, Cap-PEG-Insulin-Casein (CAPIC), was developed by constructing caseins around a PEG-insulin formulation. Casein provided mucoadhesive properties as well as protection against the acidic environment. When a single dose of CAPIC was administered directly into the stomachs of fasted diabetic mice, the blood glucose levels were reduced by 80% within the first hour of treatment. CAPIC also improves the half-life of insulin leading to improved therapeutic activity (Chin *et al.,* 2012:109).

Enzyme inhibitors

Formulation of the enzyme inhibitors (i.e. chicken and duck ovomucoids) into drug delivery systems was previously attempted to increase the bioavailability of insulin by inhibition of trypsin and α-chemotrypsin. Chicken and duck ovomucoids inactivate the enzymes responsible for insulin degradation; therefore by co-administration of these ovomucoids with insulin the bioavailability may be increased. Concerns do arise in the daily usage of high concentrations of these enzyme inhibitors as they may lead to serious side effects including impaired dietary protein digestion, metabolic alterations and pancreatic hypertrophy (Rekha & Sharma, 2013:53).

Mucoadhesive systems

Enhanced insulin permeability and absorption was observed when Fluorescein isothiocyanate (FITC)-labelled insulin loaded anionic/hydrophobic modification of chitosan nanoparticles were given orally to diabetic rats. These nanoparticles showed mucoadhesive properties and increased the gastro-intestinal transit time, resulting in an extended period of insulin absorption (Rekha & Sharma, 2013:54).

Absorption enhancers

The transport of insulin was investigated across Caco-2 cell monolayers in the presence and absence of *A. vera* gel, as well as whole leaf extract solutions. The solutions showed a significant reduction in TEER compared to the control group with total recovery of cell monolayer integrity 120 min after the solutions were removed. The transport of insulin across the monolayers corresponded with the TEER results, with a higher enhanced transport at pH 5.8 compared to pH 7.4 (Chen *et al*., 2009:592).

2.6 Summary

The oral route of protein and peptide drug delivery would be more preferable than the parental route of drug administration, but overcoming poor bioavailability and pre-systemic degradation are important challenges which need to be addressed when formulating protein and peptides in oral dosage forms.

Protein and peptides encounter physical barriers after oral administration, including the unstirred water layer, intestinal epithelium itself, tight junctions, as well as efflux systems. The oral delivery of protein and peptide drugs are also pH dependant and susceptible to biochemical degradation due to enzymes and micro-organisms present in the gastro-intestinal tract.

Approaches that have been studied to overcome the above mentioned challenges include chemical modifications and formulation technologies. The use of absorption enhancers is an important formulation strategy to enhance protein and peptide absorption across the gastro-intestinal tract. The focus has been shifted to non-toxic absorption enhancers which do not influence the biological activity of the protein and peptide drugs. Natural compounds such as *A. ferox, A. marlothii* and *A. vera* leaf gel materials have proven to be excellent candidates to increase absorption enhancement.

Absorption enhancement properties and transport of insulin can be studied using different *in vitro* techniques, such as excised intestinal tissue techniques as well as *in vitro* cell models.

CHAPTER 3: MATERIALS AND METHODS

3.1 Introduction

To achieve the aim of this study, the selected aloe leaf gel materials were incorporated into spherical beads prepared by extrusion-spheronisation. A full factorial design of experiments was used to optimise the formulations based on their ability to reduce transepithelial electrical resistance (TEER) of Caco-2 cell monolayers. Thereafter, the optimised beads were evaluated for their ability to deliver insulin across excised pig intestinal tissue.

3.2 Materials

Aloe ferox leaves were sourced from Organic Aloe (Pty) Ltd in Albertinia, Eastern Cape Province, South Africa; *Aloe marlothii* leaves were collected in the Koster district in North-West Province, South Africa; *Aloe vera* gel powder was sourced from Warren Chem (Johannesburg, South Africa); Insulin was purchased from Sigma Aldrich (Johannesburg, South Africa); Avicel® (microcrystalline cellulose) was obtained from FMC (Philadelphia, USA); Ac-di-sol® (Crosscarmellose Sodium) was obtained from BASF (Midrand, South Africa); Sodium Lauryl Sulphate was obtained from Merck (Johannesburg, South Africa).

The culture medium consisted of Dulbecco's Modified Eagle Medium (DMEM), which contains 4.5 g/L D-glucose, sodium pyruvate and L-glutamine, which was further supplemented with 10% foetal bovine serum, 1% Penicillin/streptomycin, 1% amphotericin B and 1% L-glutamine (Separations, Johannesburg, South Africa). Corning Costar Transwell® 24-well plates used for TEER studies were purchased from Separations (Johannesburg, South Africa).

3.3 Design of experiments (DoE)

Computer software (i.e. MODDE 9.0™ by Umetrics from Sweden) was used in a 2^3 full factorial design of experiments to determine the composition of the initial bead formulations (i.e. the experimental runs) from which the optimum bead formulation was predicted (Table 3.1 to 3.3). Three centre points were added to measure experimental error and determine the reproducibility. The variables were entered in a new sheet in MODDE 9.0™ (i.e. aloe leaf material, Avicel® PH101 and Ac-di-sol® concentration) and the screening option was chosen in designing the experimental runs. The low and high levels for microcrystalline cellulose (Avicel® PH101) ranged from 87% to 100% (w/w), *Aloe ferox* gel, *Aloe marlothii* gel

as well as *Aloe vera* gel ranged from 0% to 10% (w/w), whereas the low and high levels of the disintegrant (Ac-di-sol®) ranged from 0% to 3% (w/w).

Table 3.1: Composition of bead formulations containing *Aloe ferox* gel as determined by the design of experiments (MODDE 9.0™)

Experimental run	*A. ferox* (% w/w)	Ac-di-sol® (% w/w)	Avicel® (% w/w)
1	10	0	90
2	10	3	87
3	5	0	95
4	10	1.5	88.5
5	10	1.5	88.5
6	5	1.5	93.5
7	5	1.5	93.5
8	5	1.5	93.5

Table 3.2: Composition of bead formulations containing *Aloe marlothii* gel as determined by the design of experiments (MODDE 9.0™)

Experimental run	*A. marlothii* (% w/w)	Ac-di-sol® (% w/w)	Avicel® (% w/w)
1	10	0	90
2	10	3	87
3	5	0	95
4	10	1.5	88.5
5	10	1.5	88.5
6	5	1.5	93.5
7	5	1.5	93.5
8	5	1.5	93.5

Table 3.3: Composition of bead formulations containing *Aloe vera* gel as determined by the design of experiments (MODDE 9.0™)

Experimental run	Aloe content (% w/w)	Ac-di-sol (% w/w)	Avicel® (% w/w)
1	10	0	90
2	10	3	87
3	5	0	95
4	10	1.5	88.5
5	10	1.5	88.5
6	5	1.5	93.5
7	5	1.5	93.5
8	5	1.5	93.5

Reduction in the TEER of Caco-2 cell monolayers, at 20 min after application of each bead formulation in suspension to the cell monolayers, was used as the response and these values were entered into the worksheets of the design of experiments (MODDE 9.0™ software). A contour plot was constructed for each aloe leaf material containing bead formulation to predict the optimum bead formulation for protein drug permeation enhancement.

3.4 Processing of *Aloe ferox* and *Aloe marlothii* leaves

The extreme ends of the *Aloe ferox* and *Aloe marlothii* leaves were cut off and the skin of the leaves was removed (Figure 3.1 A & B). The fillets were rinsed in cold water and cut into smaller cubes (Figure 3.1 C), which were liquidised in a food processor and frozen at -80ºC, where after it was lyophilised in a freeze drier (Virtis, Gardiner N.Y. USA) (Figure 3.1 D). The dried product was pressed through a 350 µm sieve to produce a fine powder which was used in the preparation of the beads (Figure 3.1 E& F).

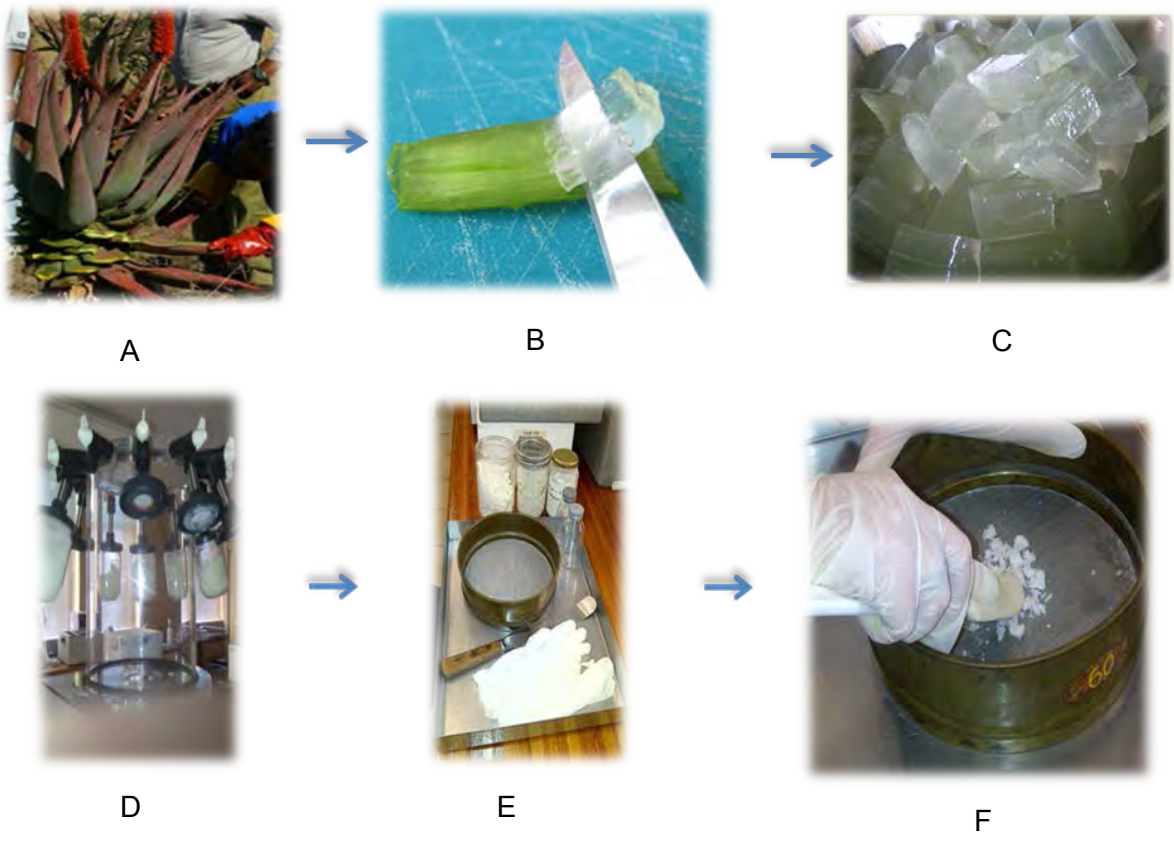

Figure 3.1: Photographic images (A-F) illustrating the processing of *A. ferox and A. marlothii* leaves into dried powder in chronological order

3.5 Fingerprinting of the aloe materials by proton nuclear magnetic resonance (^{1}H-NMR) spectrometry

Nuclear magnetic resonance (NMR) is a form of absorption spectrometry, which is based on the theory of the magnetic properties of certain atomic nuclei. The theory is based on principles that a sample can absorb electromagnetic radiation in the radio frequency region at frequencies governed by the characteristics of the sample under appropriate conditions in a magnetic field. An NMR spectrum represents a plot of the frequencies of the absorption peaks versus peak intensities (USP, 2014:381).

A quantity of 40 mg of each of the *A. ferox, A. marlothii* and *A. vera* gel materials, together with a very small amount of the reference compound, 3-(Trimethylsilyl)-propionic acid-D4 (TPS), were dissolved in 2 ml D_2O water and the ^{1}H-NMR spectra recorded with a 600 MHz spectrometer (Bruker, Germany).

3.6 Preparation of beads that contain selected aloe gel materials

3.6.1 Extrusion-spheronisation

Extrusion-spheronisation was used as the technique for the preparation of the beads with different compositions. Weighed amounts of all the ingredients, as determined by the full factorial design of experiments (refer to Tables 3.1-3.3 for formulation compositions) namely aloe materials (i.e. *A. ferox, A. marlothii and A. vera* gel), insulin (only included in the optimised bead formulations for transport studies), Ac-di-sol® and Avicel®, were mixed in a Turbula® mixer (Willy. A. Bachofen, Switzerland) for 5 min at 69 rpm for all bead formulations.

The total weight of each powder mixture for each formulation was 50 g in total. A mixture of de-ionised water and ethanol in a 80:20 ratio was slowly added (100 ml) with a burette to the powder mixture of each bead formulation while blending the powder mass in a Kenwood® planetary mixer for 2 min. The wetted powder mass of each bead formulation was passed through a 1 mm extrusion screen (Type 20 Caleva®, Caleva Process Solutions, England) at a speed of 25 rpm to form spaghetti-like extrudates. This was followed by spheronisation of the extrudate using a Caleva® spheroniser MBS (Caleva Process Solutions, England) at 1100 rpm for 5 min to form spherical beads. The beads were dried in a conventional oven for 72 h at 37°C.

The optimum formulations (as determined by the DoE and containing insulin) were freeze dried to overcome the degradation of the insulin. This was done by freezing the prepared

optimum bead formulations at -80ºC and then freeze drying them under vacuum (Virtis, Gardiner N.Y. USA) for up to 3 days.

3.6.2 Mass variation

Ten individual hard gelatine capsules (size 0) filled with beads were taken randomly from each bead formulation batch and the content of each capsule was individually weighed. The mass of the beads in each capsule was compared to that of the average mass. The mass variation of capsules containing granules (uncoated, single–dose) weighing more than 300 mg should not have a percentage deviation of more than ± 7.5% from the average (USP, 2014:492).

3.6.3 Friability

According to the British Pharmacopoeia (2013:XVII), friability is the reduction in mass of the beads when they are subjected to mechanical strains such as tumbling produced by a friabilator. Tumbling of the beads may cause abrasion, deformation or breakage and indicate their ability to withstand physical strain during packaging and handling.

A sample of beads from each formulation weighing 3 g was placed in a friability tester (NWU, Potchefstroom, South Africa) along with 25 glass beads (diameter of 5 mm). The friabilator was operated at 25 rpm for 4 min to apply 100 revolutions to each test sample. The content was emptied onto a Madison 425 µm sieve, the glass beads were removed and smaller powder particles were allowed to pass through the sieve prior to weighing the beads. Friability (F) was determined by calculating the percentage loss in mass according to the following equation:

$$F = \frac{W_1 - W_2}{W_1} \times 100 \quad \text{(Equation 3.1)}$$

Where W_1 is the initial mass of the beads and W_2 is the mass of the same beads after they were exposed to the friability test. The friability of each batch of beads was assessed in triplicate (BP, 2013:XVII).

3.6.4 Bead surface morphology by scanning electron microscopy (SEM)

Scanning electron microscopy (SEM) makes it possible to visualise the surface and internal morphology of solid dosage forms on microscopic level, which can be used to investigate the relationship between materials and dosage form structure and to relate drug release to physical characteristics such as the presence of pores (Cheng *et al*., 2014:348)

The beads' outer and cross-sectional surfaces were evaluated by scanning electron microscopy. Samples of beads were mounted on a metal disc with silicon adhesive. The beads were coated in an Eiko® ion coater (model IB-2, Eiko engineering, Japan) using a mixture of gold and palladium (66:34) under a vacuum of 1.5 torr. After coating, the beads were placed in a scanning electron microscope (SEM) (FEI quanta FEG 250) and micrographs were taken of the external surface and internal structure of the beads at different magnifications.

3.6.5 Particle size analysis

Laser light diffraction is used to determine the particle size distribution and is based on the principle that a representative sample is dispersed at an adequate concentration in a suitable liquid, which is passed through a beam of monochromatic light. A multi-element detector then measures the light scattering caused by the particles (e.g. beads) at various angles. Further analysis is done on the numerical values representing the scattering pattern through the use of mathematical algorithms and an appropriate optical model. These methods deliver the proportion of total volume to a number of size ranges, which forms a volumetric particle-size distribution (BP, 2014:Appendix XVII).

The size of the beads was determined by laser diffraction using a Malvern® Mastersizer 2000 (Malvern Instruments Ltd. Worcestershire, UK) fitted with a Hydro 2000MU sample dispersion unit and a 300 mm lens. A volume of 600 ml of 98% w/v ethanol was used to flush the system to align the lasers within the apparatus and as the liquid dispersant for the sample. The Mastersizer software was used to capture and process the data to obtain the mean particle size and particle size distribution.

3.6.6 Assay

The insulin content of 1 g of beads sample was determined from each formulation. The bead samples were each crushed using a pestle and mortar and transferred to a volumetric flask, which was made up to volume (100 cm^3) with distilled water. The insulin content in the solution was determined with high-performance liquid chromatography (HPLC). The insulin present in the solution was used to compare the experimental value to that of the theoretical value in order to express the insulin content as a percentage, calculated with the following equation:

$$\% \text{ Content} = \frac{(\text{experimental value of insulin content})}{(\text{theoretical value of insulin content})} \times 100 \quad \text{(Equation 3.2)}$$

3.6.7 Drug release

3.6.7.1 Preparation of potassium phosphate buffer (pH 6.8)

A potassium phosphate buffer with pH 6.8 was prepared according to the BP (2012:A332) formula. The buffer was prepared as follows: 250 ml of 0.2 M potassium dihydrogen orthophosphate (KH_2PO4) solution was added to 112 ml of 0.2 M sodium hydroxide (NaOH) solution. Distilled water was added to the mixture to make its volume up to 1000 ml.

The 0.2 M KH_2PO_4 solution was prepared by dissolving 27.22 g of KH_2PO_4 in distilled water and making its volume up to 1000 ml with distilled water. The 0.2 M NaOH solution was prepared by dissolving 8 g of NaOH and making its volume up to 1000 ml with distilled water.

The pH of the buffer solution was adjusted to 6.8 by adding sufficient volumes of 0.1 M hydrochloric acid (HCl) or 0.1 M NaOH. The 0.1 M HCl solution was prepared by measuring 8.35 ml of 37% HCl and making it up to 1000 ml with distilled water. The 0.1 M NaOH solution was prepared by dissolving 4 g of NaOH and making its volume up to 1000 ml with distilled water.

3.6.7.2 Dissolution test

Dissolution is a process where the drug particle is dissolved in a specific fluid. It is critical for a drug to be dissolved in the gastro-intestinal fluid for absorption to occur at the absorption site. Therefore, when a drug is administered orally in a solid oral dosage form, the drug molecule needs to be released from the dosage form into the surrounding fluid. Drug particles dissolve and form stagnant saturated solution layers around each particle. The dissolved drug molecules can then pass through the stagnant layers around each particle to make contact with the absorbing mucosa. Dissolution of a drug is simplified by the Noyes–Whitney equation:

$$\frac{dm}{dt} = kA\,(C_s - C) \quad \text{(Equation 3.3)}$$

$\frac{dm}{dt}$ is the dissolution rate, k is the dissolution rate constant, A is the surface area of the dissolving particle, C_s is the solubility of the drug and C is the concentration of the drug in the dissolution medium at time, t (Aulton, 2007:11).

Dissolution of insulin from the different optimised bead formulations was carried out in potassium phosphate buffer at pH 6.8 with the paddle method (USP II method) in a six

vessel dissolution apparatus (Distek 2500 dissolution apparatus as, North Brunswick, NJ, USA).

The stirring rate was set at 150 rpm in 900 ml dissolution medium and the temperature was maintained at 37 ± 0.5°C. Dissolution of insulin from the optimum bead formulations (as determined by the design of experiments, MODDE 9.0™), as well as the bead formulations used as control group in the transport study (i.e. insulin alone in Avicel® beads, was evaluated in triplicate by means of placing one capsule of each formulation in three individual dissolution vessels, respectively.

Samples (2 ml) were withdrawn from each dissolution vessel using an auto sampler (Distek evolution 4300 North Brunswick, NJ, USA), at time intervals of 15, 30, 60, 90, 120, 150 and 180 min, which were immediately replaced with 2 ml fresh dissolution medium. The stirring rate was then set at 250 rpm for a further 15 min, after which each dissolution flask was placed in an ultrasonic bath for 15 min (to allow complete release of insulin from the beads) and the last samples were taken.

The samples obtained from the dissolution study were analysed with an HPLC equipment to determine the amount of insulin released at each time point.

3.7 Growth and seeding out of Caco-2 cells

3.7.1. Culturing Caco-2 cell monolayers

Caucasian colon adenocarcinoma cells (Caco-2, ATCC catalog no. HTB-37) were grown from frozen stock and sub-cultured in 75 cm^2 cell growth flasks (Corning Costar Corporation, USA) to produce cells for seeding on culture treated polycarbonate filters. The culture medium consisted of Dulbecco's Modified Eagle Medium (DMEM), which contains 4.5 g/L D-glucose, sodium pyruvate and L-glutamine and further supplemented with 10% foetal bovine serum, 1% Penicillin/streptomycin, 1% amphotericin B and 1% L-glutamine (Separations, Johannesburg, South Africa). The cell cultures were kept in an incubator (Galaxy 170R, New Brunswick, New Jersey, USA) at 37°C in an atmosphere of 95% air and 5% CO_2. The cell culture medium was replaced with fresh medium every second day under aseptic conditions in a laminar air flow cabinet.

3.7.2 Trypsinisation of the cell cultures

The culture flasks were checked macroscopically and only flasks with cells that had reached 60 to 80% confluence were used for the trypsinisation procedure (within ± 7 days). Hank's

Balanced Salt Solution (HBSS), trypsin-versene solution (Separations Johannesburg, South Africa) and culture medium were warmed in a water bath at 37°C. These solutions and the flask with the cell culture were transferred to a laminar airflow cabinet. The cells in the flask were rinsed twice with the HBSS and 0.5 ml of trypsin-versene solution was poured onto the bottom surface of the culture flask in such a way that all the cells were covered.

The flask was then incubated for 10 min at a temperature of 37°C in an atmosphere of 95% air and 5% CO_2. After the flask was transferred to the laminar airflow cabinet and checked macroscopically if all the cells were detached, 2 ml of the warm medium (37°C) was added directly onto the bottom surface of the flask. This cell suspension was diluted by transferring it to warmed medium (37°C) in a 50 ml sterile tube and agitated with a Pasteur pipette. The flask was rinsed with 1 ml of warm medium (37°C) to ensure all the cells were removed from the flask. Three empty 75 cm^2 cell growth flasks (Corning Costar Corporation, USA) were transferred to the laminar airflow cabinet and were marked with the date and new passage number. A volume of 10 ml of the cell suspension was added to each of the three culture flasks which were then transferred to the incubator at a temperature of 37°C and an atmosphere of 95% air with 5% CO_2.

The trypsinisation procedure was repeated every week (7 days) until the cells were seeded out on Corning Costar Transwell® 24-well plates and Transwell 6-well plates for the TEER and transport studies, respectively.

3.7.3 Seeding of Caco-2 cells on Transwell® membranes

Caco-2 cells (passages 50, 53 and 54) were seeded out on tissue culture treated polycarbonate filters (area = 0.33 cm^2) in Costar Transwell® 24-well plates for TEER studies. A cell suspension was obtained in the same way as described in the trypsinisation process (paragraph 3.7.2).

The cells were counted on a haemocytometer and diluted until a concentration of 1.77 x 10^4 cells/ml was reached. The culture medium consisted of Dulbecco's Modified Eagle Medium (DMEM) and was added to both the apical (200 µl for 24-well plates) and basolateral (1 ml for 24-well plates) compartments and was changed every second day under aseptic conditions. The Transwell® plates with cell cultures were kept in an incubator at a temperature of 37°C in an atmosphere of 95% air and 5% CO_2. The Caco-2 cell monolayers were used for TEER measurements studies 21-23 days after seeding.

3.8 Transepithelial electrical resistance (TEER) studies

The TEER of Caco-2 cell monolayers was measured using a Millicell ERS meter (Millipore, USA) connected to chopstick electrodes. Prior to the TEER experiments, the medium in the basolateral chamber was replaced by DMEM buffered at pH 7.4 with 25 mM *n*-(2-hydroxymethyl) piperazine-*N*-(2-ethanesulfonic acid), (HEPES). The apical medium was replaced with 0.2 ml of each of the *A. ferox* gel, *A. marlothii* gel and *A. vera* gel solutions 0.6% w/v and 0.2 ml of each suspension of the optimised bead formulations (0.1 g/mL). The TEER was measured at 20 min time intervals, starting 20 min before application of the test solutions and bead suspensions and was continued for 120 min after application of the aloe gel solutions/bead suspensions. Control experiments were performed under the same conditions using Avicel® only beads (negative control) and beads containing Avicel® and sodium lauryl sulphate (SLS) 0.2% w/w (positive control). All the experiments were done in triplicate at 37ºC in an atmosphere of 95% air and 5% CO_2.

The percentage reduction in TEER (% of initial value) was calculated and these TEER values were plotted as a function of time to determine the effect of the test solutions and bead suspensions on the TEER of Caco-2 cell monolayers.

3.9 Insulin transport studies

3.9.1 Preparation of excised pig intestinal tissue

Directly after a pig was slaughtered at the local abattoir (Potchefstroom Abattoir, Potchefstroom, South Africa), a piece of approximately 30 cm of pig jejunum tissue was collected from the gastro-intestinal tract of each pig. The tissue was rinsed with ice cold Krebs-Ringer bicarbonate buffer (KRB) and placed in cold KRB buffer in a cooler box to adhere to the cold chain (pH 7.4).

In the laboratory, the jejunum was pulled onto a glass rod (Figure 3.2 A) where it was kept cold by applying KRB buffer on the intestinal tissue. The serosa was removed by blunt dissection (Figure 3.2 B). A piece of heavy duty filter paper was placed on the Perspex plate positioned on ice and the intestinal tissue was cut along the mesenteric border with a scalpel blade. The tissue was washed from the glass rod using cold KBR (Figure 3.2 C & D). This resulted in the apical side of the excised tissue piece to face upwards. The tissue and filter paper were cut into approximately 2 cm pieces (Figure 3.2 E), while keeping the tissue moist with KRB buffer throughout the procedure. These segments of tissue were mounted onto the half cells of the Sweetana-Grass Diffusion Chambers with the apical side facing

downwards, the filter paper (basolateral side) facing upwards and the filter paper was then removed (Figure 3.2 F). The two half cells were clamped together with metal rings (Figure 3.2 G) and these combined chambers were placed onto a heating block and filled with 7 ml heated (37°C) KRB buffer at a pH of 7.4. The half cells were connected to parallel gas flow (5% CO_2, 95%O_2) with a flow rate of 15-20 ml/min (Figure 3.2 H). The assembled cells were left for 20 min to reach an equilibrated state before transport studies commenced.

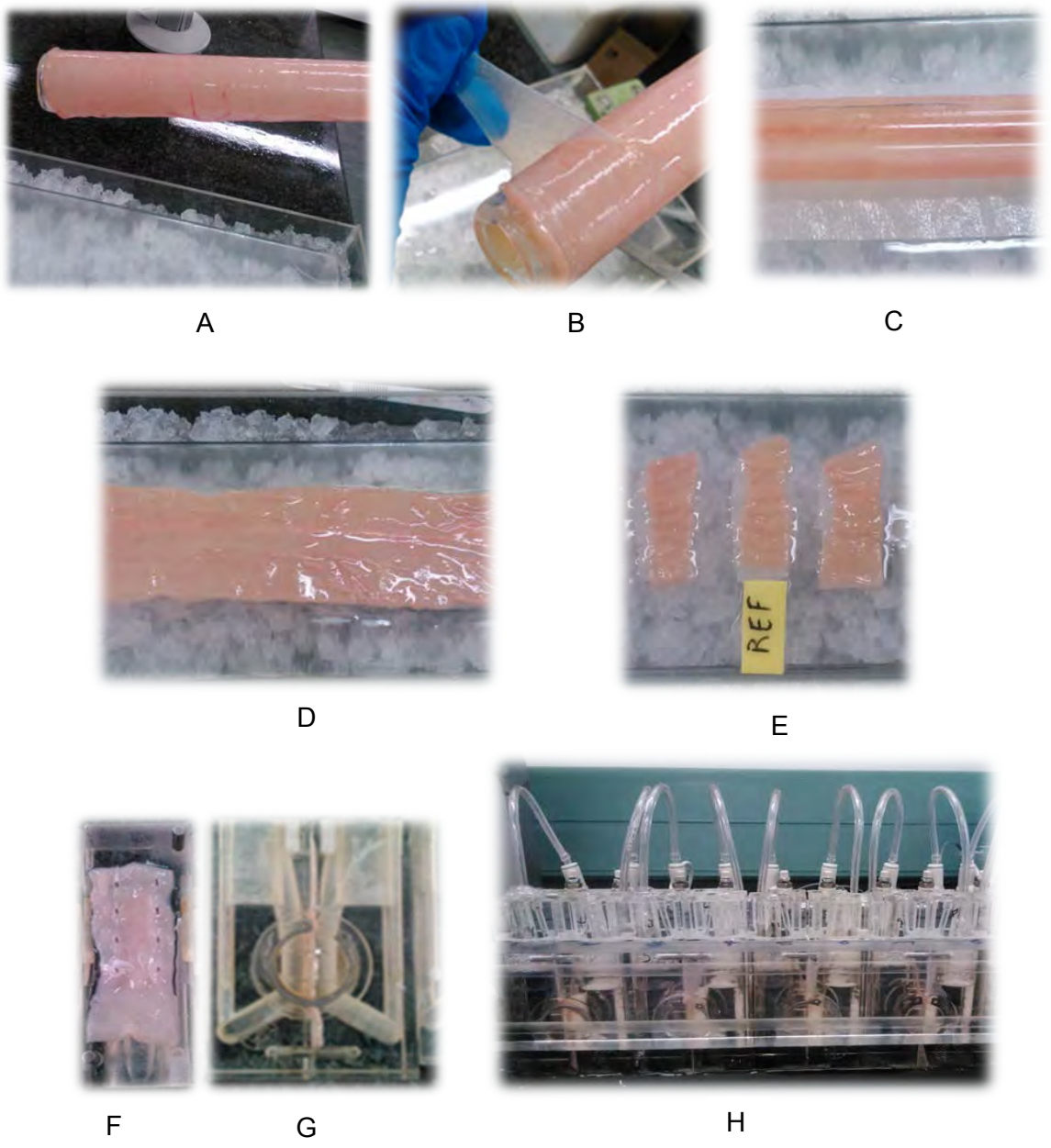

Figure 3.2: Photos (A-H) illustrating the preparation and mounting of the pig jejunum on the Sweetana-Grass Diffusion Chamber

3.9.2 Transport across excised pig intestinal tissue

The transport of insulin was determined across excised pig intestinal tissue after application of the optimum bead formulations suspended in KRB pH 7.4, as well as beads containing only insulin, (negative control group) with Avicel® using the Sweetana-Grass Diffusion Chamber apparatus. Prior to conducting each of the transport studies, the assay of each optimum bead formulation was used to determine the initial concentration of the model drug.

To study the apical to basolateral transport of the optimum bead formulations, the TEER was measured for each chamber to determine membrane viability. Thereafter a concentration of 0.1 mg/ml of each optimum bead formulation was added to the apical chamber and 200 µl samples were withdrawn from the basolateral chamber and replaced with 200 µl heated (37°C) KRB buffer every 20 min over a 2 h period in triplicate.

The percentage insulin transported was plotted as a function of time. Apparent permeability coefficient (P_{app}) values were calculated using the following equation (Hellum & Nilsen, 2008:468; Hansen & Nilsen, 2009:88):

$$P_{app} = \frac{dQ}{dt} \times \frac{1}{A.C_0.60} \quad \text{(Equation 3.4)}$$

Where P_{app} is the apparent permeability coefficient (cm/s), dQ/dt ($\mu g.s^{-1}$) represents the increase in the amount of drug in the receiver chamber within a given time period, which is equivalent to the slope of the plot of drug concentration transported versus time, A (cm^2) is the effective surface area of the excised pig intestinal cell layer between the apical and basolateral chambers and C_o is the initial insulin concentration in the apical chamber ($\mu g.cm^{-3}$).

3.10 High-performance liquid chromatography analysis of insulin

An insulin high-performance liquid chromatography analysis method which was previously developed in the Analytical Technology Laboratory of Pharmacen, North-West University, Potchefstroom, was validated before used to analyse the dissolution and transport samples for insulin concentration.

3.10.1 Chromatographic conditions

High-performance liquid chromatography is known as a multi-stage separation method where molecules in solution are distributed between a stationary and a mobile phase and insulin can be detected by a variety of techniques such as Ultra violet absorbance. The

stationary phase is packed in a column and the mobile phase is a liquid forced through the column under high pressure (USP, 2014:6378-6379). Table 3.4 summarises the chromatographic conditions used to analyse the insulin.

Table 3.4: Chromatographic conditions used to analyse the insulin in samples obtained from the dissolution and transport studies

Parameters	**Description**
Analytical Instrument	HP1100 series HPLC equipped with a pump, auto-sampler, UV detector and Chemstation Rev. A.10.01 data acquisition and analysis software.
Column	Vydac C18 Protein and peptide column, 218TP54, 300 Å, 250 x 4.6 mm (Grace Vydac, Hesperia, CA).
Mobile phase	Phase A: Degassed mixture of HPLC grade water and 0.1% orthophosphoric acid. Phase B: Acetonitrile
Flow rate	1.0 ml/min
Injection volume	50 µl
Detection	UV absorbance at 210 nm
Retention time	5.87 min
Stop time	12 min
Solvent	Phosphate buffer saline (PBS)

The mobile phase consisted of two components and was applied by means of a gradient, as shown in Table 3.5.

Table 3.5: Gradient conditions for the mobile phase used in the high performance liquid chromatography analysis method

Time (min)	Mobile Phase A	Mobile Phase B
0	80	20
6	40	60
8	40	60
8.2	80	20
12	80	20

3.10.2 Sample preparation from dissolution and transport studies

Samples (2 ml) from the dissolution test vessels were withdrawn with an auto sampler (Distek evolution 4300 North Brunswick, NJ, USA) and 200 µl from these samples were placed directly into flat bottom vial inserts with a pipette. The inserts were placed into 2 ml amber HPLC screw vials and analysed by means of HPLC.

During the transport studies, 200 µl samples were withdrawn from the basolateral chamber and placed directly into flat bottom vial inserts. The inserts were placed into 2 ml amber HPLC screw vials and analysed by means of HPLC.

3.10.3 Standard solution preparation

Approximately 15 mg of human recombinant insulin was accurately weighed and dissolved in 100 ml PBS. A volume of 5 ml of this solution was diluted to 50 ml with PBS. This standard insulin solution was transferred into an HPLC vial and volumes of 10, 20, 30, 40 and 50 µl were injected into the HPLC. This standard solution preparation was repeated to create a standard curve each time an HPLC analysis of dissolution and transport samples was conducted.

3.10.4 Calculation of insulin concentration in the samples

The peak areas on the chromatograms were plotted as a function of insulin concentration in the standard solutions and a linear regression of the curve was done by using Microsoft Excel® software.

The insulin concentration of each sample was calculated from the chromatogram peak areas using the data obtained from the regression curve by using the equation for a straight line as follows:

$$\text{Concentration in sample (µg/ml)} = \frac{\text{(peak area of sample – y-intercept)}}{\text{slope}} \quad \text{(Equation 3.5)}$$

3.10.5 Validation of the HPLC analytical method

The validation of an analytical method is the procedure to establish whether the performance characteristics of the analytical method meet the requirements for the intended analytical application (USP, 2014:1157).

3.10.5.1 Specificity

Specificity is the ability to analyse a substance in the presence of other components which may be expected to be present in the sample, e.g. impurities and degradation products (USP, 2014:1159).

Insulin was dissolved in PBS, as described in the method under standard solution preparation and samples from this solution were analysed with the HPLC in duplicate. The insulin solution was diluted 1:1 with water, 0.1 M hydrochloric acid, 0.1 M sodium hydroxide and 10% hydrogen peroxide to produce degradation products. Samples of insulin in the presence of *A. ferox*, *A. marlothii* and *A. vera* gel were furthermore analysed in duplicate with the HPLC. The chromatograms were inspected to ensure the insulin peak was completely separated from those of the other components for the analytical method to be acceptable.

3.10.5.2 Linearity

Linearity of an analytical method refers to the linear relationship between analyte concentration and analysis measurements such as peak area (USP, 2014:1160). A standard human recombinant insulin solution was prepared as described before (section 3.8.3). Concentration ranging from 0.1 µg/ml to 169 µg/ml of standard solution was injected

in duplicate into the chromatograph. The peak areas on the chromatograms were plotted as a function of insulin concentration and a linear regression of the curve was done by using Microsoft Excel® software from which the correlation coefficient (R^2) was obtained. An R^2 value of 0.99 or higher was required for the analytical method to be acceptable.

3.10.5.3 Limit of quantification and limit of detection

The limit of quantification (LOQ) is the lowest amount of an analyte in a sample that can be determined with acceptable precision and accuracy under standard experimental conditions. It is a characteristic of importance of quantitative assays for low levels of compounds in samples (USP, 2014:1160). The LOQ was determined by injecting six replicates of a low concentration standard solution (17 µg/ml). The LOQ was taken as the lowest concentration that can be determined with a relative standard deviation (RSD) of ≤ 15% for six replicates.

The limit of detection (LOD) is the lowest concentration peak which is discernible from baseline noise (USP, 2014:1160). The LOD was taken as a peak equal to three times the average baseline noise.

3.10.5.4 Accuracy

The USP (2014:1158) defines the accuracy of an analytical procedure as the closeness of the test results obtained by that procedure to the true value.

Approximately 15 mg human recombinant insulin was accurately weighed and dissolved in 100 ml DMEM. A volume of 6 ml of this solution was added to ten 20 ml volumetric flasks and filled to volume with DMEM. This was done to obtain spiked samples with known amounts of insulin at concentrations in the low, medium and high region of the standard solution range used to produce the standard curve. The samples were injected in duplicate into the chromatograph for analysis.

These samples were analysed and the amount of drug in each was determined with the aid of the standard or calibration curves by means of Equation 3.6:

$$y = mx + c \quad \text{(Equation 3.6)}$$

Where y represents the peak of the drug, m the slope, x the concentration of drug (mg/ml) and c is the y-intercept. Accuracy was given as the percentage extraction recovery for human recombinant insulin extracted from samples taken during the transport study with the equivalent drug concentrations prepared in DMEM. Recovery must be between 98 to 102%.

3.10.5.5 Precision

Precision of an analytical procedure is the degree of agreement between individual test results when the procedure is applied repeatedly to multiple samplings of the homogenous sample. The results are expressed as the standard deviation (SD), or relative standard deviation (RSD), of a series of measurements (USP, 2014:1159).

Intra-day precision (repeatability)

Repeatability refers to the use of the analytical procedure within a laboratory over a short period of time using the same analyst with the same equipment (USP, 2014:1159). The intra-day precision was determined by analysing the same standard human recombinant insulin solutions that were used during the accuracy experiment, with concentrations ranging from 46.38 to154.6 µg/ml. Repeatability must be better than 2%, (n = 9).

Inter-day precision

The same standard human recombinant insulin solutions were used as in the accuracy experiment, with concentrations ranging from 46.38 to 154.6 µg/ml on two different days in triplicate to determine the between-day variability of the analysis method. Stability was assured by keeping the samples at a stable temperature in the auto sampler. Inter-day precision must be better than 5% (n = 9).

3.10.5.6 Ruggedness

Stability of sample solutions

A standard solution was prepared and was injected into the chromatograph for analysis. The sample was left in the auto sampler tray and re-analysed at hourly intervals up to 24 h to determine the stability of the insulin. The pump was programmed to reduce the flow rate to 0.1 ml/min after elution of the peak and to reset the flow rate to 1 ml/min at 5 min before injecting the next sample.

System repeatability

An insulin standard solution was analysed six times consecutively in order to test the repeatability of the peak area and the retention time. The peak area and retention times should have an RSD of 2% or less.

3.10.5.7 Robustness

The following deliberate changes in the chromatographic operating parameters were made to determine the influence of these changes on the chromatographic results (Table 3.6):

Table 3.6: Changes in the chromatographic operating parameters, to determine the influence of these changes on the chromatographic result

Flow rate	0.9-1.1 ml/min
Injection volume	2.5, 5, 10, 20, 30, 40, and 50 µl
Wavelength	UV at 208- 212 nm
Mobile phase composition	A: A filtered and degassed mixture of HPLC grade water and 0.1% orthophosphoric acid was prepared. B: Acetonitrile The starting concentration could be 18 to 22% acetonitrile and the gradient end time could be 5.8 to 6.2 min without any ill effect. The retention time of the insulin peak will vary under different conditions, but this will not affect method performance.

3.11 Summary

The methods employed to complete the research project are described in this chapter. The selected aloe leaf gel materials were incorporated into spherical beads prepared by extrusion- spheronisation according to the 2^3 design of experiments and characterised in terms of mass variation, friability, particle size analysis, percentage content and dissolution. Optimised formulations were obtained based on their ability to reduce transepithelial electrical resistance (TEER) of Caco-2 cell monolayers. Validation of an HPLC analytical method was employed to determine the specificity, linearity, limit of quantification, limit of detection, accuracy, precision, ruggedness as well as robustness. Lastly, the optimised beads were evaluated for their ability to deliver insulin across excised pig intestinal tissue and analysed by means of HPLC.

CHAPTER 4: RESULTS AND DISCUSSION

4.1 Design of experiments

The eleven bead formulations, generated by MODDE 9.0™ design of experiments (DoE) software for each aloe gel material (Table 3.1 to 3.3), were prepared by means of extrusion-spheronisation. These beads were applied to Caco-2 cell monolayers to measure their effects on the transepithelial electrical resistance (TEER). All TEER values were entered into the software as the "response" that represented the performance of the beads. The DoE software was used to generate summary of fit plots, as well as contour plots, in order to predict the optimum formulation for each aloe material. Optimised bead formulations were subsequently tested by means of insulin transport studies across excised pig intestinal tissues.

In the summary of fit plot (Fig 4.1), which is given in the form of a histogram, the green bar (R^2) represented the model fit, the blue bar (Q^2) indicated how well future prediction would be, the yellow bar (Model validity) tested for the presence of outliers as well as incorrect model or transformational problems which might have occurred and the light blue bar (Reproducibility) was a numerical summary of variability's during replication. A good DoE model should comply with the following reference values for each parameter: the difference between R^2 and Q^2 must be ≤ 0.3, but both these values must be as close as possible to unite (i.e. 1); $Q^2 > 0.5$, model validity > 0.25 and reproducibility > 0.5 (Eriksson *et al*., 2008:78).

The contour plot is a useful tool to predict the exact amounts of ingredients to be used in the optimum bead formulations for drug absorption enhancement.

4.1.1 Beads containing *Aloe ferox* gel

The summary of fit plot (Figure 4.1), generated by MODDE 9.0™ DoE software based on TEER reduction by different formulations of *A. ferox* containing beads, shows it complied with most of the reference values for a good prediction model. The difference between R^2 and $Q^2 = 0.25$ (i.e. ≤ 0.3) and model validity = 0.72 (i.e. > 0.25, indicating a correct model with the absence of outliers and transformation problems). Although the reproducibility depicted a value of 0.75 (i.e. > 0.5), the Q^2 value was 0.33 which was lower than 0.5, indicating the model may suffer from reduced future prediction ability.

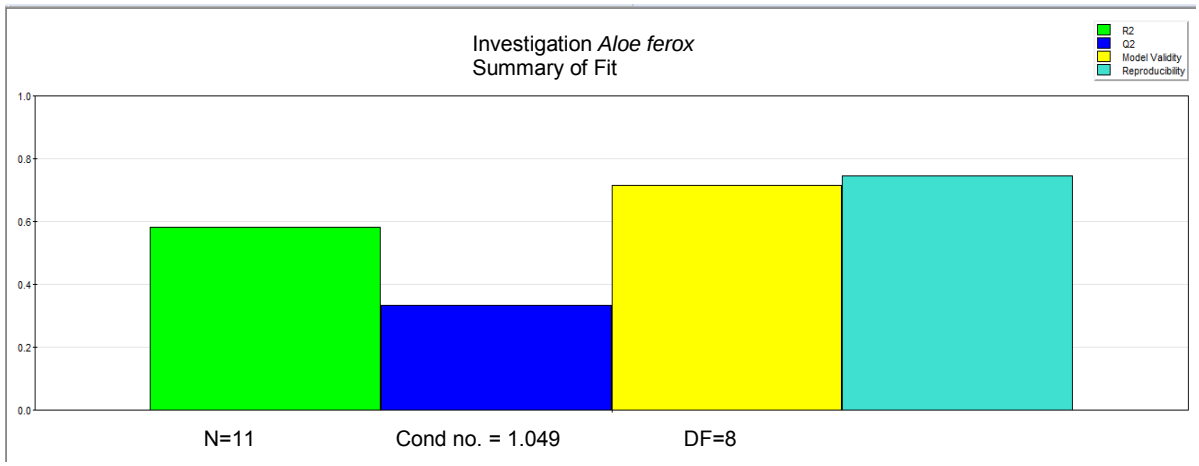

Figure 4.1: The summary of fit plot generated by the design of experiments software (MODDE 9.0™) for *A. ferox* containing beads based on TEER reduction results

The contour plot (Figure 4.2) for *A. ferox* containing beads shows the optimum bead formulation, based on the TEER reduction results (i.e. the ability to open tight junctions and thereby allow for paracellular drug transport), should consist of 9.79% w/w *A. ferox* gel, 2.89% w/w Ac-di-sol®, and 87.31% w/w MCC.

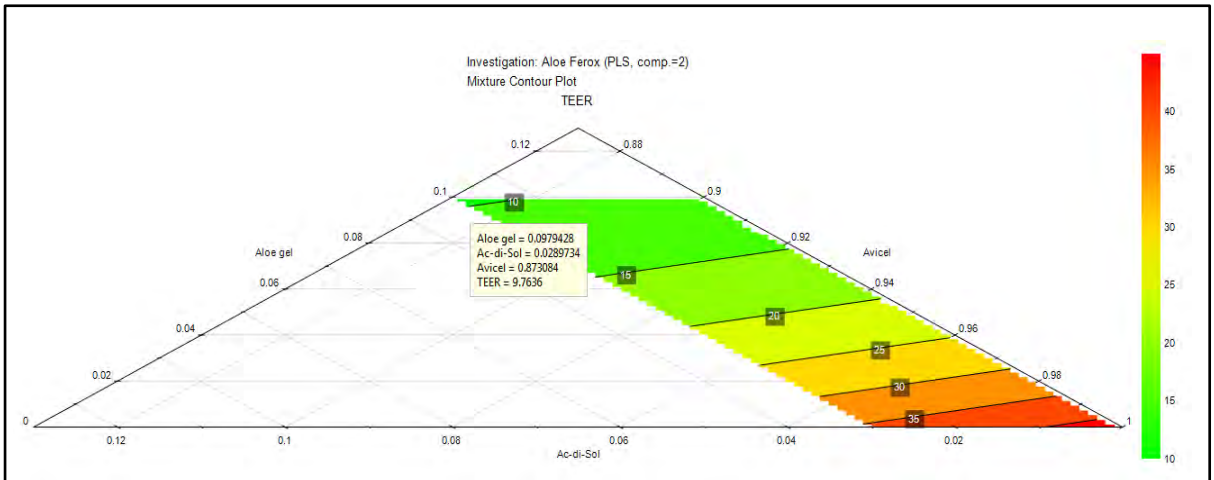

Figure 4.2: Contour plot generated by the design of experiments software (MODDE 9.0™) to determine the optimum bead formulation containing *A. ferox* as drug absorption enhancer

4.1.2 Beads containing *Aloe marlothii* gel

The summary of fit plot (Figure 4.3), generated by MODDE 9.0™ DoE software based on TEER reduction by different formulations of *A. marlothii* containing beads, shows it complied with the reference values for a good prediction model. The difference between R^2 and Q^2 = 0.11 (i.e. < 0.3), R^2 portrayed a value of 0.75 and Q^2 = 0.66 (i.e. > 0.5, indicating good future prediction). Model validity was 0.96 (i.e. > 0.25) indicating a correct model with the absence of outliers and transformation problems. The reproducibility value was 0.42 (i.e. < 0.5), which indicated potential problems with the number of variables during replication.

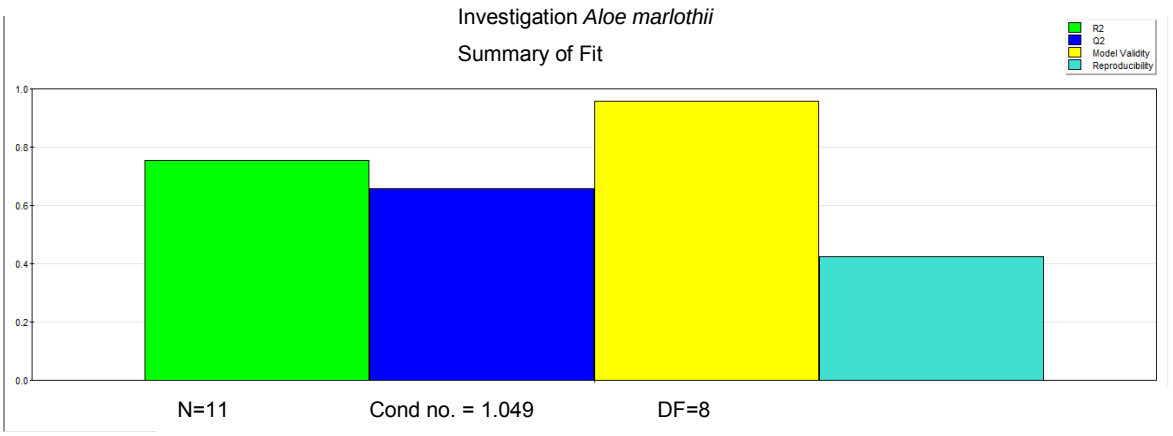

Figure 4.3: The summary of fit plot generated by the design of experiments software (MODDE 9.0™) for *A. marlothii* containing beads based on TEER reduction results

The contour plot (Figure 4.4) for *A. marlothii* containing beads shows the optimum bead formulation based on the TEER reduction results (i.e. the ability to open tight junctions and thereby allow for paracellular drug transport) should consist of 9.07% w/w *A. marlothii* gel, 1.98% w/w Ac-di-sol®, and 88.95% w/w MCC.

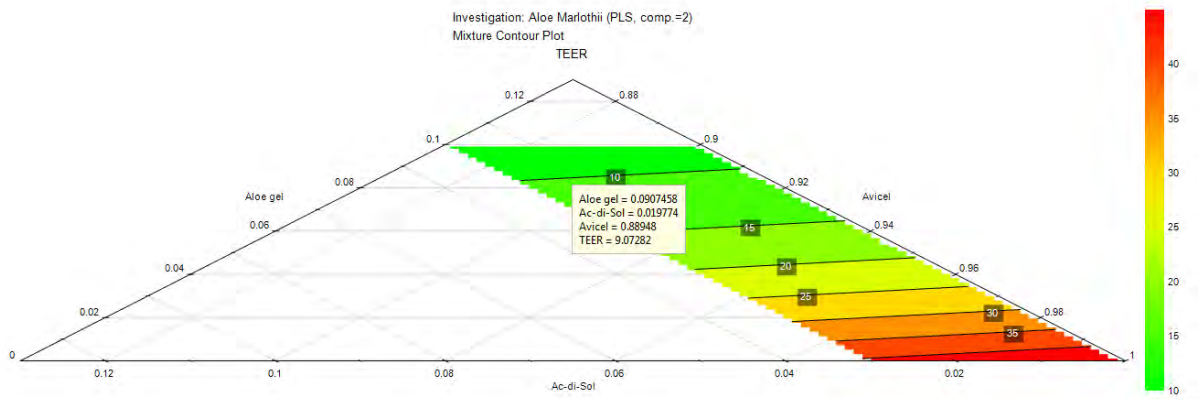

Figure 4.4: Contour plot generated by the design of experiment software (MODDE 9.0™) to determine the optimum bead formulation containing *A. marlothii* as absorption enhancer

4.1.3 Beads containing *Aloe vera* gel

The summary of fit plot (Figure 4.5) generated by MODDE 9.0™ DoE software, based on TEER reduction by different formulations of *A. vera* containing beads, shows it did not comply with most of the reference values for a good model. The difference between R^2 and Q^2 = 0.25 (i.e. < 0.3), but the R^2 value was 0.41 showing a lack of model fit. Q^2 = 0.16 (i.e. < 0.5), which indicated potential problems with future prediction. Model validity was 0.19 (i.e. < 0.25), indicating the model might be incorrect and may have outliers and transformation problems. The reproducibility = 0.96 (i.e. > 0.5) which indicated an acceptable number of variables during replication.

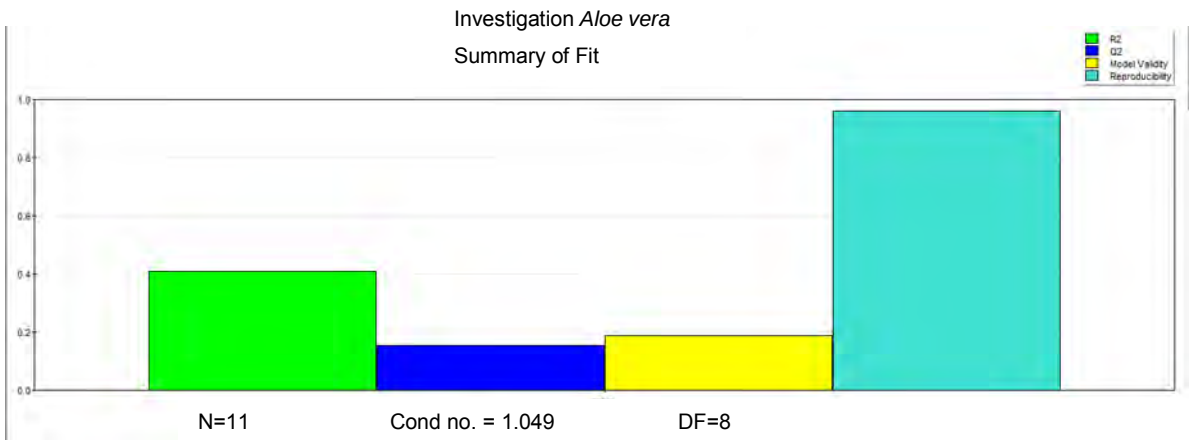

Figure 4.5: The summary of fit plot generated by the design of experiments software (MODDE 9.0™) for *A. vera* containing beads based on TEER reduction results

The contour plot (Figure 4.6) for *A. vera* containing beads shows the optimum bead formulation, based on the TEER reduction results (i.e. the ability to open tight junctions and thereby allow for paracellular drug transport), should consist of 9.50% w/w *A. vera* gel, 2.73% w/w Ac-di-sol® and 87.77% w/w MCC.

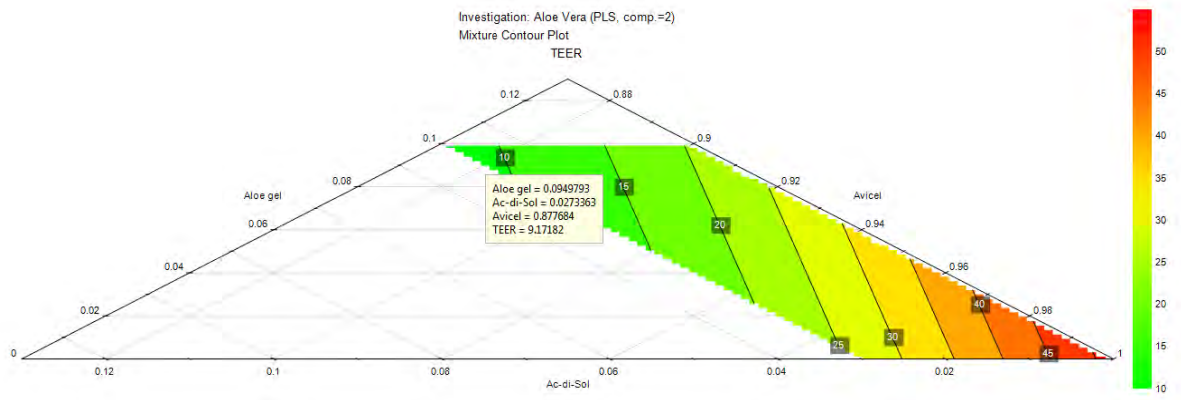

Figure 4.6: Contour plot generated by the design of experiments software (MODDE 9.0™) to determine the optimum bead formulation containing *A. vera* as absorption enhancer

4.2 Fingerprinting of aloe materials by nuclear magnetic resonance (^{1}H-NMR) spectroscopy

Chemical fingerprinting by means of ^{1}H-NMR was done to identify marker molecules present in each of the aloe gel materials. Furthermore, marker molecules were also used to indicate biological and chemical stability of the aloe leaf materials. The ^{1}H-NMR spectrum of the *A. ferox* gel material used in this study is given in Figure 4.7.

From Figure 4.7, it is clear that *A. ferox* gel contained glucose, lactic acid and malic acid. The absence of aloverose (or acetylated polymannose) is in accordance with previous findings (O'Brien *et al.*, 2011:988). The presence of lactic acid may be an indication of some bacterial degradation of the aloe gel material, but this is often present in aloe leaf materials in trace quantities.

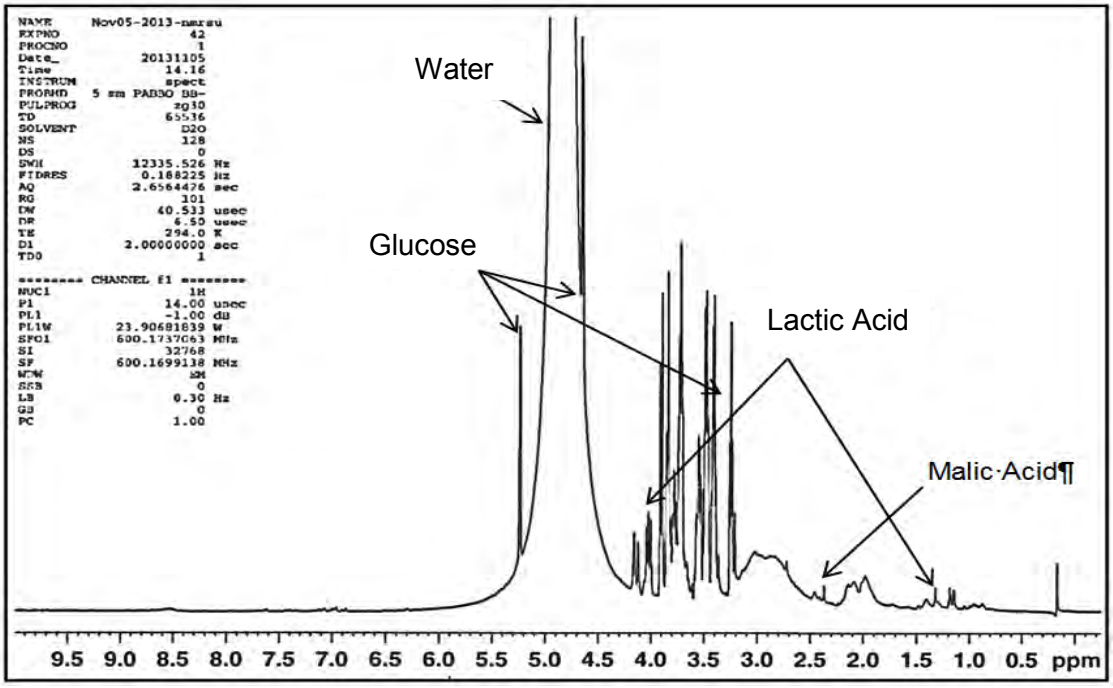

Figure 4.7: The ^{1}H-NMR spectrum of *Aloe ferox* gel material

Figure 4.8 presents the ^{1}H-NMR spectrum of the *A. marlothii* gel material used in this study.

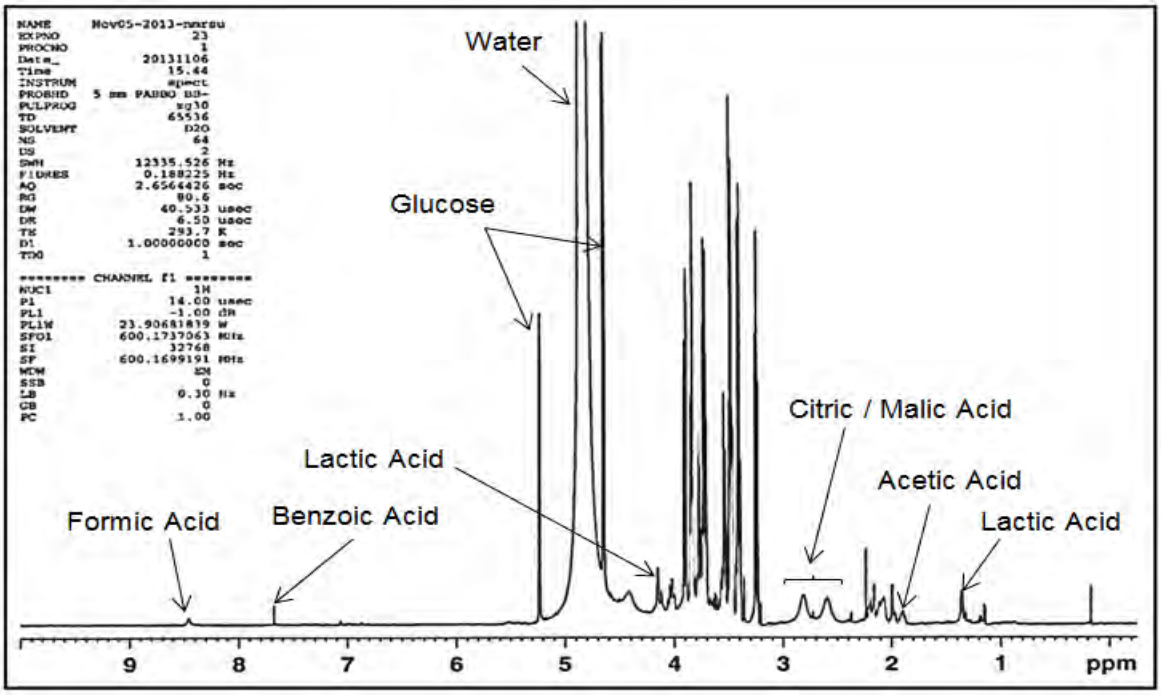

Figure 4.8: The ^{1}H-NMR spectrum of *Aloe marlothii* gel material

The most important chemical markers identified by ^{1}H-NMR in the *A. marlothii* gel material are glucose, malic acid, formic acid, benzoic acid, lactic acid, citric acid and acetic acid. Lactic acid indicated bacterial degradation by Lactobacilli, whereas the presence of formic acid and acetic acid indicated chemical degradation by hydrolysis. These compounds are often present in aloe leaf materials in trace quantities since this degradation almost always exists to a low degree.

Figure 4.9 presents the ^{1}H-NMR spectrum of the *A. vera* gel material used in this study. The three main marker molecules found in the *A. vera* gel material included aloverose, glucose and malic acid. Formic acid and lactic acid were also present due to the previously mentioned degradation processes.

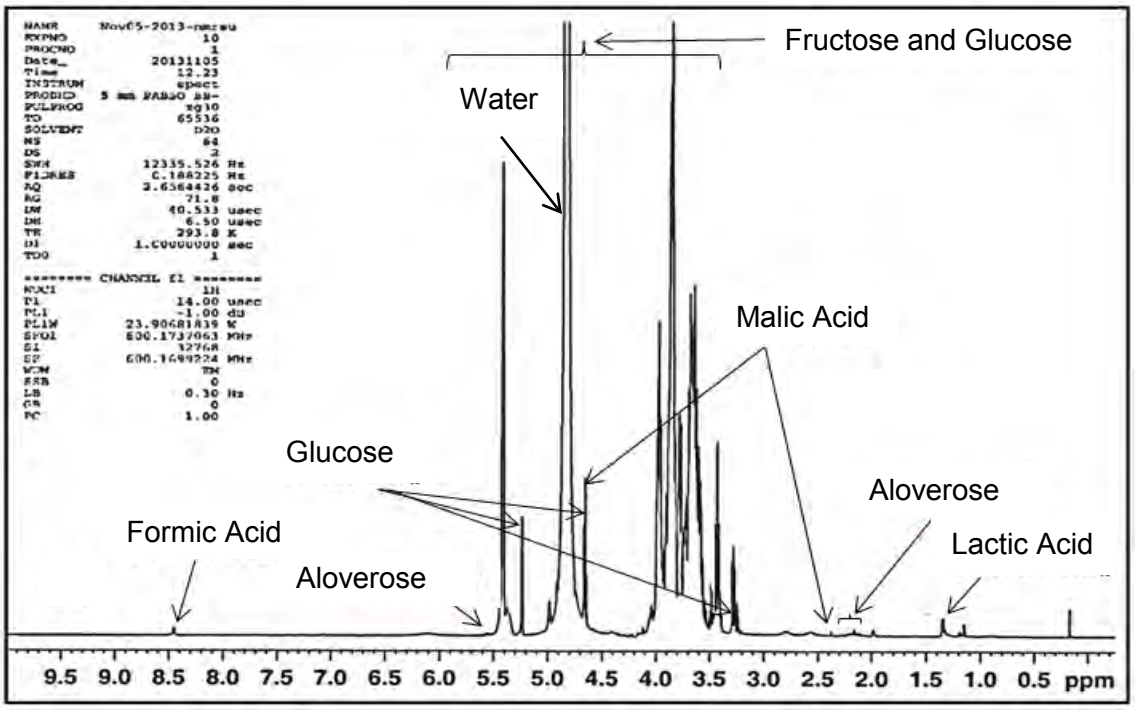

Figure 4.9: The ^{1}H-NMR spectrum of *Aloe vera* gel material

4.3 Evaluation of beads containing the selected aloe gel materials

4.3.1 Mass variation and friability

The average mass as well as percentage deviations from the average mass (i.e. the maximum deviation from the average for both masses lower and higher than the average mass) are given in Table 4.1 for all the bead formulations. Note that all the formulations contained microcrystalline cellulose and no insulin. Formulation names provided in this table, as well as in other tables that follow, only indicate the differences between the content of these formulations. All the optimum formulations did contain 0.06% w/w insulin.

According to the USP (2014:492), the mass variation of capsules, granules (uncoated, single–dose) weighing more than 300 mg, must not have a percentage deviation outside the limit ± 7.5% from the average. From Table 4.1, it is clear that all the bead formulations complied with the prescribed values of the USP.

According to the USP (2014:1146), the limit for acceptable on friability of solid oral dosage forms is <1%. The percentage friability and standard deviations for all the bead formulations are depicted in Table 4.2. Bead formulations that had an average friability of more than 1%, did not comply with the USP standard. The optimum bead formulations containing aloe gel materials, all complied with the standard, as well as the formulation containing insulin complied with the specification.

The friability of a few bead formulations could not be determined, due to the difficulty in weighing the beads after completion of the friability test because of build-up of static electricity in the friability drum. All the beads could not be removed from the drum and thus the friability of these formulations was not determined.

Table 4.1: Average mass and minimum as well as maximum percentage deviation from the average mass for all the bead formulations (n=3)

Formulation	Average mass (g)	Maximum % deviation (lower than average)	Maximum % deviation (higher than average)
MCC 100%	1.003	3.98	4.26
Ac-di-sol® 3%	0.784	3.48	2.74
Ac-di-sol® 1.5%	0.895	3.75	2.87
SLS 0.2%	0.864	2.51	1.69
A. ferox gel 10%	1.054	4.47	4.12
A. ferox gel 10%, Ac-di-sol® 3%	0.777	2.58	1.90
A. ferox gel 5%	0.967	4.49	2.44
A. ferox gel 10%, Ac-di-sol® 1.5%	0.895	3.75	2.87
A. ferox gel 5%, Ac-di-sol® 3%	0.803	3.33	2.90
A. ferox gel 5%, Ac-di-sol® 1.5%	0.861	2.78	2.87
A. ferox gel 5%, Ac-di-sol® 1.5%	0.860	5.31	3.91
A. ferox gel 5%, Ac-di-sol® 1.5%	0.927	2.55	4.01
A. marlothii gel 10%	0.902	2.96	2.42
A. marlothii gel 10%, Ac-di-sol® 3%	0.795	1.58	3.28
A. marlothii gel 5%	0.898	2.21	3.76
A. marlothii gel 10%, Ac-di-sol® 1.5%	0.846	2.60	2.89
A. marlothii gel 5%, Ac-di-sol® 3%	0.791	5.01	2.39
A. marlothii gel 5%, Ac-di-sol® 1.5%	0.757	1.59	3.53
A. marlothii gel 5%, Ac-di-sol® 1.5%	0.858	3.19	3.06
A. marlothii gel 5%, Ac-di-sol® 1.5%	0.828	2.48	3.74
A. vera gel 10%	0.841	0.45	0.24
A. vera gel 10%, Ac-di-sol® 3%	0.795	4.81	4.05
A. vera gel 5%	0.780	4.49	2.73
A. vera gel 10%, Ac-di-sol® 1.5%	0.807	2.36	5.23
A. vera gel 5%, Ac-di-sol® 3%	0.807	2.30	1.91
A. vera gel 5%, Ac-di-sol® 1.5%	0.805	1.67	3.44
A. vera gel 5%, Ac-di-sol® 1.5%	0.846	0.29	0.26
A. vera gel 5%, Ac-di-sol® 1.5%	0.827	0.17	0.18
Optimum bead formulation for *A. ferox*	0.545	3.60	4.80
Optimum bead formulation for *A. marlothii*	0.541	4.44	5.04
Optimum bead formulation for *A. vera*	0.521	3.52	1.72
Insulin bead formulation	0.519	2.44	4.24

Table 4.2: Average percentage friability and standard deviations for all the bead formulations (n=3)

Formulation	Percentage Friability	Standard deviation
MCC 100%	0.07	0.03
Ac-di-sol® 3%	4.29	1.82
Ac-di-sol® 1.5%	2.73	0.66
SLS 0.2%	1.95	0.92
A. ferox gel 10%	0.46	0.22
A. ferox gel 10%, Ac-di-sol® 3%	2.36	0.27
A. ferox gel 5%	1.05	0.26
A. ferox gel 10%, Ac-di-sol® 1.5%	0.81	0.22
A. ferox gel 5%, Ac-di-sol® 3%	ND	ND
A. ferox gel 5%, Ac-di-sol® 1.5%	1.05	0.26
A. ferox gel 5%, Ac-di-sol® 1.5%	ND	ND
A. ferox gel 5%, Ac-di-sol® 1.5%	ND	ND
A. marlothii gel 10%	0.15	0.18
A. marlothii gel 10%, Ac-di-sol® 3%	3.59	2.46
A. marlothii gel 5%	1.13	0.58
A. marlothii gel 10%, Ac-di-sol® 1.5%	0.66	0.33
A. marlothii gel 5%, Ac-di-sol® 3%	0.88	1.40
A. marlothii gel 5%, Ac-di-sol® 1.5%	0.99	0.10
A. marlothii gel 5%, Ac-di-sol® 1.5%	2.58	1.67
A. marlothii gel 5%, Ac-di-sol® 1.5%	0.60	0.65
A. vera gel 10%	2.02	0.32
A. vera gel 10%, Ac-di-sol® 3%	2.97	0.67
A. vera gel 5%	0.70	0.97
A. vera gel 10%, Ac-di-sol® 1.5%	2.62	0.22
A. vera gel 5%, Ac-di-sol® 3%	0.91	0.59
A. vera gel 5%, Ac-di-sol® 1.5%	0.91	0.59
A. vera gel 5%, Ac-di-sol® 1.5%	3.09	0.83
A. vera gel 5%, Ac-di-sol® 1.5%	2.81	1.93
Optimum bead formulation for *A. ferox*	0.00	0.00
Optimum bead formulation for *A. marlothii*	0.00	0.00
Optimum bead formulation for *A. vera*	0.00	0.00
Insulin bead formulation	0.16	0.17

*ND = not determined.

4.3.2 Scanning electron microscopy

The surface morphology and internal structure of the optimised bead formulations containing different aloe gel materials were evaluated by means of scanning electron microscopy (SEM). SEM evaluation was also conducted on beads consisting of microcrystalline cellulose (MCC) only, MCC with disintegrant (Ac-di-sol®), MCC with sodium lauryl sulphate (SLS) and MCC with insulin, respectively.

4.3.2.1 Beads consisting of microcrystalline cellulose only

Figure 4.10 presents the SEM micrographs of the bead formulation consisting of MCC only. Scale bars are specified on each micrograph as an indication of the magnification.

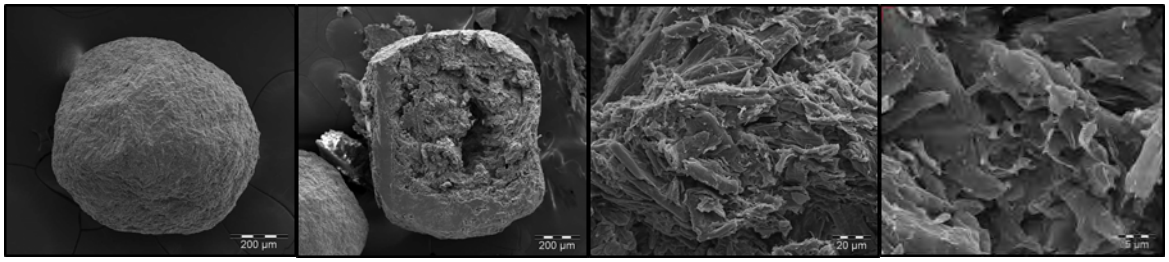

A B C D

Figure 4.10: Scanning electron micrographs of the bead formulation consisting of microcrystalline cellulose only: A) External surface morphology; B, C and D) internal structure at different magnifications

Beads consisting of MCC only appear to have a dense structure, with a relatively smooth surface morphology (Figure 4.10 A). There are only a few pores visible on the internal structure of this particular bead formulation (Figure 4.10 B, C & D). This indicates the ability of MCC to form densely structured beads by means of extrusion spheronisation, which may not easily disintegrate and will therefore probably release incorporated drug molecules relatively slowly.

4.3.2.2 Beads consisting of microcrystalline cellulose and 3% w/w Ac-di-sol®

Figure 4.11 presents SEM micrographs of the bead formulation consisting of MCC and 3% w/w Ac-di-sol®. Scale bars are specified on each micrograph as an indication of the magnification.

The beads containing Ac-di-sol® in addition to MCC have a less dense structure compared to those consisting of MCC only. Relatively large pores are visible on both the surface and internal structures of this particular bead formulation (Figure 4.11 B, C and D). The pores may facilitate relatively quick movement of water into the beads, which may contribute to fast disintegration and release of drug molecules from these beads.

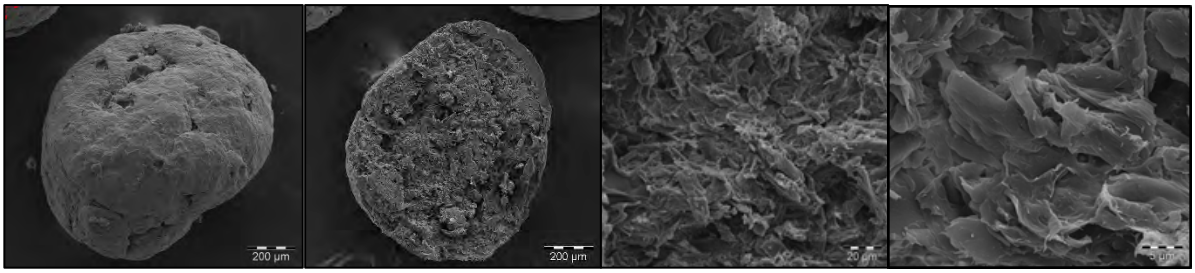

A B C D

Figure 4.11: Scanning electron micrographs of the bead formulation consisting of microcrystalline cellulose and 3% w/w Ac-di-sol®: A) External surface structure; B, C and D) internal structure at different magnifications

4.3.2.3 Beads consisting of microcrystalline cellulose and 1.5% w/w Ac-di-sol®

Figure 4.12 presents SEM micrographs of the bead formulation consisting of MCC and 1.5% Ac-di-sol® is presented in Figure 4.12. These beads exhibit an uneven form as well as a relatively rough surface morphology (Figure 4.12 A) with fewer pores visible on both the surface and internal structures (Figure 4.12B, C and D), compared to the bead formulation containing 3% w/w Ac-di-sol®.

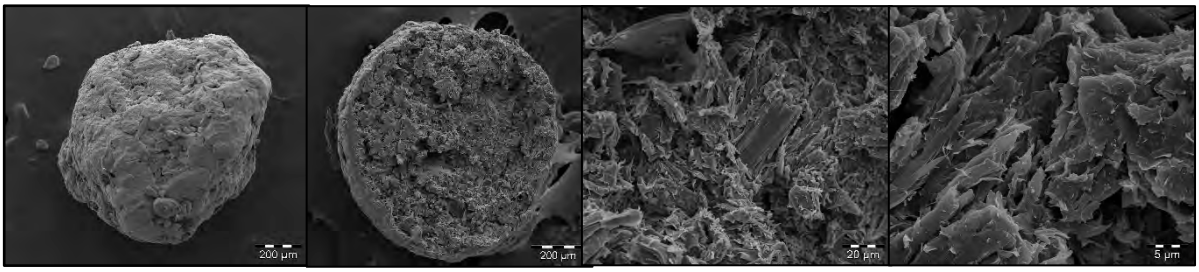

A B C D

Figure 4.12: Scanning electron micrographs of the bead formulation consisting of microcrystalline cellulose and 1.5% w/w Ac-di-sol®: A) External surface structure; B, C and D) internal structure at different magnifications

4.3.2.4 Beads consisting of microcrystalline cellulose and 0.2% w/w sodium lauryl sulphate

Figure 4.13 presents SEM micrographs of the bead formulation consisting of MCC and 0.2% w/w SLS. These beads appear to have a similar dense structure with a relatively smooth surface morphology, compared to beads consisting of MCC only (Figure 4.13 A). There are relatively small pores visible on the internal structure (Figure 4.13 B, C and D) of this particular bead formulation.

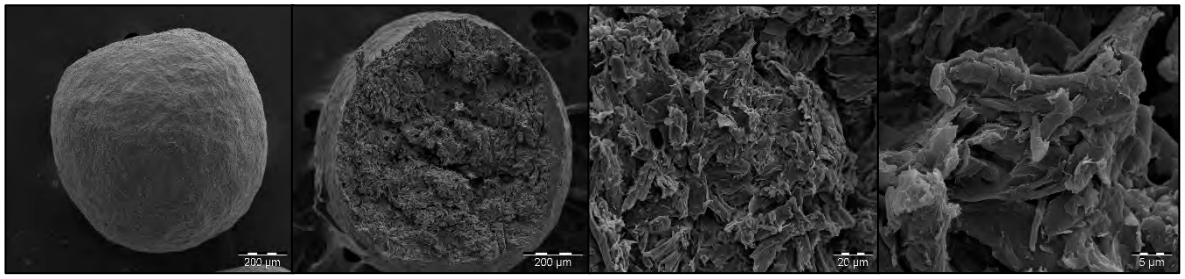

A B C D

Figure 4.13: Scanning electron micrographs of the bead formulation consisting of microcrystalline cellulose and 0.2% w/w sodium lauryl sulphate: A) External surface morphology; B, C and D) internal structure at different magnifications

4.3.2.5 Optimised bead formulation containing *Aloe ferox* gel

Figure 4.14 presents SEM micrographs of the optimised bead formulation containing *Aloe ferox*. This formulation produced relatively spherical beads with a slightly rough exterior surface (Figure 4.14 A) and porous interior structure (Figure 4.14 B).

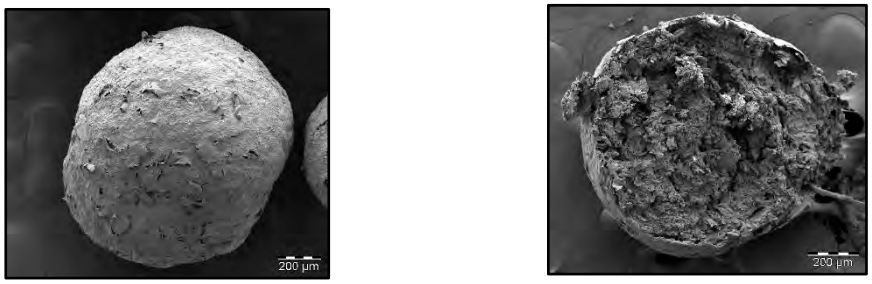

A B

Figure 4.14: Scanning electron micrographs of the optimised bead formulation containing *Aloe ferox*: A) External surface morphology and B) internal structure

4.3.2.6 Optimised bead formulation containing *Aloe marlothii* gel

Figure 4.15 presents SEM micrographs of the optimised bead formulation containing *Aloe marlothii*. This bead formulation has a relatively smooth exterior surface morphology (Figure 4.15A) and the internal surface (Figure 4.15B) density resembles the formulation consisting of MCC with 1.5% w/w Ac-di-sol®. The beads are less spherical and appear brittle, which may contribute to disintegration with potential faster release of the drug molecules than the beads consisting of MCC only.

A B

Figure 4.15: Scanning electron micrographs of the optimised bead formulation containing *Aloe marlothii*: A) External surface morphology and B) internal structure

4.3.2.7 Optimised bead formulation containing *Aloe vera* gel

Figure 4.16 presents SEM micrographs of the optimised bead formulation containing *Aloe vera*. This formulation produced elongated (almost dumbbell shaped) beads, with a relatively porous external morphology (Figure 4.16 A) and internal structure (Figure 4.16 B). The pores may contribute to faster infiltration of water into the beads with consequent faster disintegration and release of drug molecules.

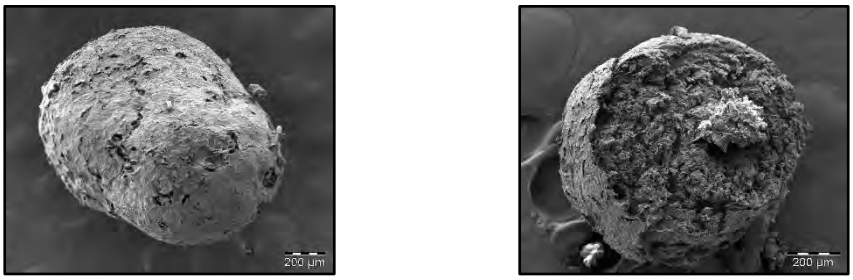

A B

Figure 4.16: Scanning electron micrographs of the optimised bead formulation containing *Aloe vera*: A) External surface morphology and B) internal structure

4.3.2.8 Bead formulation containing microcrystalline cellulose and insulin

Figure 4.17 presents SEM micrographs of the bead formulation consisting of insulin and MCC. The beads have a relatively rough exterior surface morphology and a slightly less dense internal structure compared to those consisting of MCC only. The beads are spherical, but drug release may be slower due to the absence of pores.

A B

Figure 4.17: Scanning electron micrographs of the bead formulation consisting of insulin and microcrystalline cellulose: A) External surface morphology and B) internal structure

4.3.3 Particle size and size distribution analysis of beads

The d(0.5) (average particle distribution) and D[4,3] (volume weighed mean) values obtained by the size analysis of all the initial and optimised bead formulations are given in Tables 4.3 and 4.4, respectively.

Table 4.3: The d(0.5) values obtained during particle size analysis using the Malvern® Mastersizer 2000 (n=3)

Formulation	d(0.5) µm value	Standard deviation
MCC 100%	971.62	18.49
Ac-di-sol® 3%	992.60	3.67
Ac-di-sol® 1.5%	949.43	18.53
SLS 0.2%	970.05	5.37
A. ferox gel 10%	957.34	3.68
A. ferox gel 10%, Ac-di-sol® 3%	935.49	13.62
A. ferox gel 5%	973.14	0.42
A. ferox gel 10%, Ac-di-sol® 1.5%	960.41	2.33
A. ferox gel 5%, Ac-di-sol® 3%	961.16	5.13
A. ferox gel 5%, Ac-di-sol® 1.5%	985.17	7.07
A. ferox gel 5%, Ac-di-sol® 1.5%	974.08	10.49
A. ferox gel 5%, Ac-di-sol® 1.5%	966.58	11.07
A. marlothii gel 10%	887.34	5.81
A. marlothii gel 10%, Ac-di-sol® 3%	886.83	19.65
A. marlothii gel 5%	891.51	5.53
A. marlothii gel 10%, Ac-di-sol® 1.5%	894.24	7.78
A. marlothii gel 5%, Ac-di-sol® 3%	896.32	5.98
A. marlothii gel 5%, Ac-di-sol® 1.5%	861.83	9.36
A. marlothii gel 5%, Ac-di-sol® 1.5%	890.60	15.99
A. marlothii gel 5%, Ac-di-sol® 1.5%	850.77	13.28
A. vera gel 10%	801.45	10.44
A. vera gel 10%, Ac-di-sol® 3%	935.42	9.60
A. vera gel 5%	934.60	14.26
A. vera gel 10%, Ac-di-sol® 1.5%	792.58	20.45
A. vera gel 5%, Ac-di-sol® 3%	927.03	9.68
A. vera gel 5%, Ac-di-sol® 1.5%	813.95	22.48
A. vera gel 5%, Ac-di-sol® 1.5%	997.37	11.86
A. vera gel 5%, Ac-di-sol® 1.5%	951.97	23.74
Optimum bead formulation for *A. ferox*	1048.00	5.64
Optimum bead formulation for *A. marlothii*	972.70	4.85
Optimum bead formulation for *A. vera*	1088.42	12.85
Insulin bead formulation	1135.25	3.39

Table 4.4: The D[4,3] values obtained during particle size analysis using the Malvern® Mastersizer 2000; *D[4,3] Volume weighted mean (n=3)

Formulation	D[4,3] µm*	Standard deviation
MCC 100%	1005.95	18.88
Ac-di-sol® 3%	1023.91	3.53
Ac-di-sol® 1.5%	998.01	2.56
SLS 0.2%	1002.19	5.10
A. ferox gel 10%	990.45	3.53
A. ferox gel 10%, Ac-di-sol® 3%	972.05	15.21
A. ferox gel 5%	1006.59	2.40
A. ferox gel 10%, Ac-di-sol® 1.5%	994.45	3.54
A. ferox gel 5%, Ac-di-sol® 3%	993.86	4.85
A. ferox gel 5%, Ac-di-sol® 1.5%	1016.49	6.65
A. ferox gel 5%, Ac-di-sol® 1.5%	1005.92	10.12
A. ferox gel 5%, Ac-di-sol® 1.5%	999.11	10.67
A. marlothii gel 10%	924.20	8.14
A. marlothii gel 10%, Ac-di-sol® 3%	932.74	16.77
A. marlothii gel 5%	926.37	5.36
A. marlothii gel 10%, Ac-di-sol® 1.5%	928.70	7.79
A. marlothii gel 5%, Ac-di-sol® 3%	934.81	7.36
A. marlothii gel 5%, Ac-di-sol® 1.5%	911.16	8.96
A. marlothii gel 5%, Ac-di-sol® 1.5%	929.14	17.75
A. marlothii gel 5%, Ac-di-sol® 1.5%	886.80	20.71
A. vera gel 10%	844.39	10.13
A. vera gel 10%, Ac-di-sol® 3%	982.46	10.58
A. vera gel 5%	975.26	18.19
A. vera gel 10%, Ac-di-sol® 1.5%	829.92	24.83
A. vera gel 5%, Ac-di-sol® 3%	971.27	8.91
A. vera gel 5%, Ac-di-sol® 1.5%	874.65	21.66
A. vera gel 5%, Ac-di-sol® 1.5%	1032.36	10.88
A. vera gel 5%, Ac-di-sol® 1.5%	990.12	22.02
Optimum bead formulation for *A. ferox*	1075.58	5.28
Optimum bead formulation for *A. marlothii*	1008.89	4.55
Optimum bead formulation for *A. vera*	1114.07	11.02
Insulin bead formulation	1157.31	3.11

The bead formulations containing MCC 100%, Ac-di-sol® 3%, Ac-di-sol® 1.5% and SLS 0.2% exhibit d(05) and D[4,3] values which are close to each other, indicating relatively narrow particle size distributions for the formulations.

All the initial bead formulations containing *A. ferox* gel had d(0.5) values ranging from 935.49 to 985.17 µm and D[4,3] values from 972.05 to 1006.59 µm. Although these values differ to some extent, they are still relatively close to each other and indicate the formulations

have acceptable size distributions. The formulations containing *A. marlothii* gel depicted d(0.5) values ranging from 850.77 to 896.32 µm and D[4,3] values from 886.80 to 934.00 µm. These values indicated the bead sizes of formulations containing *A. marlothii* are slightly smaller than the bead formulations containing *A. ferox* and *A. vera* gel as absorption enhancers. Formulations containing *A. vera* gel had a wider size distribution than the other two aloe materials containing bead formulations, with d(0.5) values ranging from 801.45 to 997.37 µm and D[4,3] values from 844.39 to 1032.36 µm.

The average d(0.5) values for the optimised bead formulations containing *A. ferox, A. marlothii* and *A. vera* gel were 1048.00 µm, 972.70 µm and 1088.42 µm, respectively. The D[4,3] values for these optimised bead formulations were 1075.58 µm, 1008.89 µm and 1114.07 µm, respectively. Relatively small differences between the d(0.5) and D[4,3] values of each optimised bead formulation confirmed the relative small particle size distribution of each of these formulations, as observed with the size distribution plots. The bead formulation containing insulin and MCC depicted the largest d(0.5) value (1135.25 µm) and D[4,3] value (1157.31 µm), which correlates well with the size of the beads in the optimised bead formulations which also contain insulin as the active ingredient.

Particle size distribution plots of each optimised bead formulation as well as the bead formulation containing insulin and microcrystalline cellulose are shown in Figures 4.18 to 4.20. The size distribution graphs of all four the bead formulations showed these formulations have relatively narrow size distributions with average sizes close to 1.00 mm.

4.3.3.1 Optimised bead formulation containing *Aloe ferox* gel

Figure 4.18 presents the particle size distribution plot for the optimised bead formulation containing *A. ferox*. The majority of the beads (i.e. 72.3%) in the optimised bead formulation containing *A. ferox* (Figure 4.18) ranged between 954.993 µm and 1445.440 µm. Beads with an average size of 1096.478 µm represented 21.27% of the total batch volume, whereas those measuring 1258.925 µm represented 19.47% of the total batch volume.

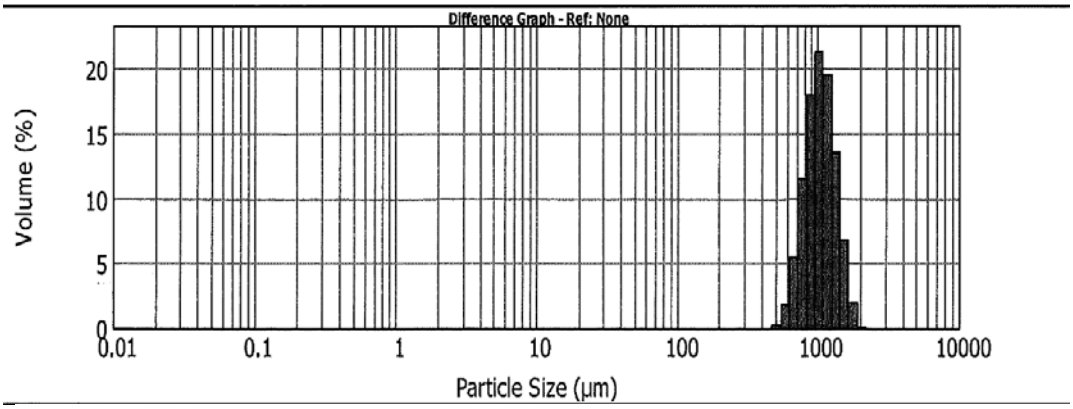

Figure 4.18: Particle size distribution plot for the optimised bead formulation containing *Aloe ferox* gel

4.3.3.2 Optimised bead formulation containing *Aloe marlothii* gel

Figure 4.19 presents the particle size distribution plot for the optimised bead formulation containing *A. marlothii*. The majority of the beads (i.e. 63.46%) in the optimised bead formulation containing *A. marlothii* (Figure 4.19) ranged between 954.993 µm and 1445.440 µm. Beads with an average size of 1096.478 µm represented 18.65% of the total batch volume, whereas those measuring 1258.925 µm represented 15.87% of the total batch volume.

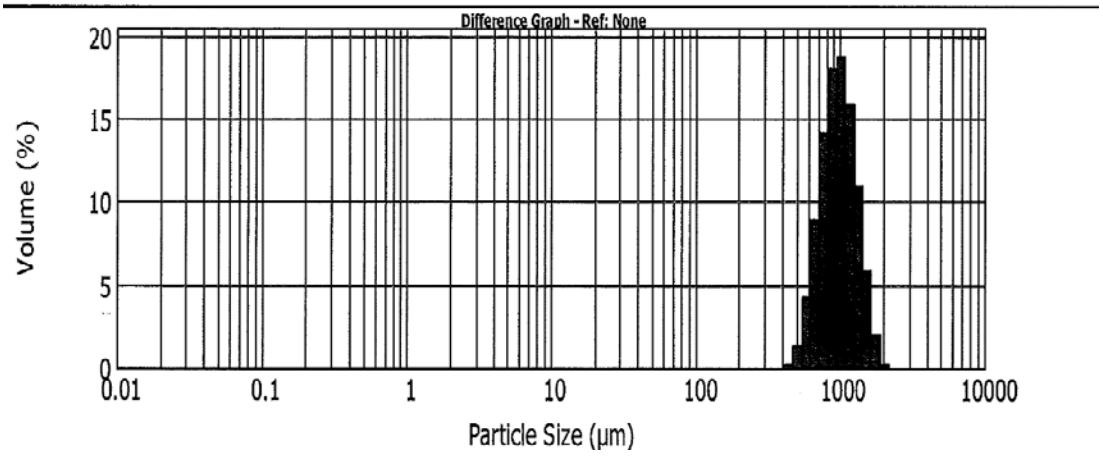

Figure 4.19: Particle size distribution plot for the optimised bead formulation containing *Aloe marlothii* gel

4.3.3.3 Optimised bead formulation containing *Aloe vera* gel

Figure 4.20 presents the particle size distribution plot for the optimised bead formulation containing *A. vera*. The majority of the beads (i.e. 75.25%) in the optimised bead formulation containing *A. vera* (Figure 4.20) varied between 954.993 µm and 1445.440 µm. Beads with an average size of 1096.478 µm denoted 21.04% of the total batch volume, those measuring 1258.925 µm denoted 21.58% of the total batch volume.

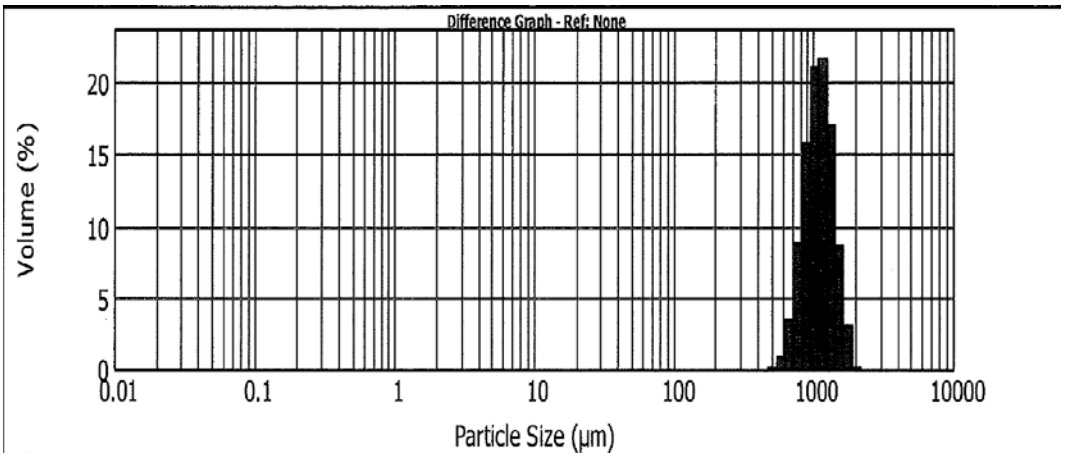

Figure 4.20: Particle size distribution plot for the optimised bead formulation containing *Aloe vera* gel

4.3.3.4 Bead formulation containing microcrystalline cellulose and insulin

Figure 4.21 presents the particle size distribution plot for the optimised bead formulation containing insulin and microcrystalline cellulose. The bulk of the beads (i.e. 75.25%) in the optimised bead formulation containing insulin (Figure 4.21) varied between 954.993 µm and 1445.440 µm. Beads with an average size of 1096.478 µm signified 20.80% of the total batch volume, whereas those measuring 1258.925 µm signified 22.82% of the total batch volume.

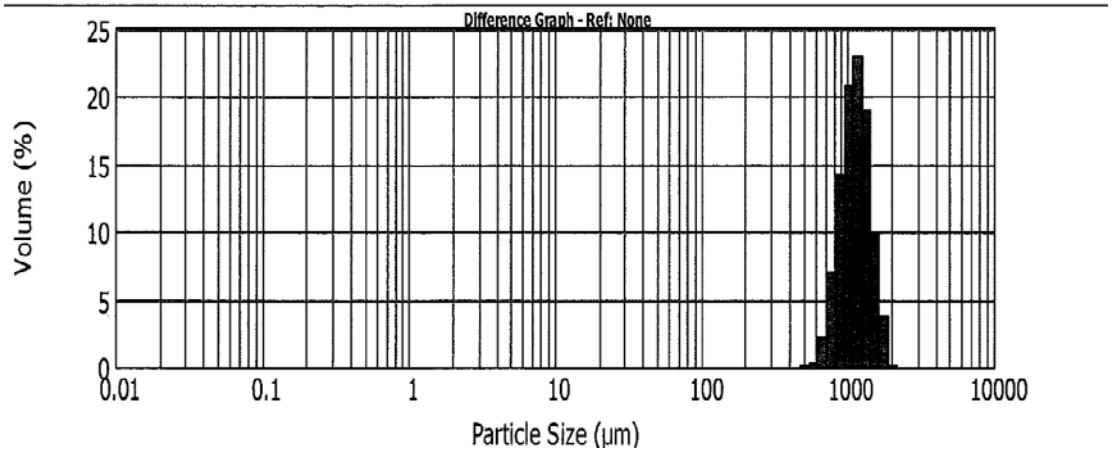

Figure 4.21: Particle size distribution plot for the bead formulation containing insulin and microcrystalline cellulose

4.4 Validation of the high-performance liquid chromatography (HPLC) analysis of insulin

4.4.1 Specificity

Figures 4.22 to 4.29 illustrate the ability of the HPLC method to separate and analyse insulin in the presence of other compounds, such as phosphate buffer saline (PBS), 0.1 M hydrochloric acid, 0.1 M sodium hydroxide, 10% hydrogen peroxide as well as *A. ferox*, *A. marlothii, A. vera* gel material and potential insulin degradation products as produced by stress conditions. Insulin elutes from 5.82 min (Figure 4.22).

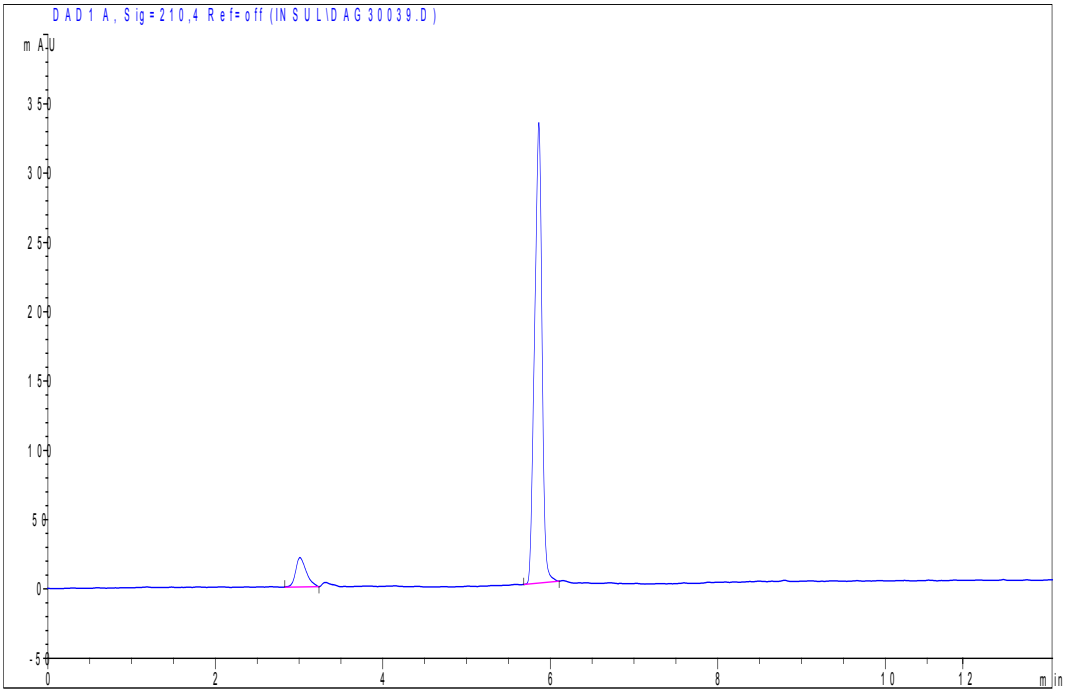

Figure 4.22: Chromatogram of insulin in the presence of PBS

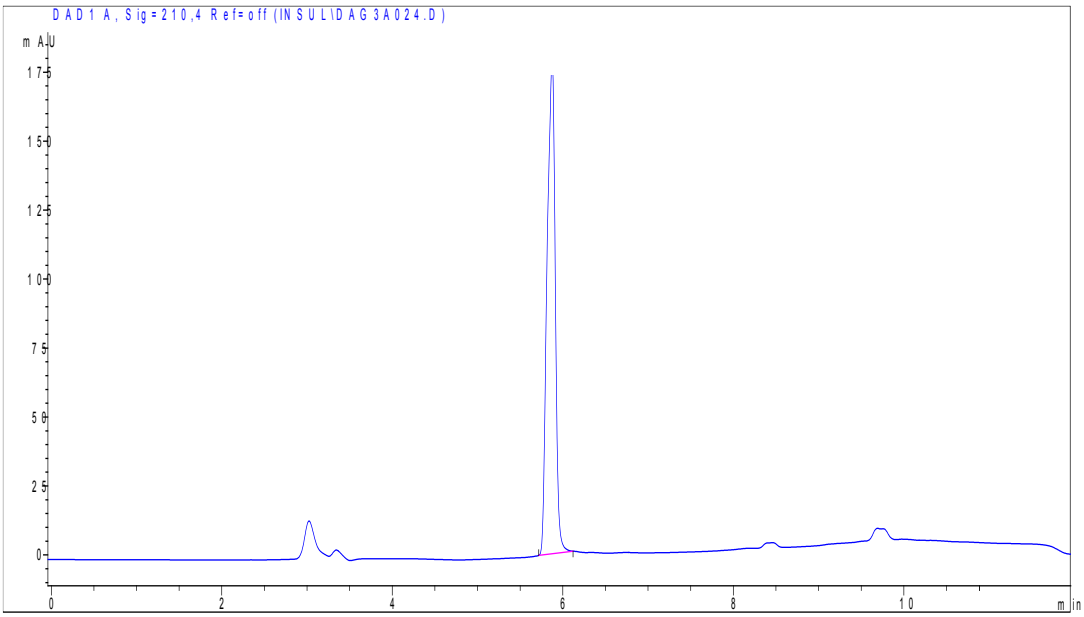

Figure 4.23: Chromatogram of insulin kept in water at 40°C for 24 h for insulin analysis in the presence of potential degradation products

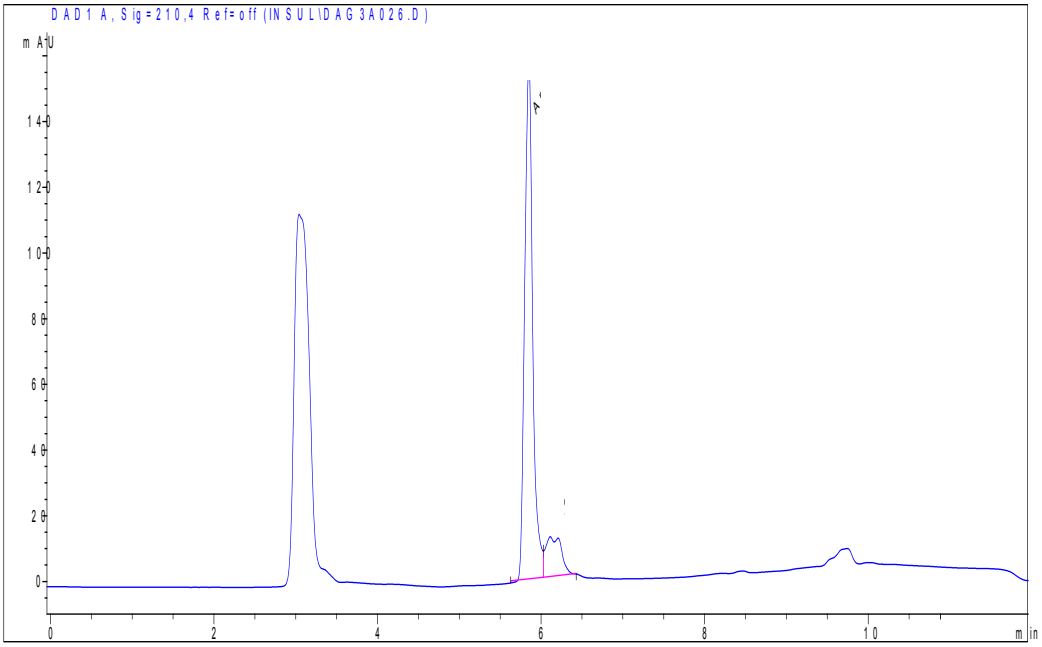

Figure 4.24: Chromatogram of insulin kept in 0.1 M hydrochloric acid at 40°C for 24 h for insulin analysis in the presence of potential degradation products

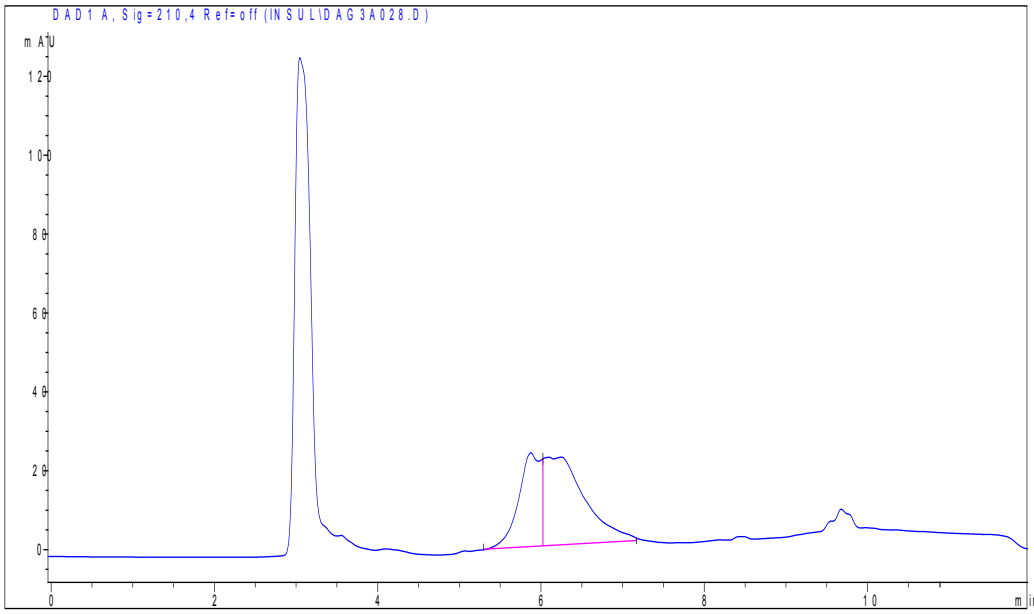

Figure 4.25: Chromatogram of insulin kept in 0.1 M sodium hydroxide at 40°C for 24 h for insulin analysis in the presence of potential degradation products

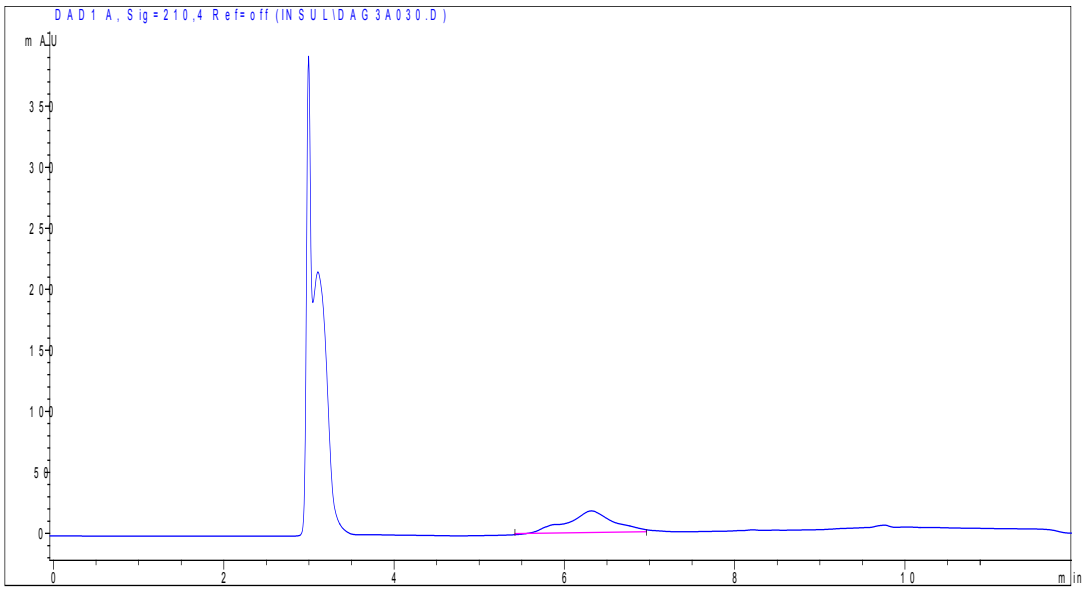

Figure 4.26: Chromatogram of insulin kept in 10% hydrogen peroxide at 40°C for 24 h for insulin analysis in the presence of potential degradation products

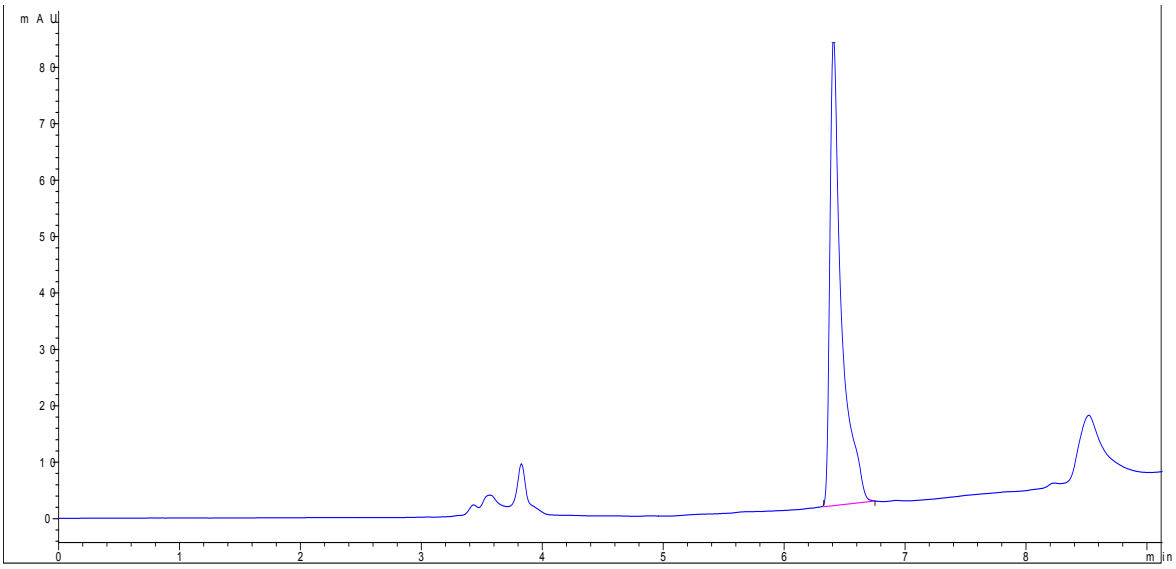

Figure 4.27: Chromatogram of insulin in the presence of *Aloe ferox* gel

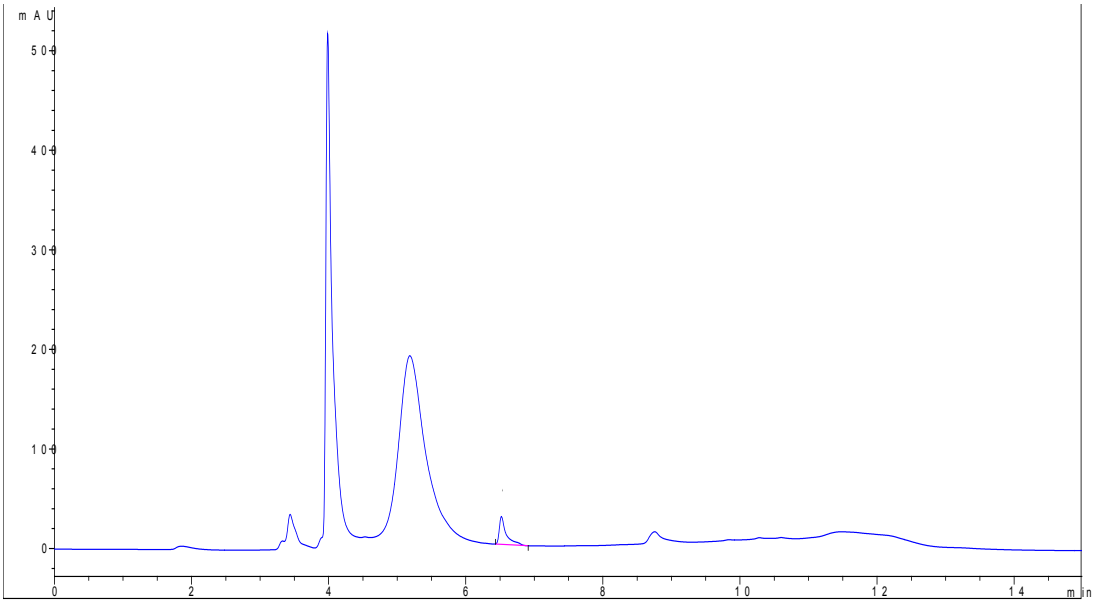

Figure 4.28: Chromatogram of insulin in the presence of *Aloe marlothii* gel

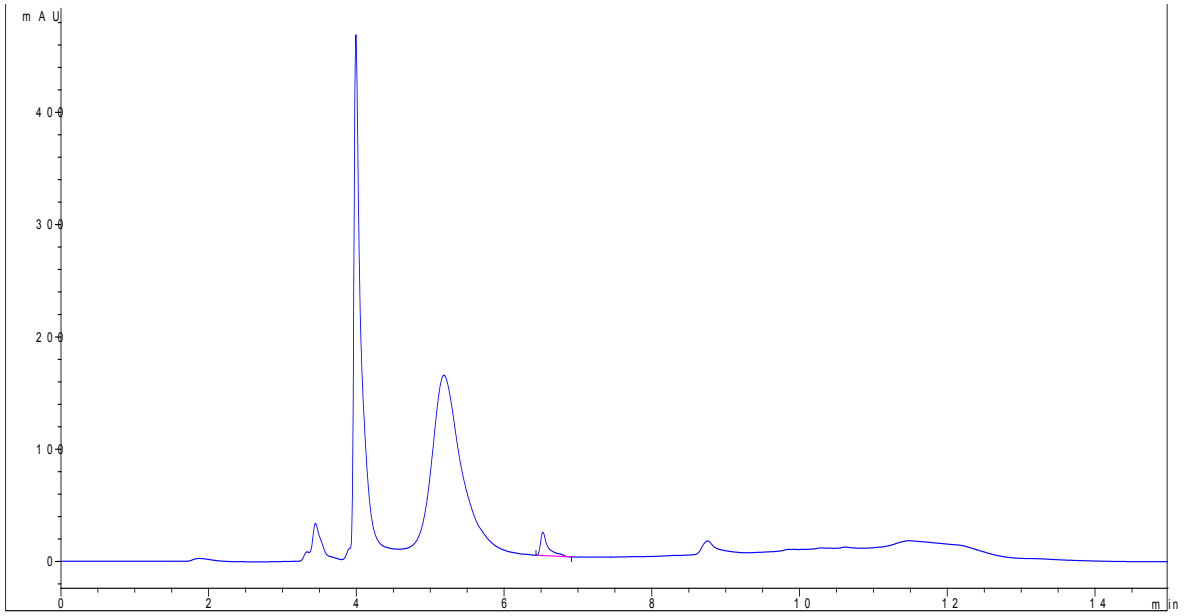

Figure 4.29: Chromatogram of insulin in the presence of *Aloe vera* gel

None of the ingredients investigated interfered with the insulin peak on the HPLC chromatograms, except for some potential peak overlaps when insulin was incubated at 40°C in 0.1 M hydrochloric acid and 0.1 M sodium hydroxide.

4.4.2 Linearity

Figure 4.30 illustrates the linear regression curve where the peak area was plotted as a function of insulin concentration, whereas the regression coefficient, slope and intercept are shown in Table 4.6. The regression coefficient (R^2) for insulin regression curve is 0.9998575, which indicates the HPLC method used in this study for insulin analysis complies with the requirements of an R^2 value of 0.99 for linearity (USP, 2014:1160). The method was linear over the concentration range 0.3 to 170 μg/ml (Table 4.5).

Table 4.5: Peak areas obtained for insulin over a concentration range to determine the linearity

µg/ml	Peak area 1	Peak area 2	Mean
0.1	3.5	3.5	3.5
0.2	8.2	9.1	8.7
0.3	19.8	18.6	19.2
0.7	40.2	39.2	39.7
1.0	57.6	56.7	57.2
1.4	74.8	79.4	77.1
1.7	98.8	95.8	97.3
3.4	251.1	250.5	250.8
6.8	495.0	494.2	494.6
10.1	737.8	739.5	738.7
13.5	986.1	985.0	985.6
16.9	1230.1	1228.8	1229.5
33.8	2657.3	2663.2	2660.3
67.6	5263.7	5282.0	5272.8
101.4	7849.4	7851.0	7850.2
135.2	10332.8	10348.4	10340.6
169.0	12730.1	12856.3	12793.2

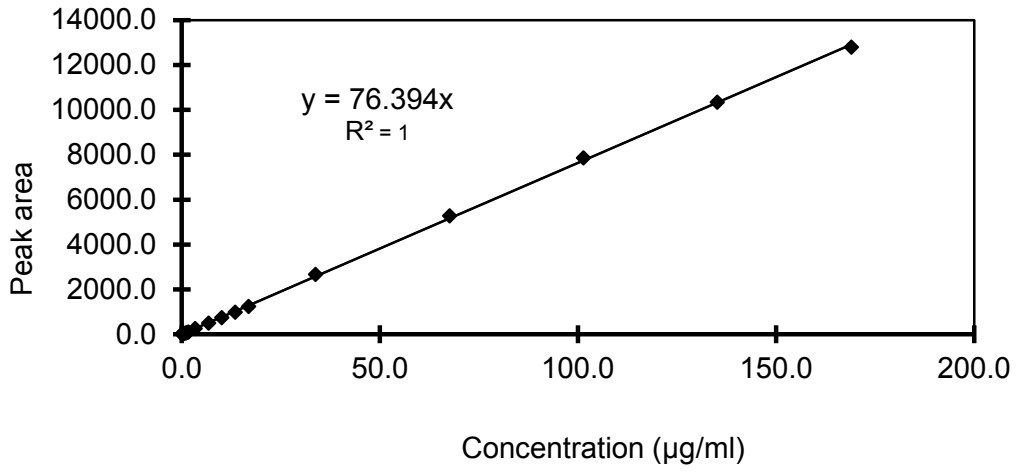

Figure 4.30: Linear regression curve for insulin

Table 4.6: Regression statistics for linearity of insulin

Regression coefficient (R^2)	0.9998575
Intercept	0
Slope	76.394

4.4.3 Limit of quantification and limit of detection

The limit of quantification (LOQ) was determined by injecting six replicates of standards at a low concentration. LOQ is the lowest concentration that can be determined with an RSD of ≤ 15%; for insulin the LOQ was 0.3 µg/ml. The limit of detection (LOD) is the lowest concentration peak that is discernible from baseline noise, usually taken as a peak that is equal to about three times the average baseline noise (USP, 2014:1160). The LOD for insulin was 0.05 µg/ml.

4.4.3 Accuracy and precision

Table 4.7 illustrates the recovery values obtained from three concentration ranges of insulin solutions and three replicates of each concentration range. Figure 4.8 illustrates the statistical analysis of the recovery of insulin from spiked samples

Table 4.7: Recovery of insulin from spiked samples

Concentration spiked	**Peak areas**			**Recovery**	
µg/ml	**1**	**2**	**Mean**	**µg/ml**	**%**
46.38	3160.3	3160.0	3160.2	45.48	98.06
46.38	3167.8	3143.8	3155.8	45.42	97.92
46.38	3148.2	3132.1	3140.2	45.19	97.44
92.76	6390.6	6388.7	6389.7	91.96	99.14
92.76	6393.0	6418.0	6405.5	92.19	99.38
92.76	6393.4	6408.8	6401.1	92.12	99.31
154.6	10610.9	10594.4	10602.7	152.59	98.70
154.6	10549.1	10724.7	10636.9	153.08	99.02
154.6	10711.8	10670.1	10691.0	153.86	99.52

Table 4.8: Statistical analysis of the recovery of insulin from spiked samples

Statistical analysis	
Mean	98.7
SD	0.7
% RSD	0.7
95% confidence intervals	
Lower limit	98.2
Upper limit	99.3
Estimated median	99.0
Confidence level (95.0%)	0.6

*SD refers to the standard deviation; **%RSD refers to relative standard deviation

The HPLC insulin analysis method yielded a mean recovery of 98.7% and a standard deviation, as well as relative standard deviation, of 0.7% from spiked samples, which is an acceptable value for accuracy where recovery has to be between 98 to 102%

4.4.4 Inter-day precision

Table 4.9 illustrates the inter-day precision parameters obtained for insulin analysis.

Table 4.9: Inter-day precision parameters for insulin

	Day 1	Day 2	Day 3	Between days
	99.1	98.1	101.7	
	99.4	98.0	101.1	
	99.3	98.7	100.9	
Mean	99.28	98.25	101.20	99.58
SD	0.10	0.29	0.34	1.22
RSD %	0.10	0.29	0.33	1.23

Table 4.10 illustrates the ANOVA single factor statistics for the inter-day precision parameters obtained and Table 4.11, the results of the inter- and intra-day precision ANOVA statistics.

Table 4.10: ANOVA single factor statistics for the inter-day precision parameters obtained

ANOVA Summary				
Groups	Count	Sum	Average	Variance
Day 1	3	297.832	99.277	0.016
Day 2	3	294.762	98.254	0.124
Day 3	3	303.613	101.204	0.171

Table 4.11: Inter- and Intra-day precision ANOVA statistics

ANOVA Summary					
Source of	SS	df	MS	F	p-value
Inter-day	13.466	2.0	6.733	65.092	$8.55E^{-05}$
Intra-day	0.621	6.0	0.103		
Total	14.087	8.0			

SS = sum of squares; df = degrees of freedom; MS = mean squares; F = F ratio

From Table 4.11 it is clear the inter-day and the intra-day precision of the HPLC insulin analysis are acceptable, as the values did not differ statistically significantly from each other ($p < 0.05$). Repeatability was within acceptable limits (an RSD better than 2% for intra-day precision and 5% for inter-day precision) and the assay should perform well, even when executed by other personnel in a different laboratory.

4.4.5 Ruggedness

4.4.5.1 Stability of sample solutions

Table 4.12 illustrates the results obtained for stability testing over 24 h.

Table 4.12: Results for stability of insulin over a 24 h period

Time (h)	Peak Area	% Remaining
0	2080.07	100.0
1	2092.5	100.6
2	2064.45	99.2
3	2051.82	98.6
4	2053.02	98.7
5	2051.43	98.6
6	2039.45	98.0
7	2040.79	98.1
8	2053.41	98.7
9	2009.65	96.6
10	2035.69	97.9
11	2042.49	98.2
12	2044.11	98.3
13	2035.59	97.9
14	2039.45	98.0
15	2036.64	97.9
16	2030.15	97.6
17	2026.27	97.4
18	2026.57	97.4
19	2033.57	97.8
20	2040.5	98.1
21	2025.89	97.4
22	2029.77	97.6
23	2026.96	97.4
24	2034.12	97.8
Mean	2041.8	98.2
SD	17.33	0.83
RSD %	0.85	0.85

The insulin degraded by approximately 2% over 24 h, which is acceptable.

4.4.5.2 System repeatability

Table 4.13 presents the results attained from the repeatability experiment.

Table 4.13: System repeatability parameters for insulin analysis

Injection sample	Peak area	Retention time (min)
1	6747.9	5.893
2	6713.3	5.859
3	6730.5	5.853
4	6788.5	5.869
5	6705.9	5.888
6	6679.9	5.906
Mean	6727.7	5.878
SD	34.35	0.019
RSD %	0.51	0.324

System repeatability proved sound, with percentage RSD values of 0.51% for peak area and 0.324% for retention time, respectively, which complies with the criteria of 2% or less.

4.4.6 Robustness

The HPLC method for insulin analysis was able to tolerate changes in the chromatographic conditions and should therefore perform well under normal conditions (Table 4.14).

Table 4.14: Changes in the chromatographic operating parameters to determine the influence of these changes on the chromatographic result

Flow rate	0.9 -1.1 ml/min
Injection volume	2.5, 5, 10, 20, 30, 40 and 50 µl
Wavelength	UV at 208- 212 nm
Mobile phase composition	A: A filtered and degassed mixture of HPLC grade water and 0.1% orthophosphoric acid was prepared. B: Acetonitrile The starting concentration could be 18 to 22% acetonitrile and the gradient end time could be 5.8 to 6.2 min without any ill effect. The retention time of the insulin peak will vary under different conditions, but this will not affect method performance.

4.4.7 Summary

Table 4.15 presents the results obtained for the HPLC validation of insulin.

Table 4.15: Summary of results obtained for the HPLC validation of insulin

Test	Result
Specificity	Complies
Range	0.3 to 170 µg/ml
Linearity	R^2 = 0.99986
Accuracy	98.7%
Precision	RSD = 1.23%

4.5 Assay

The theoretical concentration (mg/ml) (theoretical value of insulin content) of each optimum bead formulations was 0.06 mg/ml

4.5.1 Optimised bead formulation containing *Aloe ferox* gel

According to the calibration curve, c (y-intercept) = 0, m (slope) = 271734.7948 and substituting these values into the equation for a straight line (y = mx + c) to obtain the experimental value of insulin content (x) is done as follows:

$$\frac{(695.7674 - 0)}{271734.7948} = 0.0026$$

Table 4.16 displays the parameters for the assay for insulin in beads containing *Aloe ferox*

Table 4.16: Parameters for the assay for Insulin of beads containing *Aloe ferox* gel

Peak area	mg/ml
695.7674	0.0026

From Table 4.16, it is clear there is 0.256 mg insulin in 1 g beads, or 0.00026 g insulin in 1 g beads (or 0.026 g insulin in 100 g beads = 0.026 % w/w). The percentage content can then be calculated as follows:

$$\% \text{ insulin content} = \frac{0.026}{0.06} \times 100 = 43.33\%$$

The percentage content of insulin in the bead formulation containing *A. ferox* is 43.33% of the amount of insulin added to the formulation, which was 0.06 % w/w. Loss of content may have occurred during the production (i.e. extrusion and spheronisation), drying, handling or storage of the beads.

4.5.2 Optimised bead formulation containing *Aloe marlothii* gel

According to the calibration curve, c (y-intercept) = 0, m (slope) = 271734.7948 and substituting these values into the equation for a straight line (y = mx + c) to obtain the experimental value of insulin content (x) is done as follows:

$$\frac{(1965.2913 - 0)}{271734.7948} = 0.0072$$

The parameters for the assay for insulin in beads containing *Aloe marlothii* are depicted in Table 4.17.

Table 4.17: Parameters for the assay for insulin in beads containing *Aloe marlothii* gel

Peak area	mg/ml
1965.29126	0.0072

From Table 4.17 it is clear there is 0.72 mg insulin in 1 g beads containing *Aloe marlothii,* or 0.00072 g insulin in 1 g beads (or 0.072 g insulin in 100 g beads = 0.072% w/w). The percentage content can thus be calculated as follows:

$$\% \text{ Content} = \frac{0.072}{0.06} \times 100 = 120\%$$

The percentage content of insulin in the bead formulation containing *A. marlothii* was 120% of the amount of insulin (0.06% w/w) added to the formulation.

4.5.3 Optimised bead formulation containing *Aloe vera* gel

According to the calibration curve, c (y-intercept) = 0, m (slope) = 201511.736 and substituting these values into the equation for a straight line to obtain the experimental value of insulin content (x) is done as follows:

$$\frac{(1164.3671 - 0)}{201511.736} = 0.0058$$

Table 4.18 presents the parameters for the assay for insulin in beads containing *Aloe vera.*

Table 4.18: Parameters for the assay for insulin in beads containing *Aloe vera* gel

Peak area	mg/ml
1164.36707	0.0058

From this table it is clear there is 0.58 mg insulin in 1 g beads, or 0.00058 g insulin in 1 g beads (or 0.058 g insulin in 100 g beads = 0.08% w/w). The percentage content can then be calculated as follows:

% Content = $\frac{0.058}{0.06} \times 100 = 96.67\%$

The percentage content of insulin in the bead formulation containing *A. vera* was 96.67% of the amount of insulin added to the formulation, which was 0.06% w/w.

4.5.4 Optimised bead formulation containing microcrystalline cellulose

According to the calibration curve, c (y-intercept) = 0, m (slope) = 211949.9386 and substituting these values into the equation for a straight line to obtain the experimental value of insulin content (x) is done as follows:

$\frac{(1344.6632 - 0)}{211949.9386} = 0.0063$Table 4.19 shows the parameters for the assay for insulin in beads containing microcrystalline cellulose

Table 4.19: Parameters for the assay for insulin in beads containing insulin and microcrystalline cellulose

Peak Area	mg/ml
1344.66321	0.0063

From the above table, it is clear there is 0.63 mg insulin in 1 g beads, or 0.00063 g insulin in 1 g beads (or 0.063 g insulin in 100 g beads = 0.063 % w/w). The percentage content can then be calculated as follows:

% Content = $\frac{0.063}{0.06} \times 100 = 105\%$

The percentage insulin content in the bead formulation containing insulin and microcrystalline cellulose was 105% of the amount of insulin added to the formulation, which was 0.06 % w/w.

4.6 Dissolution test

Figure 4.31 presents the percentage dissolution for each of the optimised bead formulations were plotted as a function of time.

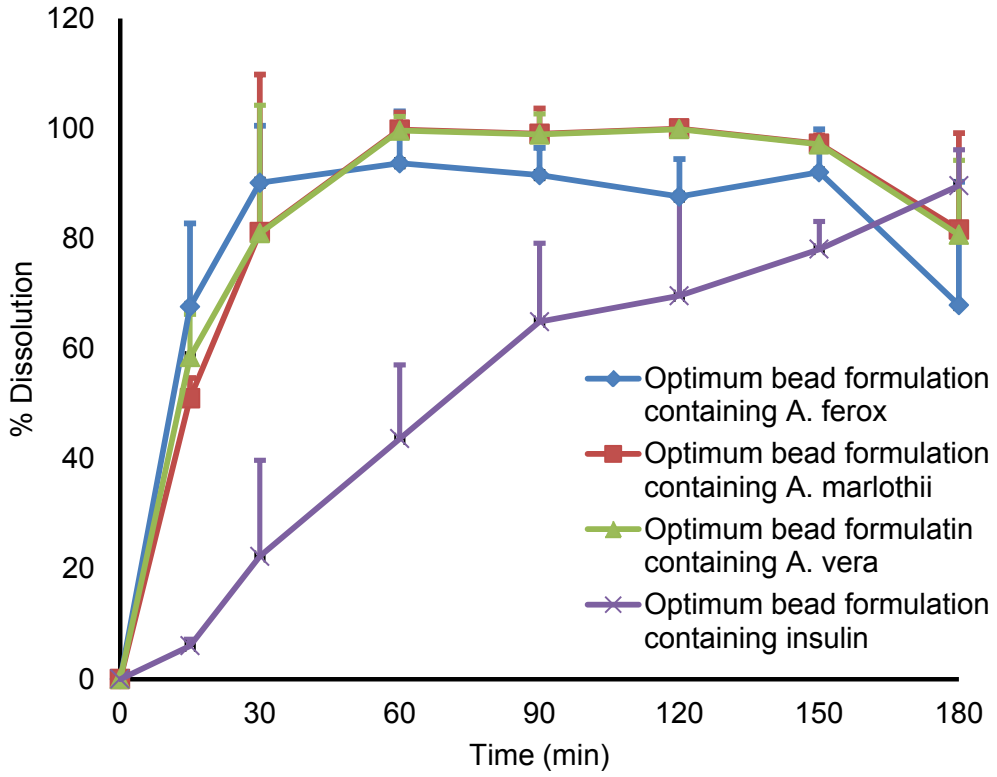

Figure 4.31: Percentage dissolution of the optimised bead formulations plotted as a function of time

All the optimised bead formulations containing aloe gel materials showed immediate release of insulin, with relatively a high percentage of insulin being released after 15 min of dissolution. A plateau in insulin release was already reached after 30 min for the beads containing *A. ferox*, whereas the bead formulations containing *A. vera* and *A. marlothii* reached a plateau in insulin release after 60 min.

The bead formulation containing insulin and MCC exhibited a slower release of insulin than the beads containing the aloe gel materials. This slower release of the active ingredient from the MCC beads may be explained by the relatively dense beads and lack of pores as illustrated by the SEM (refer to sections 4.3.2.1 and 4.3.2.8), as well as the slow disintegration of MCC beads prepared by extrusion spheronisation (Sousa *et al*., 2001:98-105). The faster release of insulin from the beads containing the aloe materials can be explained by the presence of pores in the beads (refer to sections 4.3.2.5 and 4.3.2.8) with

subsequent quick infiltration of water into the beads and diffusion of the dissolved drug out of the beads.

4.6.1 Summary

The optimum bead formulations containing aloe gel material showed immediate insulin release from the formulations, the formulation that consisted of only MCC and insulin released insulin slower due to slower disintegration.

4.7 Transepithelial electrical resistance studies

The percentage TEER reduction values of Caco-2 cell monolayers treated with the bead formulations containing each aloe material (as determined by the DoE) were plotted as a function of time and illustrated graphically (Figure 4.32, 4.35, 4.38). In the negative control group, the Caco-2 cell monolayers were exposed to exactly the same conditions, but without bead formulations over the 2 h period (i.e. the cell monolayers were exposed to DMEM only). In the positive control group, the Caco-2 cell monolayers were exposed to bead formulations containing 0.2% w/w SLS.

Results of the statistical analysis of the TEER reduction effects of the bead formulations containing the different aloe materials compared to the negative control group are also graphically presented (Figure 4.33, 4.34, 4.36, 4.37, 4.39, 4.40).

The Tukey-Kramer HSD test was included during statistical analysis to overcome the possible shortcoming of the student t-test rejecting a correct zero-hypothesis when analysing multiple formulations.

4.7.1 TEER reduction by bead formulations containing *Aloe ferox* gel

The TEER reduction values of the cell monolayers treated with the bead formulations containing *A. ferox* plotted as a function of time are presented in Figure 4.32. This figure clearly illustrates all the formulations containing *A. ferox* gel materials, as composed by the DoE, reduced the TEER immediately and effectively compared to the negative control group (i.e. DMEM). The TEER of the Caco-2 cell monolayers exposed to DMEM remained close to 100% for the duration of the experiment, which confirms the integrity of the cell monolayers over the entire experimental period. The *A. ferox* gel material formulated into beads therefore showed the ability to open tight junctions between the Caco-2 cells to different extents.

Formulations containing Ac-di-sol® together with aloe gel materials reduced the TEER values in a concentration dependant manner; this might have been due to increased disintegration because of the Ac-di-sol®. A larger amount of aloe gel is released from the formulation, which significantly reduces TEER compared to the control group. This can be seen in Figure 4.32, where the formulation containing *A. ferox* gel 5% and Ac-di-sol® 3% decreased TEER more, compared to the formulations containing *A. ferox* 5% and *A. ferox* gel 10% with Ac-di-sol® 1.5%.

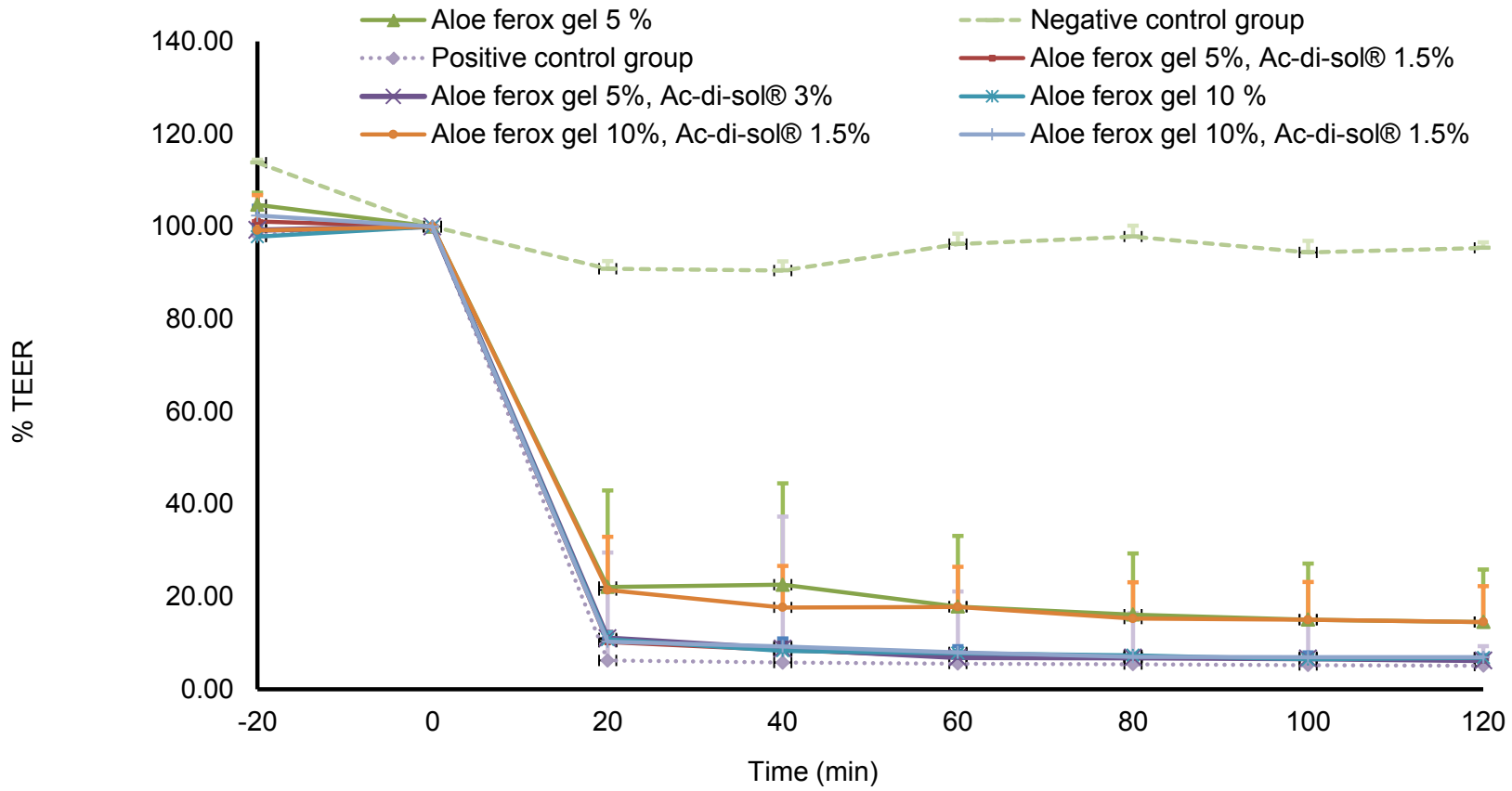

Figure 4.32: Percentage TEER reduction of Caco-2 cell monolayers treated with bead formulations containing *Aloe ferox* gel

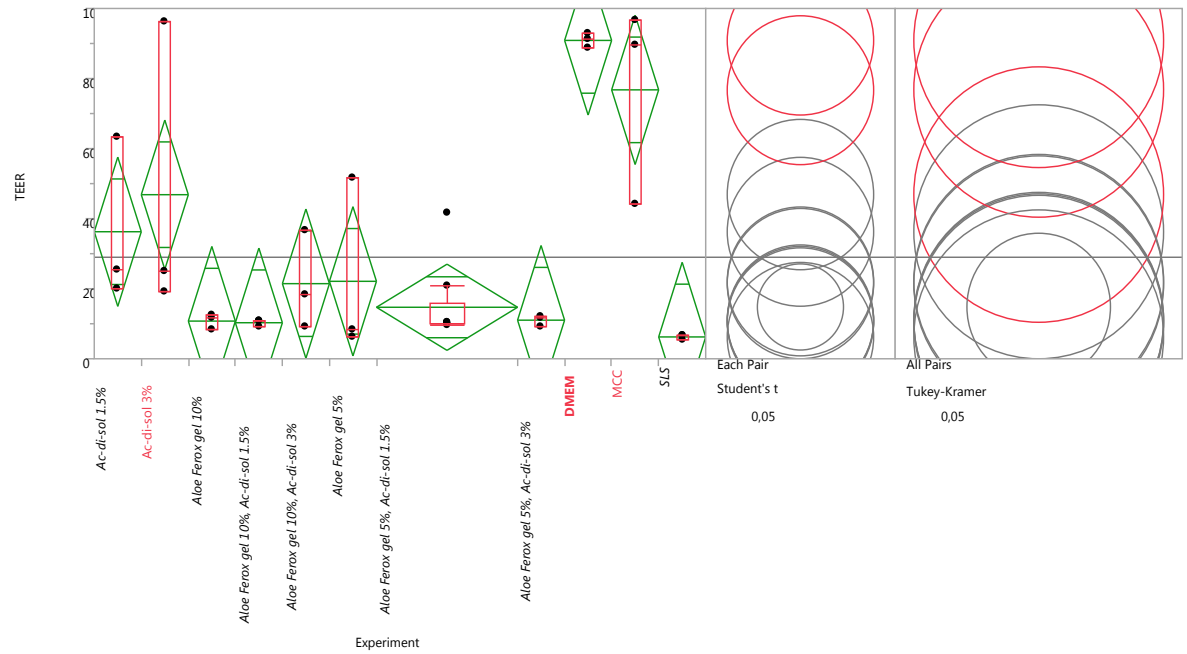

Figure 4.33: Box plot depicting the TEER reduction effects of the bead formulations containing *A. ferox* gel when compared to the negative control group by means of a one-way analysis of variance (ANOVA)

Figure 4.33 illustrates all the formulations containing *A. ferox* reduced the TEER statistically significantly compared to the negative control group ($p < 0.05$). This indicated that the effect of *A. ferox* gel materials formulated into beads on the TEER of Caco-2 cell monolayers was significant and it is therefore expected that these dosage forms will be able to increase macromolecular drug delivery across intestinal epithelial surfaces via the paracellular pathway.

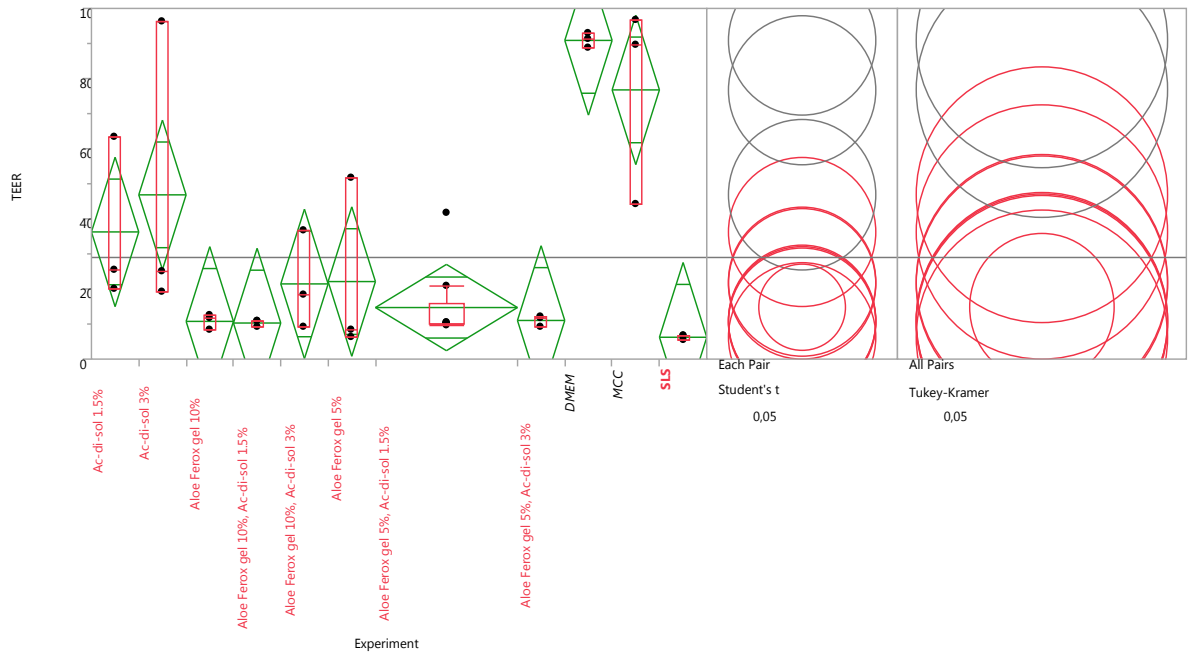

Figure 4.34: Box plot depicting the TEER reduction effects of the bead formulations containing *A. ferox* gel when compared to the positive control group (0.2% w/w SLS) by means of a one-way analysis of variance (ANOVA)

In Figure 4.34, none of the bead formulations containing *A. ferox* gel material differed statistically significantly($p < 0.05$) from the positive control group (i.e. 0.2% w/w SLS) in terms of TEER reduction, which indicated their ability to open the tight junctions to a similar extent as the positive control group.

4.7.2 TEER reduction by bead formulations containing *Aloe marlothii* gel

Figure 4.35 presents the TEER reduction values of the cell monolayers treated with the bead formulations containing *A. marlothii* plotted as a function of time. This clearly illustrates all the formulations containing *A. marlothii* gel materials, as composed by the DoE, reduced the TEER immediately and effectively compared to the negative control group (i.e. DMEM). The TEER of the Caco-2 cell monolayers exposed to DMEM remained close to 100% for the duration of the experiment, which confirmed the integrity of the cell monolayers over the entire period of the experiment. The *A. marlothii* gel material formulated into beads therefore showed the ability to open the tight junctions between the Caco-2 cells to different extents. Ac-di-sol® played a role in the disintegration of the beads and the release on aloe gel material from the formulation, thereby effecting reduction in TEER.

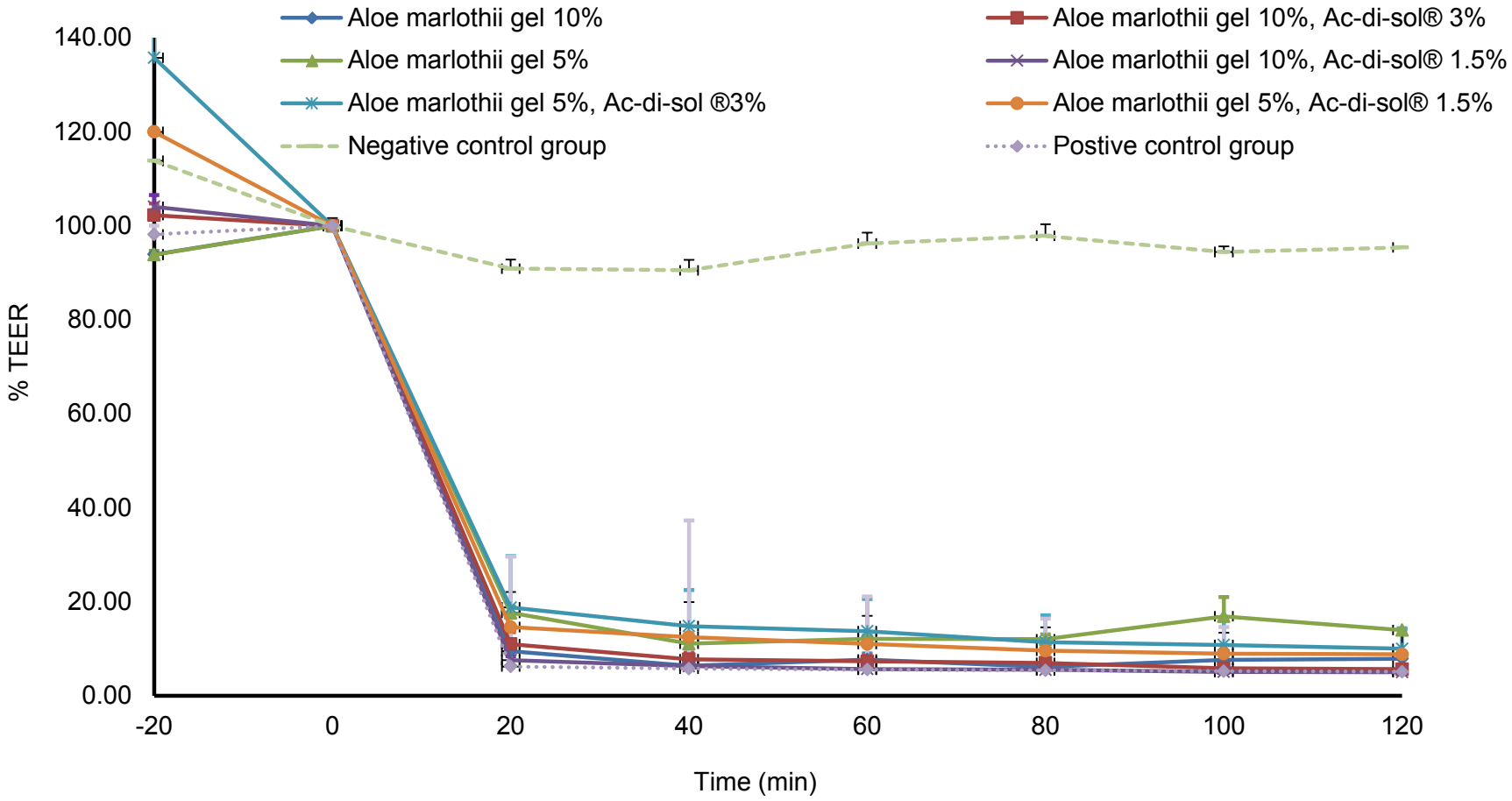

Figure 4.35: Percentage TEER reduction of Caco-2 cell monolayers treated with bead formulations containing *Aloe marlothii* gel

All the formulations containing *A. marlothii* reduced the TEER statistically significantly compared to the negative control group ($p < 0.05$) (Figure 4.36). This indicated the effect of *A. marlothii* gel materials formulated into beads on the TEER of Caco-2 cell monolayers was significant and it is therefore expected that these dosage forms will be able to increase macromolecular drug delivery across intestinal epithelial surfaces via the paracellular pathway.

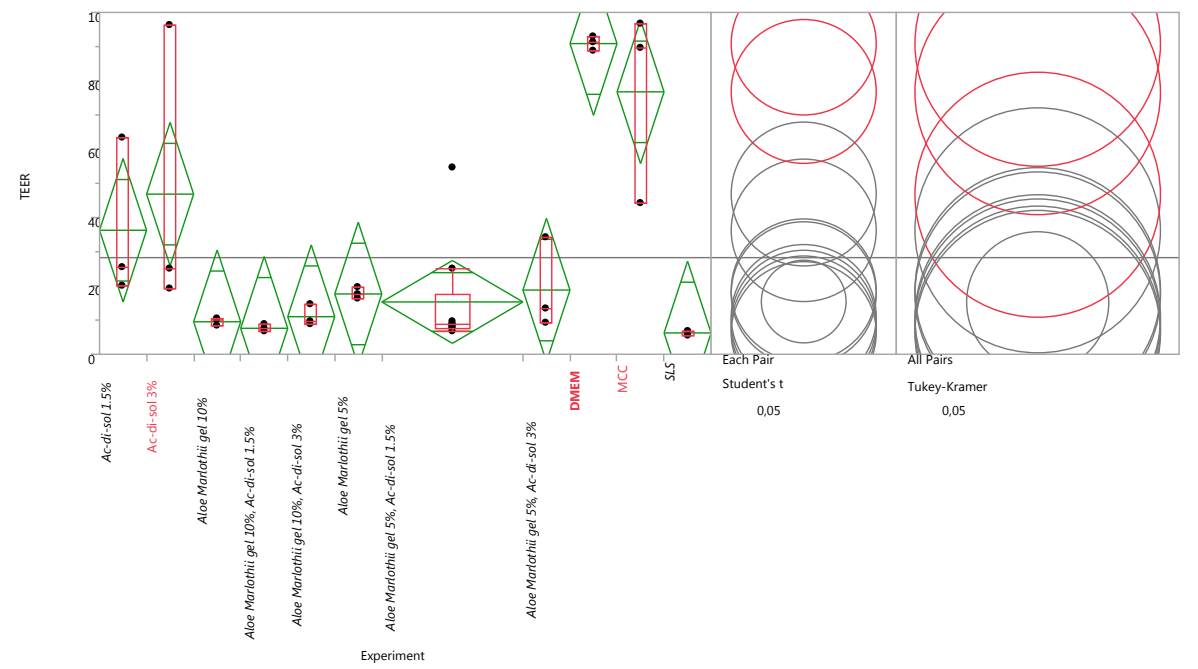

Figure 4.36: Box plot depicting the TEER reduction effects of the bead formulations containing *A. marlothii* gel when compared to the negative control group by means of a one-way analysis of variance (ANOVA)

Figure 4.37 illustrates none of the bead formulations containing *A. marlothii* gel material differed statistically significantly from the positive control group (i.e. 0.2% w/w SLS) in terms of TEER reduction, which indicated their ability to open the tight junctions similar to the positive control group.

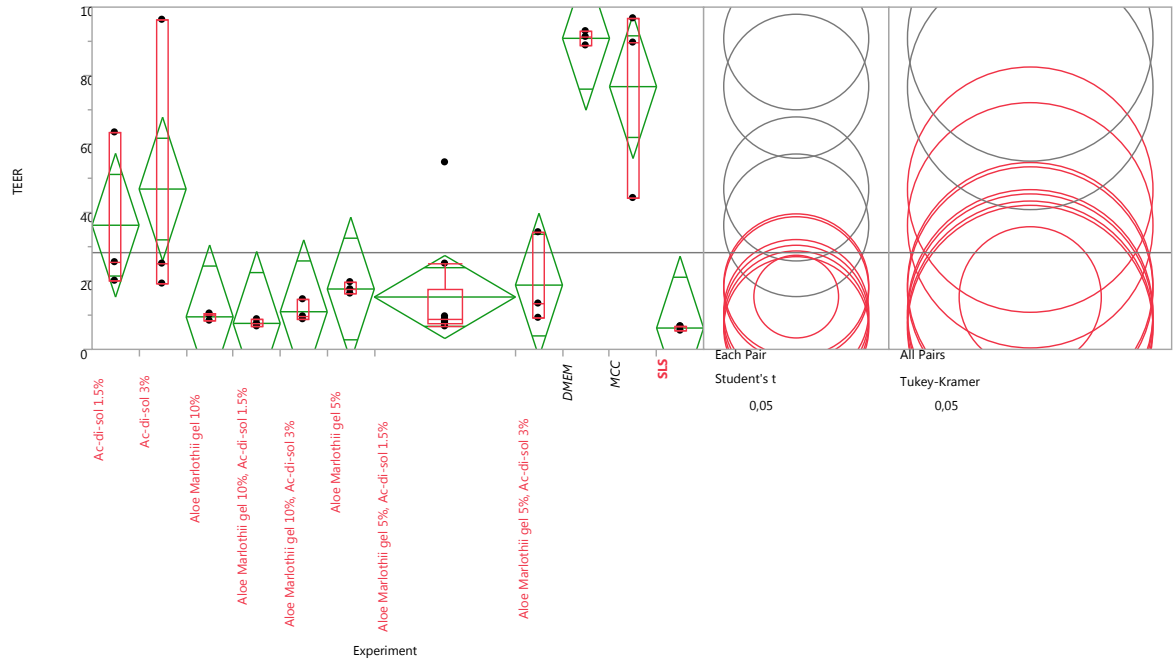

Figure 4.37: Box plot depicting the TEER reduction effects of the bead formulations containing *A. marlothii* gel when compared to the positive control group (0.2% w/w SLS) by means of a one-way analysis of variance (ANOVA)

4.7.3 TEER reduction by bead formulations containing *Aloe vera* gel

Figure 4.38 presents the TEER reduction values of the cell monolayers treated with the bead formulations containing *A. vera* plotted as a function of time. This figure clearly illustrates that all the formulations containing *A. vera* gel materials, as composed by the DoE, reduced the TEER immediately and effectively compared to the negative control group (i.e. DMEM). The TEER of the Caco-2 cell monolayers exposed to DMEM remained close to 100% for the duration of the experiment, which confirmed the integrity of the cell monolayers over the entire period of the experiment. The *A. vera* gel material formulated into beads, therefore showed the ability to open the tight junctions between the Caco-2 cells to different extents.

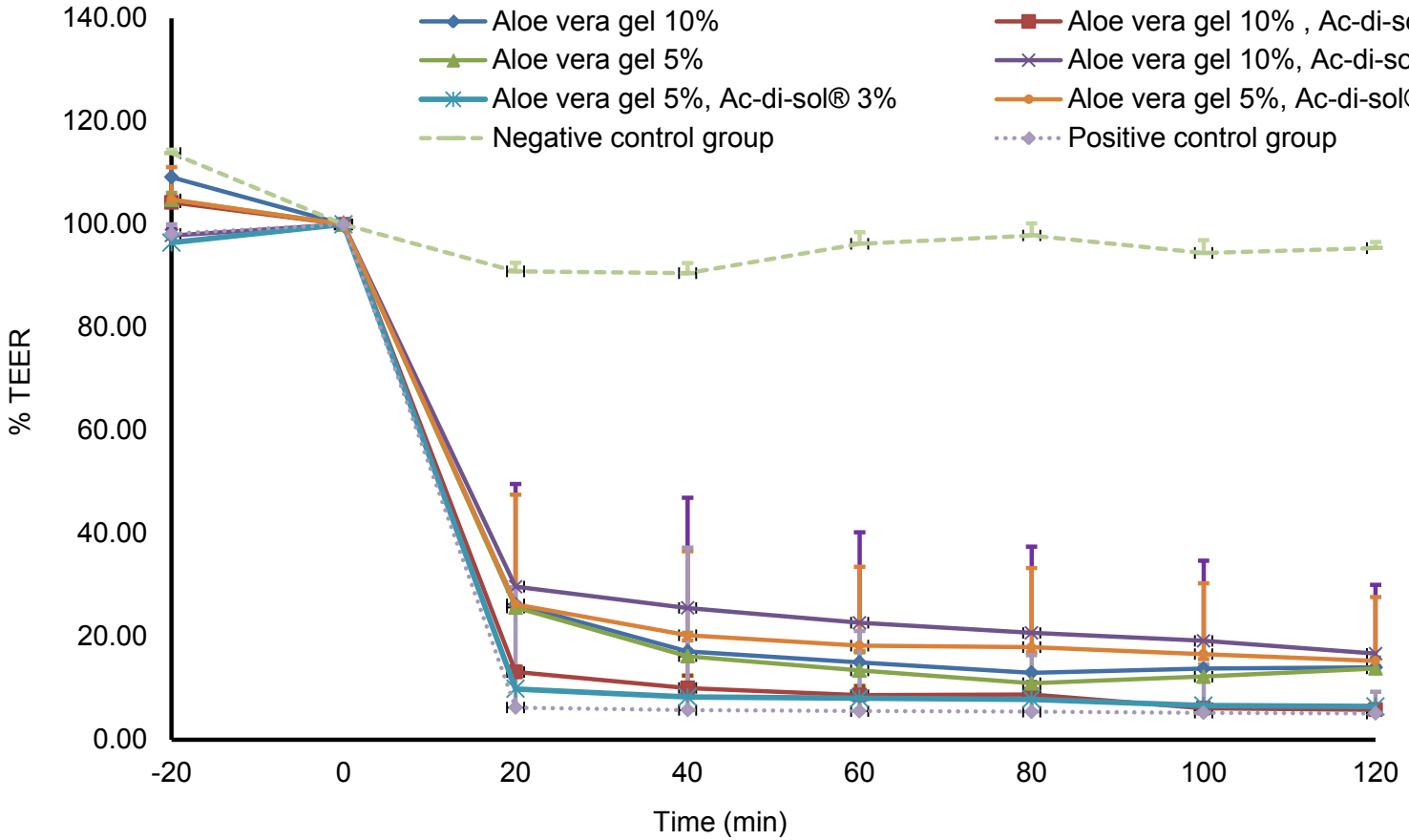

Figure 4.38: Percentage TEER reduction of Caco-2 cell monolayers treated with bead formulations containing *Aloe vera* gel

In Figure 4.39, all the formulations containing *A. vera* reduced the TEER statistically significantly compared to the negative control group ($p < 0.05$). This indicated that the effect of *A. vera* gel materials formulated into beads on the TEER of Caco-2 cell monolayers is significant and it is therefore expected that these dosage forms will be able to increase macromolecular drug delivery across intestinal epithelial surfaces via the paracellular pathway.

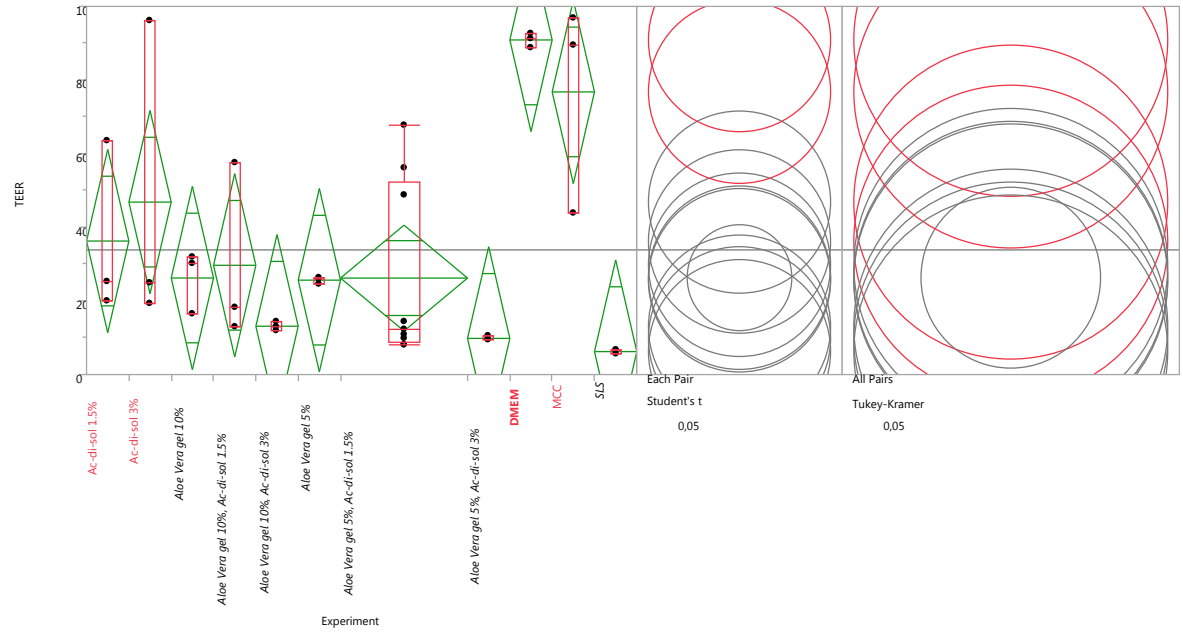

Figure 4.39: Box plot depicting the TEER reduction effects of the bead formulations containing *A. vera* gel when compared to the negative control group by means of a one-way analysis of variance (ANOVA)

Figure 4.40 illustrates that none of the bead formulations containing *A. vera* gel material differed statistically significantly ($p < 0.05$)from the positive control group (i.e. 0.2% w/w SLS) in terms of TEER reduction, which showed their ability to open the tight junctions in a similar manner to the positive control group.

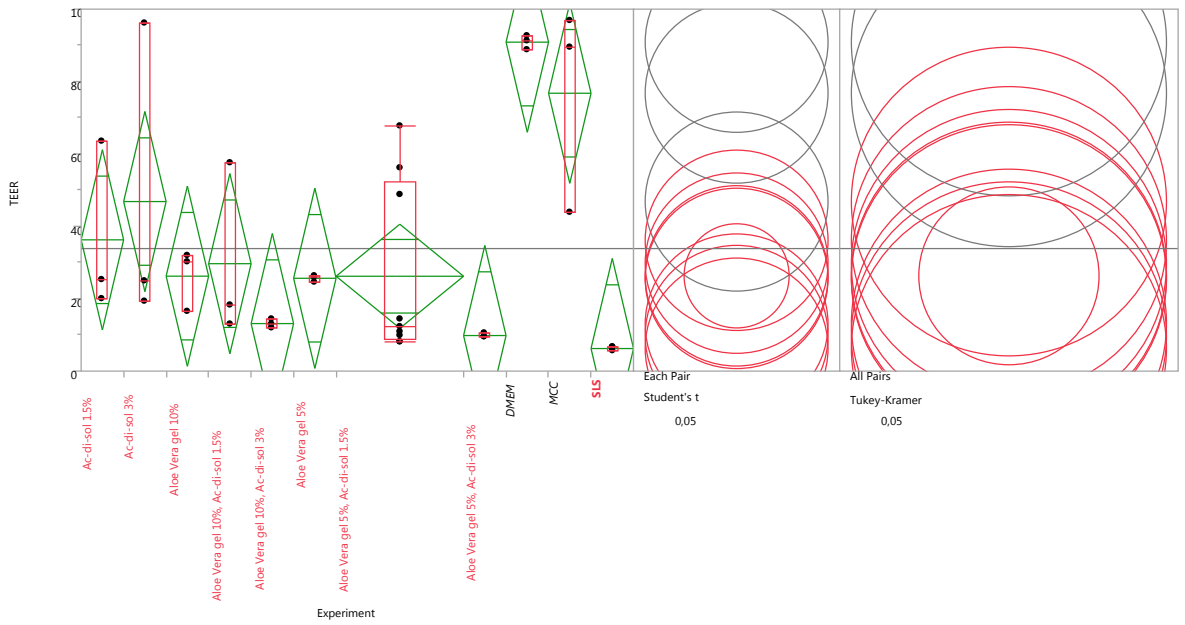

Figure 4.40: Box plot depicting the TEER reduction effects of the bead formulations containing *A. vera* gel when compared to the positive control group (0.2% w/w SLS) by means of a one-way analysis of variance (ANOVA)

4.7.4 Summary

Statistical analysis of TEER studies showed that bead formulations containing the aloe gel materials depicted significant different ($p < 0.05$) reduction in the percentage TEER reduction compared to the control group (i.e. DMEM without absorption enhancer). None of the bead formulations containing aloe gel material differed statistically significantly ($p < 0.05$) from the positive control group (i.e. 0.2% w/w SLS) in terms of TEER reduction, which showed their ability to open the tight junctions in a similar manner to the positive control group.

The addition of Ac-di-sol® in the formulations containing aloe gel material led to enhanced disintegration of the beads and release of the gel material in order to reduce the TEER values and increase tight junction opening.

4.8 Insulin transport studies

Figure 4.41 illustrates the cumulative percentage insulin transported across the excised pig intestinal tissue after application of the optimised bead formulations as a function of time.

The apparent permeability coefficient (P_{app}) values for each optimised bead formulation across excised pig intestinal tissue are shown in Figure 4.42 and Figure 4.43 illustrates a box plot depicting the transport of the bead formulations containing aloe gel material when compared to the formulation containing insulin and microcrystalline cellulose by means of a one-way analysis of variance (ANOVA).

From Figure 4.41, it is clear that the optimised bead formulations containing *A. vera* and *A. marlothii* gel improved insulin transport across the excised pig intestinal tissue compared to the control group (bead formulation consisting of insulin and MCC without any drug absorption enhancer). The optimised bead formulation containing *A. ferox* gel unexpectedly showed a lower transport of insulin than the control group, which does not correlate with the TEER reduction results (Figure 4.33). However, the lack of drug absorption enhancement by *A. ferox* gel materials has been shown previously for certain drugs, such as atenolol (Lebitsa *et al.,* 2012:303). In general, the transport results are in line with previous studies which suggested that the absorption enhancing effects of the aloe gel materials occur by opening of tight junctions and thereby producing increased paracellular transport (Beneke *et al*., 2012:475).

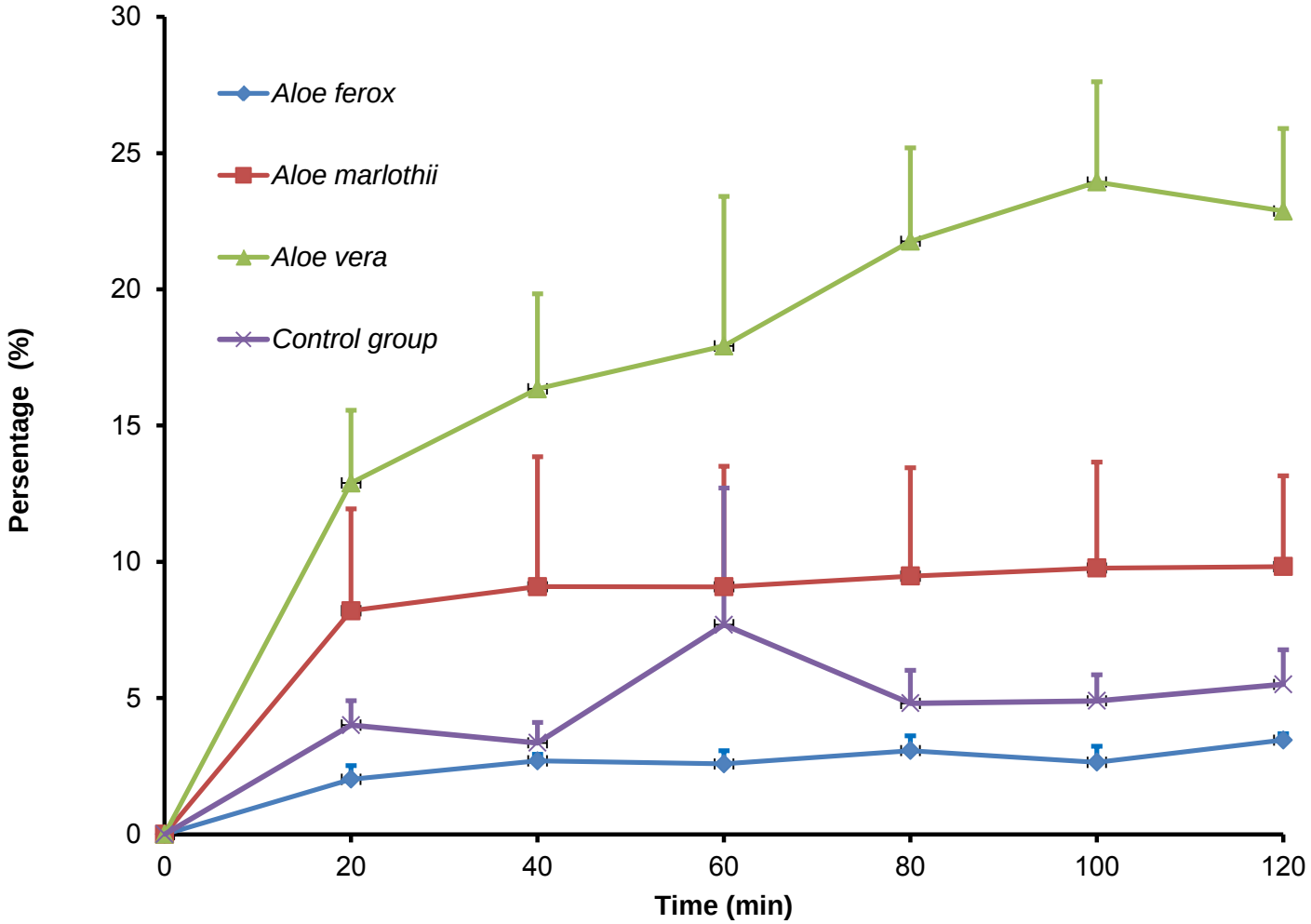

Figure 4.41: Cumulative percentage insulin transport of the optimum bead formulations plotted as a function of time

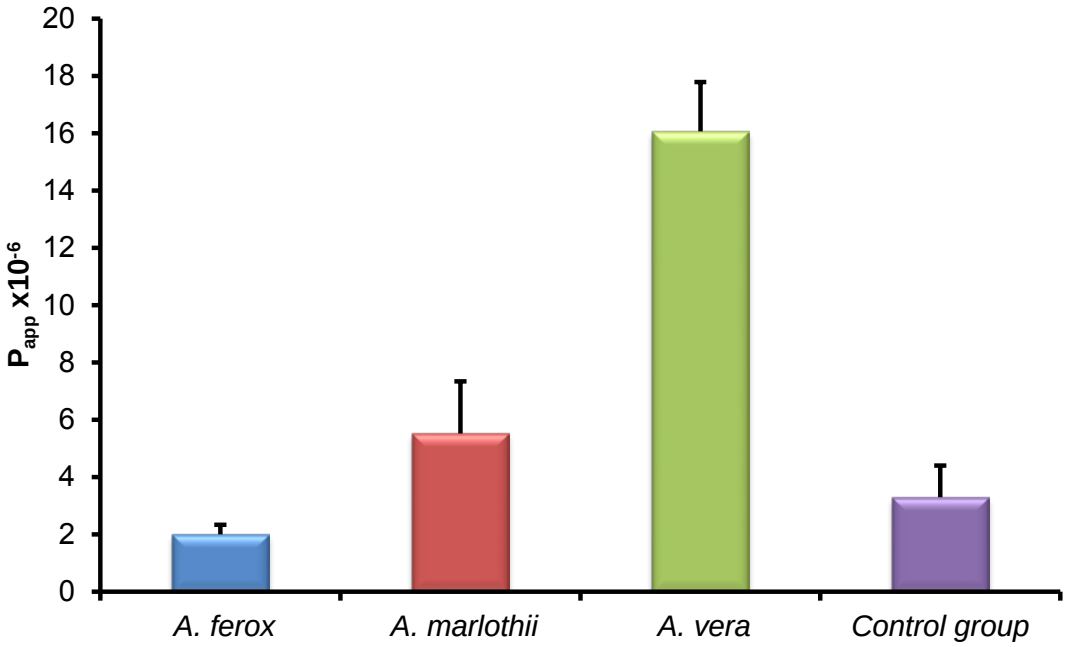

Figure 4.42: Mean P_{app} values for insulin transport of each optimum bead formulation across excised pig tissue

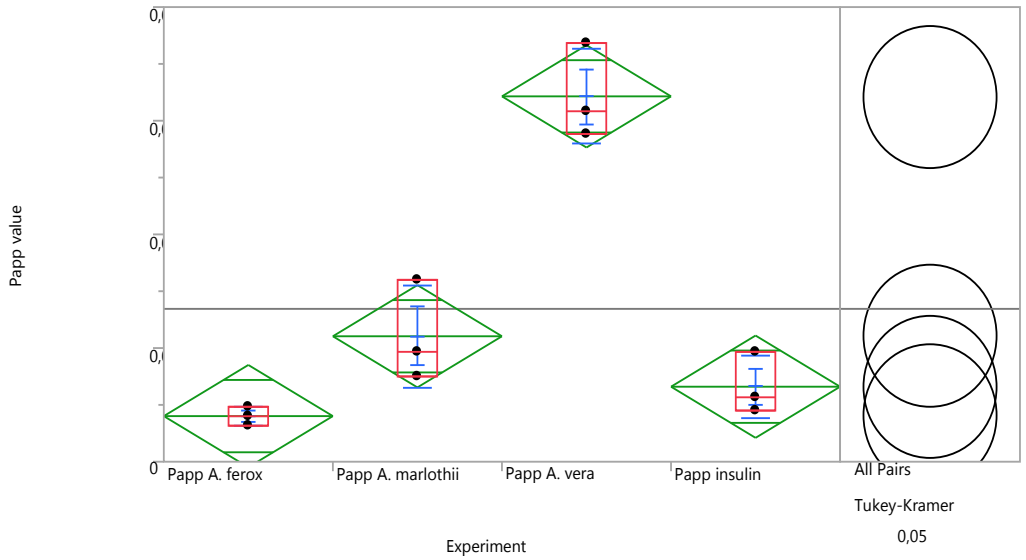

Figure 4.43: Box plot depicting the transport of the bead formulations containing aloe gel material when compared to the formulation containing insulin and microcrystalline cellulose by means of a one-way analysis of variance (ANOVA)

Figure 4.42 illustrates the optimised bead formulation containing *A. vera* gel had the highest P_{app} value, indicating the highest amount of insulin transport occurred across the excised pig intestinal tissue when this formulation was administrated. This correlates with the statistical analysis results (Figure 4.43) which depicts the permeability coefficient of *A. vera* differed statistically significant ($p < 0.05$) from the permeability coefficient of *A. ferox* ($p < 0.0001$), the control group insulin ($p < 0.0001$) as well as the permeability coefficient of *A. marlothii* ($p = 0.003$).

4.8.1 Summary

According to the permeability coefficient values *A. marlothii* and *A. vera* showed to improve transport across excised pig tissue, however only *A vera* showed to improve transport statistically significantly compared to the other aloe gel materials and the control group. *A. ferox* did not improve transport of insulin across the intestinal tissue; the lack of absorption enhancement properties of *A ferox* has been reported in previous literature (Lebitsa *et al.,* 2012:303).

CHAPTER 5: FINAL CONCLUSIONS AND FUTURE RECOMMENDATIONS

5.1 FINAL CONCLUSIONS

Investigation of the *in vitro* drug permeation enhancing effect of *Aloe ferox*, *Aloe marlothii* and *Aloe vera* leaf gel materials formulated into spherical beads across excised pig intestinal tissue, was successfully conducted.

A. ferox, A. marlothii and *A. vera* gel materials were chemically fingerprinted by means of proton nuclear magnetic resonance (^{1}H-NMR) spectroscopy. The following marker molecules were identified in *A. ferox* and *A. marlothii* gel materials: glucose, lactic acid, malic acid, formic acid, benzoic acid, lactic acid, citric acid and acetic acid. *A. vera* contained the following marker molecules: aloverose, glucose, malic acid, formic acid and lactic acid.

Optimisation of bead formulations containing *A. ferox, A. marlothii* and *A. vera* gel materials, was done by means of a 2^3 full factorial design utilising MODDE 9.0™ DoE software. A regression analysis indicated the prediction models for *A. ferox* and *A. marlothii* containing beads were good models, but the model for the *A. vera* beads had some shortcomings.

The bead formulations complied with USP mass variation and friability standards. Low friability indicated that the beads depicted acceptable physical strength. The minimal mass variation might have been due to the relatively narrow particle size distribution of beads, with uniform flow and filling of hard gelatine capsules.

SEM photomicrographs showed the optimised bead formulations were all relatively spherical with different surface morphologies. The porosity of some the bead formulations suggested immediate release of the insulin, which was confirmed by the dissolution data.

Validation of the HPLC analytical method for insulin complied with specificity and linearity. The LOQ of insulin was 0.3 µg/ml and the LOD, 0.05 µg/ml. The method yielded a mean recovery of 98.7%; an acceptable value for accuracy with 0.7% precision, with no significant difference of inter- and intra-day samples. The insulin only degraded by 2% over a 24 h time period.

Dissolution profiles obtained from the optimised bead formulations showed that insulin can be formulated into immediate release bead formulations when aloe gel materials and Ac-di-sol® are included in these formulations. As expected, slower insulin release was obtained from the bead formulation consisting of microcrystaline cellulose only.

Statistical analysis of TEER studies showed that bead formulations containing the aloe gel materials depicted significant different ($p < 0.05$) reduction in the percentage TEER reduction compared to the control group (i.e. DMEM without absorption enhancer).

Transport studies across excised pig intestinal tissue showed that optimised bead formulations containing *A. vera* and *A. marlothii* had higher percentage transport than the beads containing insulin only, which may be due to the permeation enhancing properties of the aloe materials. *A. vera* showed to statistically significantly ($p < 0.05$) improved the transport of insulin across the excised pig intestinal tissue. The optimum bead formulation containing *A. ferox* did not increase transport of insulin across the intestinal tissue compared to beads containing insulin only, which was unexpected because the formulations containing *A. ferox* did decrease the TEER and showed immediate release of insulin during dissolution.

5.2 FUTURE RECOMMENDATIONS

It is recommended that other formulations should be investigated using *A. vera* gel as a functional excipient in order to produce a better prediction model with the MODDE 9.0™ DoE software.

Enteric coating of the bead formulations containing aloe gel material with a mucoadhesive biopolymer and other functional excipients to produce improved bead formulations could also be further investigated. If sufficient mucoadhesion can be achieved with enteric coated beads, it may increase the retention time in the gastrointestinal tract, such as the jejunum, thereby increasing the contact time with the mucosal surface with even higher delivery potential.

Lastly, it is recommended the optimised bead formulations from this study be tested in transport studies using other *in vitro* models, such as the everted sac technique and ultimately, in animal models to evaluate the ability to deliver drugs *in vivo*.

REFERENCES

Amoo, S.O., Aremu, A.O. & Van Staden, J. 2014. Unraveling the medicinal potential of South African *Aloe* species. *Journal of Ethnopharmacology*,*153*(1):19-41.

Anon. Aloe ferox. 2014. http://www.kimpexenterprises.com/why_aloe_ferox.htm. Date of access: 18 November 2014.

Anon. 2014. The aloe vera site. http://thealoeverasite.com/aloe-vera-pictures.php. Date of access: 18 November 2014

Ashford, M. 2007. Gastrointestinal tract - physiology and drug absorption. (In: AULTON, M.E, ed. *Aulton's Pharmaceutics: The Design and Manufacturing of Medicines, 3rd ed. Churchill Livingstone*: Elsevier. p.270-285.)

Balimane, P.V., Han, Y.H. & Chong, S. 2006 . Current industrial practices of assessing permeability and P-glycoprotein interaction. *The AAPS Journal*, *8*(1):E1-E13.

Balimane, P.V. & Chong, S. 2005. Cell culture-based models for intestinal permeability: a critique. *Drug Discovery Today*, 10(5):335-343.

Beg, S., Swain, S., Rizwan, M., Irfanuddin, M. & Malini, S. 2011. Bioavailibility anhancement strategies: basics, formulation approaches and regulatory considerations. *Current Drug Delivery*, 8(6):691-702.

Beneke, C., Viljoen, A. & Hamman, J.H. 2012. *In vitro* drug absorption enhancement effects of *Aloe vera* and *Aloe ferox*. *Scientia Pharmaceutica*, 80(2):475-486.

Borchard, G., Luegen, H.L., Boer, A.G., de Verhoef, J.C., Lehr, C. & Junginger, H.E. 1996. The potential of mucoadhesive polymers in enhancing intestinal peptide drug absorption. III: Effects of chitosan-glutamate and carbomer on epithelial tight junctions *in vitro*. *Journal of Controlled Release*, 39(2):131-138.

British Pharmacopoeia. 2013. London: TSO. http://www.pharmacopoeia.co.uk.nwulib.nwu.ac.za/login.htm Date of access: 11 November 2014

Chalasani, K.B., Russell-Jones, G.J., Jain, A.K., Diwan, P.V. & Jain, S.K. 2007. Effective oral delivery of insulin in animal models using vitamin B12-coated dextran nanoparticles. *Journal of Controlled Release*, 122(2):141-150.

Chen, W., Lu, Z., Viljoen, A. & Hamman, H. 2009. Intestinal drug transport enhancement by *Aloe vera*. *Planta Medica*, 75(06):587-595.

Cheng, J.W., Frishman, W.H. & Aronow, W.S. 2009. Updates on cytochrome P450-mediated cardiovascular drug interactions. *American Journal of Therapeutics*, 16(2):155-163.

Chin, J., Mahmud, K.A.F., Kim, S.E., Park, K. & Byun, Y. 2012. Insight of current technologies for oral delivery of proteins and peptides. *Drug Discovery Today: Technologies*, 9(2):e105-e112

Choi, S. & Chung, M. H. 2003. A review on the relationship between Aloe vera components and their biologic effects. *Seminars in Integrative Medicine*, 1(1):53-62.

Choonara, B.F., Choonara, Y.E., Kumar, P., Bijukumar, D., du Toit, L.C. & Pillay, V. 2014. A review of advanced oral drug delivery technologies facilitating the protection and absorption of protein and peptide molecules. *Biotechnology Advances*, 32(7):1269-1282.

Clement, S., Dandona, P., Still, J.G. & Kosutic, G. 2004. Oral modified insulin (HIM2) in patients with type 1 diabetes mellitus: results from a phase I/II clinical trial. *Metabolism*, 53(1):54-58

Crowley, P.J. & Martini, L.G. 2004. Formulation design: New drugs from old. *Drug Discovery Today*: *Therapeutic Strategies,* 1(4):537-542.

Deferme, S., Annaert, O. & Augustijns, P. 2008. *In vitro* screening models to access intestinal drug absorption and metabolism. *Biotechnology: Pharmaceutical Aspects*, 7(2):182-215.

Deli, M.A. 2009. Potential use of tight junction modulators to reversibly open membranous barriers and improve drug delivery. *Biochimica et Biophysica Acta (BBA)-Biomembranes*, 1788(4):892-910.

Du Plessis, L.H. & Hamman, J.H. 2014. *In vitro* evaluation of the cytotoxic and apoptogenic properties of aloe whole leaf and gel materials. *Drug and Chemical Toxicology*, 37(2)*:*169-177.

Eriksson, L., Johansson, E., Kettanek-Wold, N., Wikström, C. & Wold, S. 2008. *Design of Experiments: Principles and Application, 3rd ed*. Sweden: Umetrics Academy.

Fasanoa, A. & Natarob, J.P. 2004. Intestinal epithelial tight junctions as targets for enteric bacteria-derived toxins. *Advanced Drug Delivery Reviews*, 56(6):795-807.

Fox, L.T., Gerber, M., Preez, J. L.D., Plessis, J.D. & Hamman, J.H. 2014. Skin permeation enhancement effects of the gel and whole-leaf materials of *Aloe vera, Aloe marlothii* and *Aloe ferox*. *Journal of Pharmacy and Pharmacology*,67:96-106.

Garrett, R.H. & Grisham, C.M. 2008. Principles of Biochemistry with a Human Focus, 2nd ed. Fort Worth: Harcourt College Publishers. pp.87.

Gandhi, R., Kaul, C.L. & Panchagnula, R. 1999. Extrusion and spheronisation in the development of oral controlled release dosage forms. *Pharmaceutical Science and Technology Today*, 2(4):160-170.

González-Mariscal, L., Nava, P. & Hernández, S. 2005. Critical role of tight junctions in delivery across epithelial and endothelial cell layers. *Journal of Membrane Biology*, 207(2):55-68.

Grace, O.M., Simmonds, M.S.J., Smith, G.F. & Van Wyk, A.E. 2008. Therapeutic uses of *Aloe L.(Asphodelaceae)* in Southern Africa. *Journal of Ethnopharmacology*, 119(3): 604-614.

Grass, G.M. & Sweetana, S.A. 1988. *In vitro* measurement of gastrointestinal tissue permeability using a new diffusion cell. *Pharmaceutical Research*, 5(6):372.

Hackett. M.J., Zaro, J.L., Shen, W., Guley, P.C. & Cho, M.J. 2013. Fatty acids as therapeutic auxiliaries for oral and parenteral formulations. *Advanced Drug Delivery Reviews*, 65(10):1331-1339.

Hamman, J.H. 2007. *Oral Drug Delivery: Biopharmaceutical Principles, Evaluation and Optimisation.* Content Solutions.

Hamman, J.H, Enslin, G.M. & Kotzé, A.F. 2005. Oral delivery of peptide drugs: Barriers and developments. *Biodrugs*, 19(3):165-177.

Hamman, J. & Steenekamp, J. 2012. Excipients with specialized functions for effective drug delivery. *Expert Opinion Delivery*, 9(2):219-230.

Hamman, J.H. & Steenekamp, J.H. 2011. Oral peptide delivery: Strategies to overcome challenges. (In: CASTANHO, M. & SANTOS, N.C., eds. Peptide Drug Discovery and

Development: Translational Research in Academia and Industry., Weinheim: Wiley-VCH Verlag & Co. p.71-84.)

Ishida, M., Abe, K., Hashizume, M. & Kawamura, M. 2008. A novel approach to sustained pseudoephedrine release: Differentially coated mini-tablets in HPMC capsules. *International Journal of Pharmaceutics*, 359(1):46-52.

Kotzé, A.F., de Leeuw, B.J., Lueßen, H.L., de Boer, A.G., Verhoef, J.C. & Junginger, H.E. 1997. Chitosans for enhanced delivery of therapeutic peptides across intestinal epithelia: in vitro evaluation in Caco-2 cell monolayers. *International Journal of Pharmaceutics*, 159(2):243-253.

Lebitsa, T., Viljoen, A., Lu, Z. & Hamman, J. 2012. *In vitro* drug permeation enhancement potential of aloe gel materials. *Current Drug Delivery*, 9(3):297-304.

Le Ferrec, E., Chesne, C., Artusson, P., Brayden, D., Fabre, G., Gires, P. & Scarino, M. L. 2001. *In vitro* models of the intestinal barrier. *Alternative to Laboratory Animals*, 29:649-668.

Legen, I., Salobir, M. & Kerč, J. 2005. Comparison of different intestinal epithelia as models for absorption enhancement studies. *International Journal of Pharmaceutics*, 291(1):183-188.

Lemmer, H.J.R. & J.H. Hamman. 2013. Paracellular drug absorption enhancement through tight junction modulation. *Expert Opinion Drug Delivery*, 10(1):103-114.

Leuβen, H.L., de Leeuw, B.J., Pérard, D., Lehr, C-M., de Boer, A.B.G., Verhoef J.C. & Junginger H.E. 1996. Mucoadhesive polymers in peroral peptide drug delivery. I. Influence of mucoadhesive excipients on the proteolytic activity of intestinal enzymes. *European Journal of Pharmaceutical Sciences*, 4(2):117-128

Liu, P, Davis, P., Liu, T. & Krishna, T.R. 1999. Evaluation of cytotoxicity and absorption enhancing effects of melittin. *European Journal of Pharmaceutics and Biopharmaceutics*, 48(1):85-87.

Lim, H-P., Tey, B-T. & Chan, E-S. 2014. Particle design for the stabilization and controlled-delivery of protein drugs by biopolymers: A case study on insulin. *Journal of Controlled Release*, 186:11-21.

Majumdar, S., Duvvuri, S. & Mitra A.K. 2004. Membrane transporter/reseptor-targeted prodrug design: Strategies for human and veterinary drug development. *Advance Drug Delivery Reviews*, 56(10):1437-1452.

Mallipeddi, R., Saripella, K. K. & Neau, S. H. 2010. Use of coarse ethylcellulose and PEO in beads produced by extrusion–spheronization. *International Journal of Pharmaceutics*, 385(1):53-65.

O'Brien, C., Van Wyk, B.E. & Van Heerden, F.R. 2011 Physical and chemical characteristics of *Aloe ferox* leaf gel. *South African Journal of Botany*, 77(4):988-995.

Ojewole, E., Mackraj, I., Akhundov, K., Hamman, J., Viljoen, A., Olivier, E. & Govender, T. 2012. Investigating the effect of *Aloe vera* gel on the buccal permeability of didanosine. *Planta Medica*, 78(04):354-361.

Park, J.W., Kim, S.K., Al-Hilal, T.A., Jeon, O.C., Moon, H.T & Byun, Y. 2010. Strategies for oral delivery of macromolecule drugs. *Biotechnology and Bioprocess Engineering*, 15(1):66-75.

Pauletti, G.M., Gangwar, S., Knipp, G.T., Nerurkar, M.M., Okumu, F.W., Tamura, K., Siahaan, T.J. & Borchardt, R.T. 1996. Structural requirements for intestinal absorption of peptide drugs. *Journal of Controlled Release*, 41(1):3-17.

Pfister, D. & Morbidelli, M. 2014. Process for protein PEGylation. *Journal of Controlled Release*, 180:134-149.

Raiman, J., Törmälehto, S., Yritys, K., Junginger, H.E. & Mönkkönena J. 2003. Effects of various absorption enhancers on transport of clodronate through Caco-2 cells. *International Journal of Pharmaceutics,* 261(1):129-136.

Rajasekaran, S.A., Beyenbach, K.W. & Rajasekaran, A.K. 2008. Interactions of tight junctions with membrane channels and transporters. *Biochimica et Biophysica Acta (BBA)-Biomembranes*, 1778(3):758.

Rekha, M.R., Sharma, C.P. 2013. Oral delivery of therapeutic protein/peptide for diabetes–future perspectives. *International Journal of Pharmaceutics*, 440(1): 48-62.

Renukuntla, J., Vadlapundi, A.D., Patel, A., Boddu, S.H.S. & Mitra, A.K. 2013. Approaches for enhancing oral bioavailability of peptides and proteins. *International Journal of Pharmaceutics*, 447(1):75-93

Reynolds, T. & Dweck, A.C. 1999. *Aloe vera* leaf gel: A review update. *Journal of Ethnopharmacology*, 68(1):3-37.

Rodriguez, E.R., Martin, J.D. & Romero, C.D. 2010. *Aloe vera* as a functional ingredient in foods. *Critical Reviews in Food Science and Nutrition*, *50*(4):305-326.

Rosenthal, R., Heydt, M.S., Amasheh, M., Stein, C., Fromm, M. & Amasheh, S. 2012. Analysis of absorption enhancers in epithelial cell models. *Annals of the New York Academy of Sciences*, 1258(1):86-92.

Sarmento, B., Martins, S., Ferreira, D. & Souto, E.B. 2007. Oral insulin delivery by means of solid lipid nanoparticles. *International Journal of Nanomedicines*, 2(4):743-749.

Semenya, S., Potgieter, M. & Erasmus, L. 2012. Ethnobotanical survey of medicinal plants used by Bapedi healers to treat Diabetes Mellitus in the Limpopo Province, South Africa. *Journal of Ethnopharmacology*, 141(1):440-445.

Shargel, L., Wu-Pong, S. & Yu, A.B.C. 2012. Targeted drug delivery systems and biotechnological products. (In: *SHARGEL, L., WU-PONG, S., & YU, A.B.C. Applied Biopharmaceutics and Pharmacokinetics, 6th ed.* New York: McGraw- Hill. p.514-515.)

Shen, W-C. 2003. Oral peptide and protein delivery: Unfulfilled promises? *Drug Discovery Today*, 8(14):607-608

Sousa, J.J., Sousa, A., Podczeck, F. & Newton, J.M. 2002. Factors influencing the physical characteristics of pellets obtained by extrusion-spheronization. *International Journal of Pharmaceutics*, 232(1):91-106.

Su, M., He, C., West, C.A. & Mentzer, S.J. 2001. Cytolytic peptides induce biphasic permeability changes in mammalian cell membranes. *Journal of Immunological Methods*, 252(1):63-71.

Summers, M.P. & Aulton, M.E. 2007. Granulation. (In: *AULTONS, M.E, ed. Aulton's Pharmaceutics: The design and manufacturing of medicines, 3rd ed*. Churchill Livingstone: Elsevier. pp.419.)

UNITED STATES PHARMACOPOEIAL CONVENTION. 2014.
USP37: NF32. http://www.uspnf.com/uspnf/login Date of access: 11 November 2014

Van Itallie, C.M. & Anderson, J.M. 2014. Architecture of tight junctions and principles of molecular composition. *Seminars in Cell & Developmental Biology* 36:157-165

Van Wyk, B. E. 2008. A broad review of commercially important southern African medicinal plants. *Journal of Ethnopharmacology*, 119(3), 342-355.

Van Wyk, B.E., De Wet, H. & Van Heerden, F.R. 2008. An ethnobotanical survey of medicinal plants in the southeastern Karoo, South Africa. *South African Journal of Botany*, 74(4), 696-704.

Vervaet, C., Baert, L. & Remon, J.P. 1995. Extrusion-spheronisation. A literature review. *International Journal of Pharmaceutics*, 116(2):131-146.

Vinson, J.A., Al Kharrat, H. & Andreoli, L. 2005. Effect of *Aloe vera* preparations on the human bioavailability of vitamins C and E. *Phytomedicine*, 12(10):760-765.

Wallis, L., Kleynhans, E., Du Toit, T., Gouws, C., Steyn, D., Steenekamp, J. & Hamman, J. 2014. Novel non-invasive protein and peptide drug delivery approaches. *Protein and Peptide Letters*, 21(11):1087-1101.

Werle, M. & Bernkop-Schnürch, A. 2006. Strategies to improve plasma half-life time of peptide and protein drugs. *Amino Acids*, 30(4):351-367.

Westerhout, J., Van der Steeg, E., Grossouw, D., Zeidner, E.E., Krul, C.A.M., Verwei, M. & Wortelboer, HM. 2014. A new approach to predict human intestinal absorption using porcine intestinal tissue and biorelevant matrices. *European Journal of Pharmaceutical Sciences*, 63:167-177.

Yin, L., Ding, J., He, C., Cui, L., Tang, C., & Yin, C. 2009. Drug permeability and mucoadhesion properties of thiolated trimethyl chitosan nanoparticles in oral insulin delivery. *Biomaterials*, 30(29):5691-5700.

York, P. 2007. Design of dosage forms. (In: *AULTON, M.E., ed. Aulton's Pharmaceutics: The Design and Manufacturing of Medicines, 3rd ed*. Churchill Livingstone Elsevier. p.7-8.)

ANNEXURE A: ARTICLE AND CONFERENCE PROCEEDINGS

A1: Kleynhans, E., Hamman, J.H., Viljoen, J.M. & Tiedt, L. Multiple-unit solid oral dosage forms for effective peptide drug delivery. 17th World Congress of Basic and Clinical Pharmacology (WCP2014). Cape Town, South Africa. 2014 (Poster presentation)

A2: Kleynhans, E., Hamman, J.H., Viljoen, J.M. Aloe gel materials as absorption enhancers in multiple-unit solid oral dosage forms for effective peptide drug delivery. 35th annual conference of the Academy of Pharmaceutical Sciences. Nelson Mandela Metropolitan University, Port-Elizabeth, South Africa. 2014. (Presentation)

A3: Wallis, L., Kleynhans, E., Du Toit, T., Gouws, C., Steyn, D., Steenekamp, J. Viljoen, J.& Hamman, J. Novel non-invasive protein and peptide drug delivery approaches. *Protein and Peptide Letters*, 2014, Vol. 21, No. 11 (Article)

30 July 2014

CERTIFICATE OF PRESENTATION

This is to certify that

Miss. Elmarie Kleynhans
North-West University

Presented the following Abstract Poster titled
Multiple-unit solid oral dosage forms for effective peptide drug delivery

On Monday 2014/07/14 12h00 - 13h30

At the 17th World Congress of Basic and Clinical Pharmacology (WCP2014) held at the Cape Town International Convention Centre (CTICC) in Cape Town, South Africa from 13-18 July 2014

Prof Douglas W Oliver
President: WCP2014
Tel: +27 (0)11 463 5085
carina@soafrica.com
www.wcp2014.org

No.1039
MULTIPLE-UNIT SOLID ORAL DOSAGE FORMS FOR EFFECTIVE PEPTIDE DRUG DELIVERY

E. Kleynhans, J.H. Hamman, J.M. Viljoen, L. Tiedt
Centre of Excellence for Pharmaceutical Sciences, North-West University,
Private Bag X6001, Potchefstroom, 2520, South Africa
20682115@nwu.ac.za

NORTH-WEST UNIVERSITY
YUNIBESITI YA BOKONE-BOPHIRIMA
NOORDWES-UNIVERSITEIT
POTCHEFSTROOM CAMPUS

INTRODUCTION

The oral route of drug administration is the most popular way of administering medicines, because it is simple, convenient, has a high patient acceptability and compliance and has the benefit of providing a large surface area for systemic drug absorption. It further avoids discomfort, pain and infections that frequently occur by administration of injectable dosage forms (Hamman, 2006:58).

Oral administration has some disadvantages such as a relative slow onset of action, while protein and peptide drugs undergo enzymatic degradation, are chemically instable with poor absorption (Rekha *et al.*, 2013:49).

Formulating a solid oral dosage form for protein and peptide drugs requires addressing challenge; such as overcoming physiological and biochemical barriers to achieve acceptable plasma concentrations. Formulation strategies include the use of enzyme inhibitors, developing bioadhesive systems, site-specific delivery and inclusion of absorption enhancers (Rekha *et al.*, 2013:53).

Absorption enhancers are compounds used in pharmaceutical preparations to increase drug absorption across the intestinal epithelium and thereby improving bioavailability. When *Aloe vera* juice was co-administered with certain vitamins to humans, the bioavailability of the vitamins were increased (Vinson *et al.*, 2005:760). Aloe leaf materials also showed *in vitro* drug absorption enhancement properties with the potential to improve oral protein and peptide drug delivery (Chen *et al.*, 2009:587; Beneke *et al.*, 2012:475).

However, the formulation of these aloe leaf materials in multiple-unit solid oral dosage forms for oral delivery of oral peptide drugs have not been investigated yet.

METHODS AND MATERIALS

Plant collection, processing and chemical fingerprinting

Aloe ferox leaves were sourced from Organic Aloe (Pty) Ltd, South Africa. *Aloe marlothii* leaves were obtained from natural growing populations in the North West Province of South Africa. The Aloe *ferox* and Aloe *marlothii* leaves were processed and freeze dried to obtain a fine dry gel product which was used in the preparation of the beads. *Aloe vera* gel (Daltonmax 700) was donated by Improve Inc. (Texas, USA). All the plant materials were chemically fingerprinted by ^{1}H-NMR to identify the presence of aloe marker molecules.

Design of experiments

A 2^3 full factorial design of experiments was used to optimise bead formulations (MODDE 9.0™ software by Umetrics, Sweden). The reduction in transepithelial electrical resistance (TEER) of Caco-2 cell monolayers was used as the response and contour plots were then constructed to predict the optimum bead formulation for drug permeation enhancement.

Bead manufacture and characterisation

Beads were prepared by extrusion spheronisation (Caleva Process Solutions, England). The beads were characterised in terms of mass variation, friability, particle size and dissolution profiles. Bead surface morphology was determined by scanning electron microscopy (SEM).

Transepithelial electrical resistance (TEER) studies

Caco-2 cells were seeded out onto tissue culture treated polycarbonate filters (area = 0.33 cm^2) in Costar Transwell 24-well plates (Corning Costar Corporation, USA). The transepithelial electrical resistance (TEER) of the Caco-2 cell monolayers was measured in the absence (control group) and presence of *A. ferox*, *A. marlothii* and *A. vera* gel materials formulated into beads (experimental groups).

RESULTS

The compositions of the bead formulations for *A. vera (as determined by the design of experiments)* and their effects on TEER of Caco-2 cell monolayers are shown in Table 1.

Table 1: Composition of beads containing *Aloe vera* gel as determined by MODDE 9.0™

Type of aloe material	Aloe content (% w/w)	Ac-di-sol (% w/w)	Avicel® (% w/w)	Reduction in TEER
Aloe vera gel	10	0	90	23.2 ± 6.66
Aloe vera gel	10	3	87	13.13 ± 1.11
Aloe vera gel	5	0	95	25.64 ± 0.6
Aloe vera gel	10	1.5	88.5	29.68 ± 19.92
Aloe vera gel	10	1.5	88.5	9.83 ± 0.51
Aloe vera gel	5	1.5	93.5	11.35 ±21.25
Aloe vera gel	5	1.5	93.5	7.93 ± 24.94
Aloe vera gel	5	1.5	93.5	10.92 ± 1.04
Aloe vera gel	0	0	100	76.8 ± 23.35
Aloe vera gel	0	3	97	46.8 ± 1.57
Aloe vera gel	0	1.5	98.5	36.3 ± 19.83

The contour plots for the optimised bead formulations are shown in Figure 1, while figure 2 indicates SEM micrographs of the optimum bead formulations.

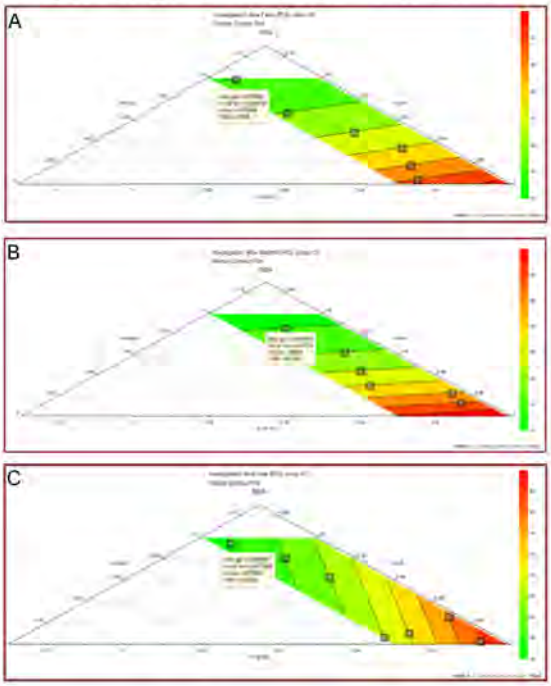

Figure 1: Contour plots to determine the optimum bead formulations for A) *Aloe ferox*, B) *Aloe marlothii* and C) *Aloe vera*

Figure 2: SEM micrographs of the optimised beads: A) *Aloe ferox*, B) *Aloe marlothii*, C) *Aloe vera*, D) Insulin alone, E) Insulin and sodium laurel sulphate

CONCLUSION

Multiple-unit solid oral dosage forms containing drug absorption enhancing agents were optimised in terms of reduction in TEER. The optimised formulations showed high potential to open tight junctions and therefore also to deliver insulin effectively across human intestinal epithelial cells.

ACKNOWLEDGEMENTS

The financial support of the National Research Foundation (NRF) of South Africa to conduct this research is acknowledged. Any opinion, findings and conclusions or recommendations expressed in materials are those to the authors and therefore the NRF do not accept any liability in regard thereto. The financial support of the WCP2014 organising committee to attend this conference is acknowledged.

CONFLICT OF INTEREST

The authors declare no conflict of interest.

REFERENCES

BENEKE, C., VILJOEN, A., HAMMAN, J.H. *In Vitro* Drug Absorption Enhancement Effects of *Aloe vera* and *Aloe ferox*. *Scientia Pharmaceutica*. 2012:475.

CHEN, W., LU, Z., VILJOEN, A. & HAMMAN, H. 2009. Intestinal Drug Transport Enhancement by Aloe vera. *Planta Medica*, 75:587-595.

HAMMAN, J.H. 2006. Oral drug delivery: Biopharmaceutical principles, evaluation and optimisation. Content Solutions.

REKHA, M.R.; SHARMA, C.P. Oral delivery of therapeutic protein/peptide for diabetes – Future perspectives. *International Journal of Pharmaceutics*, 2013:48-62.

VINSON, J.A., AL KHARRAT, H., ANDREOLI. Effect of Aloe vera preparations on the human bioavailability of vitamins C and E. *Phytomedicine*, 2005:760.

35TH CONFERENCE OF THE ACADEMY OF PHARMACEUTICAL SCIENCES

INTEGRATING EDUCATION, RESEARCH & PRACTICE

CERTIFICATE OF ATTENDANCE

This is to certify that

Miss Elmarie Kleynhans

has attended the 35th Conference of the Academy of Pharmaceutical Sciences held from 12 – 14 September at the Summerstrand Hotel in Port Elizabeth

Proudly hosted by the Department of Pharmacy at the Nelson Mandela Metropolitan University

_____

Prof Gareth Kilian

Conference Convenor

Nelson Mandela Metropolitan University

for tomorrow

ALOE GEL MATERIALS AS ABSORPTION ENHANCERS IN MULTIPLE-UNIT SOLID ORAL DOSAGE FORMS FOR EFFECTIVE PEPTIDE DRUG DELIVERY

Elmarie Kleynhans, Josias Hamman, Joe Viljoen

Centre of Excellence for Pharmaceutical Sciences, North-West University,
Private Bag X6001, Potchefstroom, 2520, South Africa

Purpose: The most popular and convenient route of drug administration remains the oral route; however, protein and peptide drugs such as insulin have poor membrane permeability and stability in the gastrointestinal tract. Absorption enhancers can be added to the drug delivery system to overcome the epithelial cell membrane permeability problem. Although previous studies have shown that aloe leaf materials improve the transport of drugs across intestinal epithelia, their performance in solid oral dosage forms has not been investigated yet.

Methods: Beads containing insulin and each of the absorption enhancers were produced by extrusion-spheronisation using a full factorial design to optimise the formulations based on transepithelial electrical resistance reduction of Caco-2 cell monolayers as response. The optimum bead formulations were evaluated in terms of friability, mass variation, particle surface texture, shape, size and dissolution. The transport of insulin across Caco-2 cell monolayers from the optimised bead formulations were determined over a 2 h period and compared to that of the aloe gel materials in solution. The samples obtained from the transport studies were analysed for insulin content by means of high-performance liquid chromatography (HPLC).

Results: The results showed that the TEER reduction, as an indication of tight junction modulation, obtained for the bead formulations containing aloe materials was concentration dependent. Furthermore, inclusion of croscarmellose sodium (Ac-di-sol®) as disintegrant showed an enhanced TEER reduction effect in combination with the aloe gel materials. Dissolution profiles were seen to release the insulin within the first hour from the beads. In accordance with the TEER reduction results, the aloe material containing beads showed similar insulin delivery across Caco-2 cell monolayers compared to the solutions, which were pronouncedly higher than that of the control group (insulin alone).

Conclusion: The optimised aloe gel material containing bead formulations showed high potential to deliver insulin effectively across human intestinal epithelial cells.

Send Orders for Reprints to reprints@benthamscience.net

Protein & Peptide Letters, 2014, *21*, 1087-1101

Novel Non-Invasive Protein and Peptide Drug Delivery Approaches

L. Wallis, E. Kleynhans, T. Du Toit, C. Gouws, D. Steyn, J. Steenekamp, J. Viljoen, J. Hamman*

Centre of Excellence for Pharmaceutical Sciences, Private Bag X6001, Potchefstroom, 2520, South Africa

Abstract: Protein and peptide based therapeutics are typically administered by injection due to their poor uptake when administered via enteral routes of drug administration. Unfortunately, chronic administration of these drugs through multiple injections presents certain patient related problems and it is difficult to mimic the normal physiological release patterns via this mode of drug administration. A need therefore exists to non-invasively deliver these drugs by means of alternative ways such as via the oral, pulmonary, nasal, transdermal and buccal administration routes. Although some attempts of needle free peptide and protein drug delivery have progressed to the clinical stage, relatively limited success has been achieved in terms of commercially available products. Despite the low frequency of clinical breakthroughs with non-invasive protein drug delivery this far, it remains an active research area with renewed interest not only due to its improved therapeutic potential, but also due to the attractive commercial outcomes it offers. It is the aim of this review article to reflect on the main strategies investigated to overcome the barriers against effective systemic protein drug delivery in different routes of drug administration. Approaches based on chemical modifications and pharmaceutical technologies are discussed with reference to examples of drugs and devices that have shown potential, while attempts that have failed are also briefly outlined.

Keywords: Absorption enhancers, enzymatic and physical barriers, needle-free, non-invasive, peptide, protein.

1. INTRODUCTION

Advances in biotechnology have led to an increased number of therapeutic proteins and peptides that have become commercially available on a large scale at an affordable price and the number of these therapeutics is expected to accelerate further in the future [1]. A relatively quick rise in the development of biotechnology based therapeutics due to advanced technologies (e.g., recombinant DNA technology) has unfortunately not been matched by the same rate in the development of effective delivery systems for these types of drugs. The challenges associated with effective systemic delivery of these types of drugs can be related to their unfavourable physicochemical properties [2]. Protein-based drugs usually fall within class III of the Biopharmaceutics Classification System (BCS) and the main reasons for their low oral bioavailability include susceptibility to enzymatic degradation, hydrophilic properties, large molecular size and in some cases low solubility [3,4]. Despite the enormous challenges associated with the effective delivery of biotechnology based drugs via non-invasive routes of drug administration, investigations with respect to this concept remain active due to its large clinical and commercial potential and the ever-increasing role that these drugs can play in the effective treatment of diseases [5,6].

Although there is room for parenteral delivery of protein drugs, a need exists for less invasive delivery of therapeutic proteins that are administered chronically (e.g., more than 60 000 insulin injections need to be administered during a patient's lifetime to effectively control blood glucose levels) [2,6]. Other shortcomings associated with peptide drug delivery by injection besides the pain, discomfort and potential for infections include a lack of replication of the physiological release pattern. Examples of this problem include insulin with its basal and post-prandial release patterns that are difficult to mimic with a series of injections and growth hormone with several secretion events spaced unevenly throughout the day [7,8]. Furthermore, fear of needles and resistance to self-injection are considered to be some of the main reasons for limiting insulin therapy and reduced compliance in diabetic patients [9]. The clinical advantages of non-invasive protein and peptide drug delivery include enhanced patient compliance and potentially improved efficacy by certain routes of drug administration due to a better resemblance of the physiological secretion patterns [10]. Therefore, non-invasive protein and peptide drug delivery is still a relevant area of investigation by formulation scientists [11].

This review aims to reflect on different strategies employed for non-invasive protein and peptide drug delivery via different routes of drug administration as demonstrated in Figure 1.

2. CHEMICAL APPROACHES

Chemical modification of peptide and protein drugs to improve bioavailability has received considerable attention. This interest is primarily due to enhanced enzymatic stability, intestinal permeability and immunogenicity [12,13]. Promising chemical modifications that have been employed to improve the unfavourable properties of peptide and protein drugs include amino acid substitution (analogue forma-

*Address correspondence to this author at the Centre of Excellence for Pharmaceutical Sciences, North-West University, Private Bag X6001, Potchefstroom, 2520, South Africa; Tel: +2718 299 4035; Fax: +2787 231 5432; E-mail: Sias.Hamman@nwu.ac.za

0929-8665/14 $58.00+.00

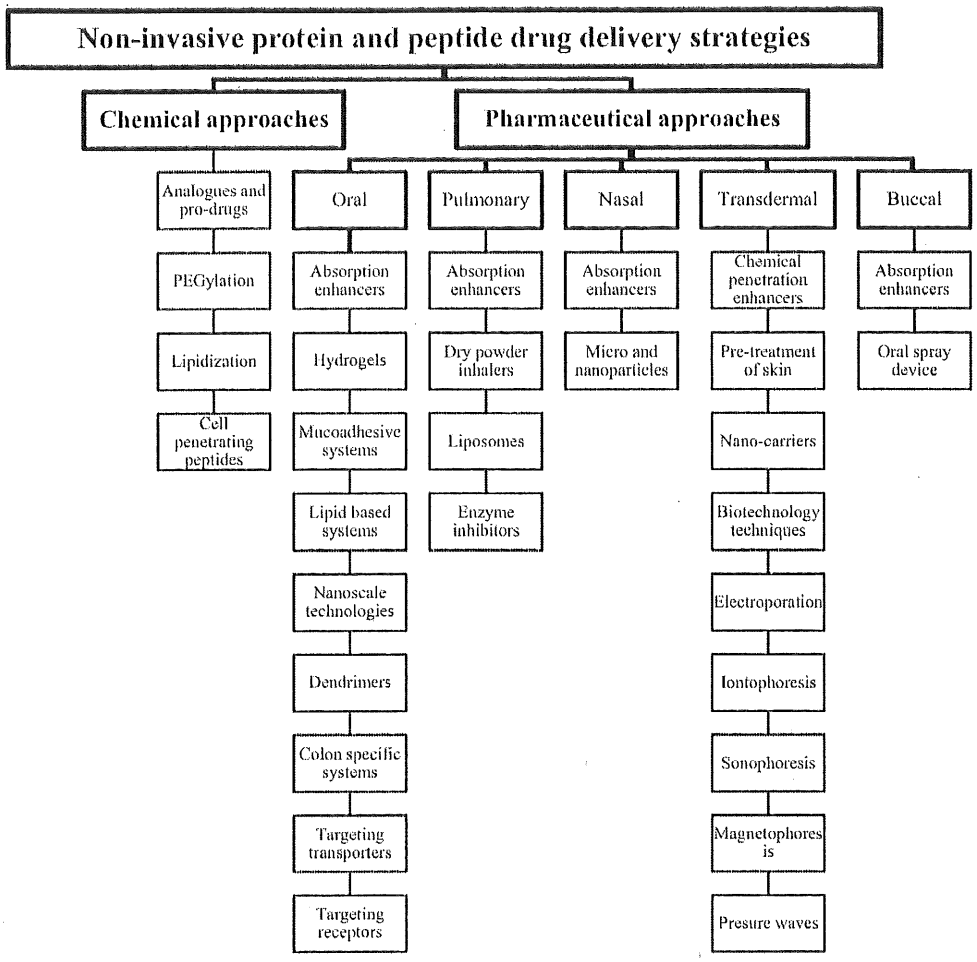

Figure 1. Summary of strategies for non-invasive protein and peptide drug delivery via different routes of drug administration.

tion), synthesis of pro-drugs, conjugation with fatty acids (lipidisation) and conjugation with polyethylene glycol (PEGylation) [12,14,15].

2.1. Analogues and Pro-Drugs

Substituting a specific amino acid in the structure of a peptide or protein with a different amino acid is known as analogue formation. Modifications based on amino acid substitution can be done by substituting an L-amino acid with a D-amino acid or by replacing a particular amino acid with a different amino acid [13]. Desmopressin acetate (DDAVP), a synthetic cyclic analogue of 8-arginine vasopressin (a 9-amino acid peptide), is an example of analogue formation which is currently the treatment of choice for diabetes insipidus and is marketed by Aventis Pharmaceuticals. In contrast to vasopressin, DDAVP is available as injection, intranasal solution and tablets for oral administration. Although the oral bioavailability of DDAVP is <1%, this produces a sufficient antidiuretic effect. Although analogue formation for non-invasive delivery of peptides has been successful for DDAVP, it seems that the application of this modification technique will be limited to small peptides [16].

2.2. PEGylation

PEGylation is a technique that has attracted considerable research attention in terms of structural modifications of peptides and proteins and is defined as the conjugation of poly(ethylene glycol) (PEG) with peptide or protein drugs [17,18]. In research done by Hinds and Kim [19], PEG was successfully conjugated with insulin via an amide bond. This conjugation did not alter insulin's secondary/tertiary structure or potency *in vivo*. However, the conjugate was almost completely devoid of immunogenicity, allergenicity and antigenicity. The conjugated insulin also remained in the systemic circulation for longer periods of time compared to unmodified insulin after subcutaneous administration. In terms of the non-invasive delivery of insulin, perhaps one of the most promising insulin formulations to date for oral administration into the gastrointestinal tract is hexal-insulin-monoconjugate-2 (HIM2). HIM2 was developed by Nobex

Corporation in partnership with GlaxoSmithKline. This conjugate has a small polyethylene glycol 7-hexyl group attached to the B29 amino acid (i.e. lysine) of recombinant human insulin. Clinical trials suggested an oral bioavailability of approximately 5%, which is thought to result in acceptable glucose lowering. HIM2 was as effective as a subcutaneous injection of 8 units of regular insulin to control postprandial glycemia with respect to parameters such as 2 h postprandial glucose concentration, maximum glucose concentration, and glucose $AUC_{0\text{-}240}$ [20,21,22]. However, Biocon acquired the technology from Nobex and conducted clinical studies. One of the longer-term studies in type 2 diabetes mellitus patients did not meet the endpoint of a reduction of HbA1c of greater than 0.7% compared to the placebo. The reduction in HbA1c in the placebo group was, however, larger than expected, thereby decreasing the difference between the two treatment groups. Unfortunately, the statistics of the trial are not freely available [8]. Currently, Biocon in co-operation with Bristol-Myers Squibb are pursuing further clinical development of this conjugated molecule [23].

2.3. Lipidisation

Another conjugation technique that has been used successfully to improve the lipophilicity and thereby the bioavailability of peptide drugs is lipidisation. This technique usually involves the conjugation of a fatty acid to a peptide or protein [21,24]. Due to difficulties associated with the conjugation of fatty acids to peptides and proteins, a modified technique to overcome the drawbacks of conventional lipidisation, was developed. This method is referred to as "reversible aqueous lipidisation" (REAL) and can be carried out in an aqueous solution, while the original peptide can be regenerated in the blood or tissues. With regard to oral peptide delivery, Wang and co-workers [25] have shown that REAL-technology improved the oral bioavailability of salmon calcitonin, however, the exact mechanism of improved absorption from the gastrointestinal tract was not clear. The authors concluded that REAL-technology can be used in future for designing polypeptide drugs for oral delivery. In another study, a non-reversible aqueous-soluble lipid conjugate of calcitonin was prepared [26]. This derivative of salmon calcitonin produced hypocalcaemic activity comparable to salmon calcitonin after subcutaneous injection, however, activity after oral administration was inconclusive due to within group variation in the rat model. With regard to calcitonin, Nobex Corporation and Elan Corporation initiated Phase I clinical trials with Oratonin™, an oral calcitonin derivative for the treatment of osteoporosis. This derivative of calcitonin encompasses the attachment of a polymer to calcitonin, however, the nature of this polymer is not revealed, only that it involves proprietary Nobex technology [27]. Currently Oratonin™ has completed Phase I clinical trials and is ready for Phase II clinical trials (Seachaid Pharmaceuticals). Publicly available information on Oratonin™ is limited.

2.4. Cell-Penetrating Peptides

Cell-penetrating peptides (CPPs) received considerable interest during the last two decades for the non-invasive delivery of peptides and proteins. CPPs can cross the cell membrane with limited toxicity and can act as vector for protein and peptide drugs. However, the exact mechanism by which CPP-drug conjugates cross the cell membrane and/or how they get internalised is still unclear [28,29,30]. It is postulated that the inter-molecular interactions between the CPP and the drug are important for enhanced absorption [13]. Improved absorption of insulin was obtained after nasal administration of insulin in the presence of penetratin, a CPP. This study also showed that penetratin did not cause any mucosal damage over the concentration range used [31]. However, a great deal of research is still needed before CPP-mediated delivery will be clinically utilised [29].

3. PHARMACEUTICAL APPROACHES

3.1. Oral Delivery

Oral drug delivery remains the most popular and patient compliant route of drug administration [31], which explains the numerous efforts of pharmaceutical scientists to overcome challenges such as low stability and poor permeability of protein and peptide drugs in the gastrointestinal tract. Although limited success has been achieved in terms of the clinical translation of protein based drugs into registered oral products [10], it is important to highlight formulation approaches that have shown potential for effective oral delivery of these drugs.

3.1.1. Polymeric Hydrogels

Hydrogels are three-dimensional water-absorbing networks consisting of cross-linked hydrophilic polymers that can be used in novel drug delivery systems [32]. Different types of hydrogel drug delivery systems have been investigated for improved protein and peptide drug delivery such as microparticles consisting of poly(methacrylic acid grafted with poly(ethylene glycol)) that protected insulin from degradation in the gastrointestinal tract with improved bioavailability[33,34].

An example of a polymeric hydrogel shuttle system which consisted of superporous hydrogel composite for site-specific controlled release of *N*-α-benzoyl-L-arginine ethylester. This system showed a promising time-controlled release profile with the potential to bring the drug in close contact with the intestinal epithelium at a specific site in the gastrointestinal tract and in addition also partly inhibited the activity of trypsin together with opening of the tight junctions. The system was designed to produce a double phase release profile to provide the enzyme inhibitors and absorption enhancers first before releasing the active ingredient as illustrated in Figure **2** [35].

3.1.2. Mucoadhesive Systems

Intestinal transit time can be prolonged by the use of mucoadhesive delivery systems that slows down the movement of a delivery system through the gastrointestinal tract by adhering to the mucosal surface. Furthermore, it improves the contact between the drug and the mucosa resulting in an increased drug concentration gradient preventing dilution or degradation of the drug in the luminal fluid to a certain extent [36].

In a previous study, a gastrointestinal mucoadhesive patch system was designed in the form of a four layered en-

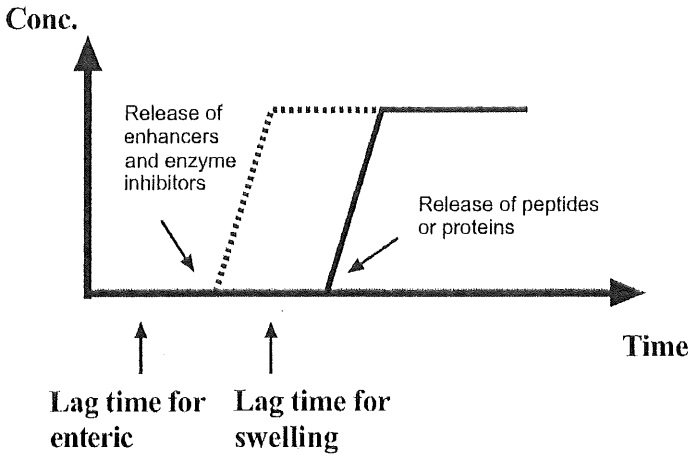

Figure 2. Graph illustrating the double phase time controlled release profile as intended to be obtained from the polymeric hydrogel shuttle system [Reprinted from 35 with permission from Elsevier].

teric coated capsule for the oral delivery of recombinant human granulocyte colony-stimulating factor. This patch system protected the drug from proteolytic enzymes and depended on environmental pH for drug release [37]. Thiolated polymers (thiomers, e.g., thiolated chitosan) contain thiol-bearing ligands that are bound to the polymer backbone and have been shown to enhance intestinal macromolecular drug absorption by means of mechanisms such as mucoadhesion and opening of tight junctions. A third generation of pre-activated thiomers have recently been introduced that enhanced the stability of the polymer, improved its mucoadhesive properties and further increased macromolecular drug delivery [38,39,40].

3.1.3. Lipid-Based Formulations

Solid lipid nanoparticles (SLNs) is an example of a lipid-based drug delivery system formulated to contain part of the drug dose in the internal core and part in the external coat of solid lipid delivery systems [41]. A significant hypoglycaemic effect was observed in diabetic rats after the oral administration of insulin loaded SLNs. It was found that glucose levels of rats were lower when given insulin-loaded SLNs due to the ability of the matrix of the SLNs to protect insulin against chemical degradation [42]. Self-dispersing or self-emulsifying lipid formulations consist of a drug that is solubilised in oil, surfactant and co-surfactant, which form an emulsion when in contact with the gastrointestinal fluid. Another type of lipid based formulations is colloidal lipid carriers that are capable of solubilising drugs in the locus of the bilayer lipid domain to enhance the dissolution of drugs. Both self-dispersing lipid formulations and colloidal lipid carriers are recent examples of lipid-based formulations investigated for the oral delivery of protein drugs [41].

3.1.4. Nanoscale Technologies

The development of nanoparticles has been considered to be a revolutionary step in the delivery of drugs with the potential of not only improving drug bioavailability, but also targeting drugs towards certain tissues in the body. However, despite the high potential of nanoparticles to provide new treatment opportunities only a few nanoparticle-based systems have reached the market due to challenges such as low encapsulation efficiencies, too rapid drug release profiles and toxicological issues [43,44].

Vitamin B_{12} conjugated dextran nanoparticles demonstrated increased bioavailability of insulin due to particle receptor mediated endocytosis and the protection of insulin from proteolytic degradation [45]. N-trimethyl chitosan chloride (TMC) insulin loaded nanoparticles were modified with a targeting peptide (i.e. CSKSSDYQC or CSK) and compared with unmodified nanoparticles. In comparison to the unmodified nanoparticles, the CSK modification facilitated the uptake of the nanoparticles in the villi, enhanced permeation of the insulin across the epithelium and induced higher internalisation of insulin via endocytosis on goblet cell-like HT29-MTX cells. The modified CSK nanoparticles also showed enhanced transport across Caco-2/HT29-MTX co-cultured cell monolayers and produced improved hypoglycemic effects with a 1.5-fold higher relative bioavailability compared to unmodified nanoparticles [46].

In another study, the anti-diabetic effect of an oral insulin nanoparticulate system consisting of an alginate-dextran sulfate core and a chitosan-polyethylene glycol-albumin shell was evaluated. The nanospheres were loaded with insulin (25, 50, 100 IU/kg) and when administered to diabetic rats, blood glucose reduced in a dose-dependent manner with maximal effect after 14h and a continued effect for up to 24h. The success of these nanospheres was attributed to the reason that albumin prevents protease attack on the insulin and PEG stabilises the nanosphere [47].

3.1.5. Dendrimers

Dendrimers are defined as spherical, macromolecules in the nanosize range with a specific architectural structure consisting of branches stretching from the core containing terminal functional groups [48]. Peptide and protein dendrimers that are synthesised without a core using lysine and

consisting of cationic and aromatic groups in the structure attracted attention due to their potential applications as protein mimetics or drug delivery vehicles [49].

Conjugation of SN38, the active metabolite of irinotecan to poly(amido amine)dendrimers was studied by determining their *in vitro* transport profiles using Caco-2 cell monolayers. The conjugated dendrimers resulted in an increase in the transepithelial transport with decreased toxicity [50].

3.1.6. Colon-Specific Delivery Systems

Site-specific delivery in the colon is considered an attractive approach for oral delivery of proteins and peptides due to decreased proteolytic activity, increased residence time and potentially improved absorption [38]. Approaches for colon-specific delivery include pressure-induced drug delivery, micro-activated systems, pH and time dependent delivery systems and particulate drug delivery systems [51].

Cross-linked bovine serum albumin nanospheres layered with fatty acids presented little drug release in the gastric area and were capable to control the release of vancomycin in the colon area responding to stimuli such as pH, mucin interactions and enzyme absorption [52]. CODES™ (Colon-targeted delivery system), developed by Katsuma and co-workers achieved colon-specific delivery in humans and dogs by releasing the drug content when the lactulose is degraded by enterobacteria in the colon [53].

3.1.7. Targeting Active Transporters

Drug molecules can be transported against a concentration gradient across intestinal epithelium and oral mucosa by means of active transport. This is an energy dependent, carrier-mediated transport of small or macromolecules by transmembrane proteins [13,54]. Transporter proteins exist for amino acids, monosaccharides, monocarboxylic acids, nucleosides, dipeptides, organic cations, phosphates and water-soluble vitamins. These active transporters are driven by Na^+- or H^+-ion electrochemical gradients, or by adenosine tri-phosphate (ATP) hydrolysis [56]. Absorption of di- and tri-peptides across intestinal epithelium has been shown to be facilitated by carrier-mediated oligopeptide transporters [13,55].

A strategy to enhance intestinal absorption of protein and peptide drugs involves its covalent conjugation to carrier molecules, creating targeted pro-drugs, which facilitates membrane transport by enabling recognition by the endogenous membrane transporters [13,56].

Of these endogenous systems, peptide transporters have several advantages as a target system including broad substrate specificity [57]. Although a number of peptide transporters have been identified, including PHT1, PHT2 and PepT2, the proton-coupled PepT1 has been described extensively and is known to be widely distributed in the small intestine and in Caco-2 cells [55,57]. It has been shown that a variety of derivatised dipeptides may be targeted to PepT1, thereby possibly improving the compound's oral bioavailability including dipeptidyl derivatives of α–methyl-Dopa. Although studies indicate that di/tripeptidomimetic and dipeptidyl pro-drugs targeting PepT1/2 showed promise for effective delivery of small drug molecules, its use for larger peptides or macromolecules appears to be limited [58,59].

3.1.8. Targeting Receptors

Receptors, unlike active transporters, transport drug molecules across epithelial and enterocytic cells via receptor-mediated transcytosis and are not limited by their ability to transport molecules based on their size [13,60]. Therefore, the conjugation of protein or peptide drugs to receptor ligands (e.g., vitamin B_{12}, biotin, transferrin, etc.) can enable site specific absorption without affecting the cellular membrane integrity [13,60,61]. This has made receptor-mediated endocytosis an important target for drug delivery research. One study showed that oligomeric transferrin has the potential to act as a carrier of protein and peptide drugs such as insulin for oral delivery with sustained release. They cross-linked insulin with transferrin, which resulted in increased intracellular retention in enterocyte-like Caco-2 cells and CF-1 mice. Insulin conjugated to the tranferrin oligomer was also more effective after oral administration in streptozotocin-induced diabetic rats [61].

The folate receptor has been identified as an ideal marker to target drug delivery to various tumours, including ovarian carcinomas and, in various studies, folate was attached directly to drugs or chemically bound to polymer-drug or polymer/lipid-drug conjugates [59,62]. Kim and co-workers proposed a poly(L-lysine)-poly(ethylene glycol)-folate conjugate (a di-block copolymer conjugate) for therapeutic proteins, since physical PEGylation might prolong circulation in the blood [62]. Folate has also been conjugated to trimethyl chitosan chloride (TMC) to protect it from enzymatic degradation, but to decrease the toxicity of TMC and to increase binding of folate to its receptor, a folate-poly(ethylene glycol)-grafted-trimethylchitosan complex was prepared [63]. Both conjugated molecules demonstrated enhanced intracellular delivery of fluorescein isothiocyanate conjugated bovine serum albumin as a model protein in a folate receptor over-expressing cell line (KB cells or SKOV3 cells) through folate receptor-mediated endocytosis when compared with A549 cells (a folate receptor deficient cell line). It is possible that this intracellular protein delivery system can be suitable to enhance delivery of other negatively charged therapeutic proteins. However, Kim and co-workers noted that intracellular delivery of the model protein was decreased when serum proteins were present, and suggested that for *in vivo* applications the protein complexes should have enhanced stability [62]. Bi-functional fusion proteins, including a human growth hormone-transferrin fusion protein for oral delivery, have been genetically engineered to link protein and peptide drugs with carrier antibodies which target transferrin receptors, and this system has been shown not to be limited to the rat [64,65].

3.2. Pulmonary Delivery

A promising non-invasive delivery route for protein and peptide drugs is via the airway or pulmonary system, in the form of dry powder inhalants and nanoparticles [66]. Macromolecules are promptly absorbed from the alveolar airspace mainly because of the large alveolar surface area, decreased enzymatic activity as well as the thin epithelial air-blood barrier [67]. As with many other delivery routes, the pulmonary route of administration also has its drawbacks such as the thick mucus layer covering the upper and central

respiratory tract, which prevents adequate absorption of proteins [68]. This mucus layer along with the closely joined tight junctions in the respiratory epithelium act as a significant physical barrier against the penetration of macromolecules [69], which needs to be overcome before therapeutic levels of the drug could be reached.

Macrophage targeting carrier systems, mucoadhesive systems as well as compounds that could reversibly open tight junctions is some novel approaches that have been explored to optimise pulmonary delivery of macromolecules [69,70]. Optimal deep lung delivery of drug molecules is ideally obtained by particles with a diameter of between 1 and 5 μm. Polymeric micro and nanoparticles that comprise of degradable and biocompatible materials such as polyethylene glycol and poly(lactide-co-glycolide) are retained well in the pulmonary tissues and are able to evade macrophages [71,72]. Besides these novel dosage form designs, various devices such as metered dose inhalers, jet and ultrasonic nebulisers and dry-powder inhalers have been used in the pulmonary drug delivery [73].

3.2.1. Absorption Enhancers

The use of absorption enhancers is one of the common methods employed to improve absorption of molecules across different mucosal surfaces. Several mechanisms of action are known for absorption enhancers employed in pulmonary drug delivery, which include reduction of the mucus viscosity, reversible opening of tight junctions, increase in membrane fluidity and momentarily disruption of the structural integrity of epithelial membranes [13]. Various absorption enhancers have been investigated for the improvement of protein and peptide absorption through the pulmonary epithelium such as surfactants, chelating agents, fatty acids, bile salts, anionic and cationic polymers [13,74]. Studies over recent years have, however, proved that only few absorption enhancers are regarded as safe for use in humans. Some of these include: chitosan, alkylsaccharides and polyethylene glycol (PEG) [75,76].

Chitosan and its derivatives have long been used in improving uptake of proteins across epithelial tissue mainly because of its muco-adhesive and absorption enhancing properties, but also because of its low toxicity [69,70]. Microencapsulation of dry insulin powder in chitosan nanoparticles significantly increased the distribution of the drug to the deep lung after intra-tracheal administration thereof. The inhaled nanoparticles induced a more pronounced and prolonged hypoglycaemic effect in rats compared to the control group [71].

3.2.2. Dry Powder Inhalers

Exubera® is a spray-dried inhalation product that contains mannitol, glycine and sodium citrate in addition to recombinant human insulin and proved to enhance the pulmonary absorption of insulin when compared to regular subcutaneous administration [77,78]. The manufacturing of this product, marketed by Pfizer, was discontinued in 2007 due to several reasons such as its high cost, relative difficulty to use the device, poor acceptance by patients and clinicians, considerations of damage to lungs and a potential increased risk in bronchial carcinoma of smokers [77,79].

Technosphere® technology (Afrezza®, Mannkind Corp) is a system developed for insulin delivery to the pulmonary area by an inhaler containing single dose cartridges [78]. This technology uses fumaryl diketopiperazine as a particle substrate, which enables improved absorption of insulin in the deep lung because it encapsulates the drug, which can be lyophilised into dry powder. The surface charge of each particle is slightly negative, which causes a charge difference between the particle and the pulmonary tissue, thereby enhancing the adsorption of the particles to the tissue. The dry powder is inhaled and the particles disintegrate in the neutral pH of the lung, where encapsulated peptide drugs are then released to be absorbed into the systemic circulation [80]. This technology has been used in delivering not only insulin, but also parathyroid hormone (PTH) and salmon calcitonin (sCT) in healthy human volunteers, as well as felbamate in mice [81]. Aspirair® is a new device, which makes use of compressed air and a vortex separation chamber in order to enhance fine particle fraction lung delivery by de-agglomeration [82].

3.2.3. Liposomes

Liposomes are spherical lipid bilayer vesicles capable of encapsulating drugs and are formulated from cholesterol and phospholipids. Insulin was encapsulated in muco-adhesive liposomes, which caused a reduced plasma glucose level in the blood of rats over a period of 12 h [70]. In another *in vivo* study that was carried out in rats, elactonin, a peptide drug used in the treatment of osteoporosis, had increased absorption in pulmonary tissue when administered in surface-modified liposomes [78].

3.2.4. Enzyme Inhibitors

Enzyme inhibitors, for example N-lauryl-ß-D-maltopyranoside, have shown the ability to enhance the pulmonary absorption of peptide drugs, such as insulin, when *in vivo* testing on rats was carried out [74]. However, limited information on the use of enzyme inhibitors for pulmonary peptide delivery is available in literature which can probably be explained by the problems experienced with long term enzyme inhibition.

3.3. Nasal Delivery

Although the nasal route of drug administration was mainly utilised for the treatment of local diseases of the upper respiratory tract, researchers later acknowledged the value of this route for the systemic delivery of peptide and protein based drugs [83,84].

The structure and composition of the nasal mucosa provides a challenging barrier, especially for the systemic delivery of large molecules (i.e. above 1.0 kDa). Nasal delivery of hydrophilic proteins and peptides usually exhibit bioavailability values of less than 1%. The sub therapeutic bioavailability of these drugs can predominantly be attributed to weak mucosal membrane permeability and degradation due to proteolytic enzyme activity in the nasal mucosa. The rapid mucocilliary clearance of drugs from the nasal mucosa also has a negative effect on bioavailability. It is therefore common practice to make use of nasal absorption enhancers to achieve therapeutic systemic drug levels [75,85].

The following approaches have been pursued to improve the nasal absorption of drugs with a peptide and/or protein nature: 1) chemical structure modification to improve metabolic stability and/or permeability [86]; 2) the addition of enzyme inhibitors to protect the drug from mucosal enzymatic degradation [87]; 3) the addition of absorption enhancers to aid the passage of drug molecules through the nasal mucosa [88]; 4) development of novel drug carrier systems such as liposomes, niosomes, nano and microparticles [89,90,91]. Recent trends showed that the focus is primarily on the use of absorption enhancers as well as nano and microparticulate systems and these strategies will therefore be discussed in more detail.

3.3.1. Absorption Enhancers

As mentioned before, chemical absorption enhancers are co-administered with drugs to improve their absorption across mucosal surfaces via different mechanisms of action. Cyclopenta decalactone is derived from the plant *Angelica archangelica* and is listed on the Food and Drug Administration (FDA) approved inactive ingredient list for use in drug delivery applications. This excipient acts as an absorption enhancer; however, thespecific mechanism of its drug absorption enhancement property in the nose is only speculative at this stage. The surfactant nature of the molecule suggests that interaction with the nasal membrane may increase fluidity, which in turn may result in improved transcellular absorption of co-administered substances. Cyclopenta decalactone has proved effective in enhancing the nasal delivery of insulin (e.g., Nasulin®) in phase I and phase II clinical trials [92].

Alkylsaccharides (e.g., Intravail®) consist of a polar sugar head (e.g., sucrose, maltose), which is esterified with non-polar alkyl chains of varying lengths. Tetradecyl maltoside, with an alkyl chain length of C_{14}, has been shown to be a very effective nasal absorption enhancer for various drug molecules [93,94]. The proposed mechanism of drug absorption enhancement is attributed to a stimulation of the rate of endocytosis and an increase in fluidity of the mucosal membrane. Studies also showed a significant reduction in transepithelial electrical resistance (TEER) after treatment of human tracheal/bronchial cell cultures, which suggested that paracellular transport enhancement may also contribute to improved absorption [95]. Tetradecyl maltoside was tested in an anaesthetised rat model in concentrations ranging from 0.06 - 0.50%. The study showed that tetradecyl maltoside had improved the nasal absorption of insulin (5.7 kDa), leptin (16.0 kDa), somatropin (22.1 kDa) and epoetin-α (30.4 kDa) to varying degrees of success when administered within the specified concentration range [96]. Another study showed that the alkylsaccharide, N-dodecyl-β-D-maltoside (DDM), enhanced the nasal delivery of a PTH analogue in rodent and primate models when used at a concentration of 0.18%. A relative bioavailability of 35 - 40% was achieved in a primate model when comparing the bioavailability of the DDM-PTH combination to that of a subcutaneous injection [97].

Hydroxy fatty acid esters of polyethylene glycol (e.g., CriticalSorb™ containing macrogol 15 hydroxy stearate) are well known as effective mucosal absorption enhancers. A relatively recent study in a conscious rat model has shown that the nasal absorption of insulin can be dramatically enhanced when combined with fatty acid esters. In a previous study, a solution of insulin (4 IU/kg) and macrogol 15 hydroxy stearate was nasally administered that resulted in a relative bioavailability of 100% when compared to a subcutaneous injection based on an $AUC_{0\text{-}1h}$ [98]. Macrogol 15 hydroxy stearate was also used in a similar study to enhance the nasal absorption of human growth hormone (hGH). A 5 mg/kg dose of hGH was administered nasally to conscious rats in a simple solution of macrogol 15 hydroxy stearate. The results showed a relative bioavailability of 49.9% as compared to a control group (i.e. hGH solution) with a bioavailability of 0.7% based on an $AUC_{0\text{-}2h}$. The optimal ratio of Macrogol 15 hydroxy stearate to hGH, when used as a solution for nasal administration, was reported to be 4:1 on a weight:weight basis [99,100]. The mechanism of action of Macrogol 15 hydroxy stearate was reported to be related to improved permeation in conjunction with a 60% reduction in TEER values which were observed in Caco-2 cell monolayers after a 2 h exposure period [101].

3.3.2. Micro- and Nanoparticles

Micro and nanoparticulate systems for nasal drug delivery usually consist of mucoadhesive polymers, which improve the retention time of the drug on the nasal mucosa that lead to enhanced drug absorption. These particulate systems not only protect the incorporated peptide and protein drugs against enzymatic degradation, but also establish a tight contact between the drug and nasal mucosa [102].

Chitosan is a positively charged polymer with pronounced mucoadhesive properties and is regularly used to aid in the nasal delivery of macromolecules. Chitosan improves drug penetration primarily by transiently opening the tight junctions in the nasal mucosa and by improving bioadhesive properties [103,104]. Chitosan glutamate or hydrochloride salts with a degree of deacetylation of approximately 83% and molecular weight of approximately 200 kDa (e.g., ChiSys®) are mostly used. A study in a sheep model showed that chitosan microspheres were capable of improving the nasal absorption of goserelin. The relative bioavailability of the microsphere formulation as compared to a subcutaneous injection was 36.6% [105,106].

In another study, a thiomer microparticulate system containing polycarbophil-cysteine and gluthatione (as permeation enhancer) was used to sucessfully administer hGH via the nasal cavity. The polycarbophil-cysteine/gluthatione combination microparticulate system achieved a 3-fold increase in bioavailability when compared to a polycarbophil-cysteine formulation which did not contain gluthatione [107].

3.4. Transdermal Delivery

The main diffusional barrier against effective transdermal drug delivery remains the stratum corneum (SC). The SC particularly excludes the transit of polar, hydrophilic molecules such as proteins and peptides. Several strategies have been followed to increase the number of compounds that can be administered transdermally without permanently compromising the SC. These strategies can be divided into two

categories namely passive and active approaches [108,109, 110,111].

3.4.1. Passive Approaches

Passive approaches to improve transdermal drug delivery include chemical penetration enhancers, pre-treatment of skin, nano-carriers and biotechnologies such as peptide cell-penetrating enhancers and peptide chaperones [38,112,113].

3.4.1.1. Chemical Penetration Enhancers

Chemical penetration enhancers facilitate transdermal delivery of drugs by different mechanisms such as enhancing solubility, increasing partitioning into the SC, fluidising the crystalline structure of the SC and/or disrupting ordered skin lipids. Examples of transdermal penetration enhancers include fatty acids/esters, solvents, surfactants, terpenes, ureas, essential oils and sulfoxides [114,115,110,111,116]. Only a relatively small number of chemical enhancers have been able to induce substantial therapeutic enhancement of drug transport across the skin without causing toxic effects and even less depicted enhanced delivery of peptides and proteins [117,118]. Fatty acids were used as penetration enhancers for arginine vasopressin and insulin delivery [119,120] and urea for leuprolide delivery through the skin [121].

3.4.1.2. Pre-Treatment of Skin

The skin contains sulfhydryl groups that may react with certain peptide and protein molecules and thereby presenting a potential biochemical barrier. Neutralisation of this barrier by means of topically applying oxidising agents could increase transdermal delivery of disulphide containing peptides such as insulin, calcitonin, somatostatin lanreotide, octreotide and oxytocin/vasopressin analogues. Sintov and Wormser showed that skin pre-treatment with iodine followed by dermal application of insulin resulted in significantly reduced glucose levels and elevated insulin concentrations in the plasma presumably through inactivation of endogenous sulfhydryl groups [122]. Another study reported that pre-treatment with menthol modifies the barrier properties of the SC by distributing into the intercellular spaces and possibly causes reversible disruption of lipid domains [114]. Skin pre-treatment with ethanol usually increases the permeation of hydrophilic drugs, whereas it decreases diffusion of hydrophobic drugs [38]. Ethanol skin pre-treatment has been investigated for transdermal delivery of leoprolide [123], while dimethyl sulfoxide was used for amphotericin B delivery [124].

3.4.1.3. Nanocarriers

Lipososmes (including niosomes and ethosomes), transfersomes, dendrimers, nanoparticles and nanoemulsions are nanocarriers most commonly utilised for transdermal drug delivery. Although liposomes are considered as nanocarriers in this discussion, it is important to note that they may also fall within the micro size range [112,115,125].

Niosomes, analogues of liposomes, are non-phospholipid vesicles created by the self-assembly of non-ionic surfactants in aqueous dispersions. Liposomes with high alcohol content are known as ethosomes. The surfactants in all of these particles aid in local fluidisation of the lipids, allowing for the particles to sit in the upper layers of the SC where they are able to form a depot for prolonged effects [112,115,125]. The encapsulation of peptides in liposomes to increase transdermal peptide delivery has been investigated for insulin [126], melatonin [127,128] and tetanus toxoid [129,130].

Transfersomes consist of a deformable structure, making them more elastic in nature and allowing them to squeeze through the pores on the surface of skin into the deeper layers [131]. Drug-loaded transfersomes can transport relatively large amounts of drug per unit time across skin (up to 100 $\mu g.cm^{-2}.h^{-1}$). Even when transfersomes are loaded with peptide-like molecules of high molecular weight, a relatively high rate of transdermal delivery remains reproducible [125,132,133]. Examples of peptide-like drugs that have been investigated for transdermal delivery with transfersomes include calcitonin, alpha-interferon, gamma-interferon, insulin and serum albumin [132,133,134].

Nanoparticles have been employed to encapsulate protein drugs for transdermal delivery. The interaction between the nanoparticles and the skin barrier leads to increased skin permeability, which was shown for example with insulin, cyclosporin A and interferon alfa-2a [135,136,137,138,139, 140,141].

Nanoemulsions can incorporate hydrophobic and hydrophilic drugs because it is possible to make both water-in-oil or oil-in-water nanoemulsions [125,142,143,144]. Examples of peptide drugs that have been incorporated in nanoemulsions for transdermal delivery include insulin [145] and bovine serum albumin [146], however, the use of this technique has become less popular due to inherent stability problems with the nanoemulsions.

3.4.1.4. Biotechnology Techniques

Increased passive delivery of insulin via the transfollicular route was achieved when a short 11-amino acid synthetic peptide (TD-1) was co-administered [147]. Enhanced transdermal delivery was also attempted for human epidermal growth factor and human growth hormone by utilising TD-1 [148,149]. A natural pore-forming peptide, magainin, was employed to increase skin permeability by a mechanism proposed to target bilayer disruption in SC lipids and not in deeper tissue [150]. Magainin was, however, only effective when utilised in combination with a surfactant.

Lipophilic derivatives of peptides were reported to have increased skin permeability, for example, covalent binding of cyclosporine to a polyarginine-heptamer cell-penetrating peptide led to improved skin absorption. However, it is important to note that alteration of the chemical structure of peptides might also affect their pharmacological activity [126,151,152,153].

3.4.2. Active Approaches

Active approaches to improve transdermal drug delivery involve the use of an energy source to overcome skin barrier properties. The device and application factors can be adjusted to accommodate the skin properties of different patients. Active transdermal delivery approaches can be subdivided into invasive (e.g., intravenous or intramuscular injection), minimally invasive (e.g., photopolymerisation, microdermabration, liquid jet injectors, powder injectors, mi-

croneedles, thermal ablation, radiofrequency ablation, laser ablation, tape stripping) and non-invasive methods (e.g., electroporation, iontophoresis, sonophoresis, magnetophoresis and pressure waves) [111,126,154]. Although some of the invasive and minimally invasive techniques have been successfully used to deliver protein based drugs across the skin, only non-invasive methods will be discussed here as delimited by the scope of this review article.

3.4.2.1. Electroporation

Electroporation is a technique that causes a temporary structural perturbation of the lipid bilayers of the SC in order to create transient pores through application of short (microsecond or millisecond), high voltage (50-1000 V) pulses to the skin. Transport of charged macromolecular drugs (up to 40 kDa) occurs mainly due to enhanced diffusion, electrophoresis and to a small extent also electro-osmosis. Electroporation has effectively been used to enhance permeability of peptides and proteins across the skin such as insulin [155], calcium regulating hormones [156] and sCT [157].

Genetronics, Inc (San Diego, California) has developed a prototype electroporation device in order to attain gene delivery and to improve drug delivery. However, safety in the clinical application of this technique is still questionable due to mild skin reactions [158,159,160].

3.4.2.2. Iontophoresis

Iontophoresis is a procedure that employs a small electrical potential difference (0.5 mA/cm^2) to enhance delivery of charged and neutral molecules with relatively low molecular weight through the skin. It offers controlled or pulsatile drug delivery, since the amount of drug delivered is directly proportional to the potential difference applied [161,162,163, 164]. Peptides that remain charged throughout transdermal delivery are ideal for iontophoretic delivery [160]. Some examples of biotechnology based drugs that have been investigated for transdermal delivery with iontophoresis include ribonuclease A [164], calcitonin [156,157,165], serum human parathyroid hormone [166,167], vasopressin [168] and luteinizing-hormone-releasing hormone [169,170].

Various companies have developed iontophoresis devices which are currently commercially available, e.g., Ionto-Patch® (Travanti Pharma Inc.) which includes the corporation's wearable electronic disposable drug delivery stand (WEDD®) that is based on a thin, elastic, low-cost battery technology within a single-use, disposable, iontophoretic patch [171,172].

3.4.2.3. Sonophoresis

Sonophoresis is the movement of compounds through intact skin into soft tissue under the influence of ultrasonic agitation. Either low-frequency ultrasound (LFS; 20-100 kHz) or high frequency ultrasound (HFS; 0.7-16 MHz) can be employed [158,173]. It was shown that LFS is significantly more effective than HFS in delivering drugs across the skin. Collapse cavitation (i.e. the generation and oscillation of gas bubbles in the skin) was identified as the mechanism of action for improved transdermal drug delivery by sonophoresis [174,175,176]. The SonoPrep® from Sontra Medical Corporation and Prelude™ SkinPrep from Echo Therapeutics are examples of skin permeation devices which employ ultrasound to increase permeability through the skin [108,160].

3.4.2.4. Magnetophoresis

Magnetophoresis is the application of a magnetic field on the skin that acts as a peripheral driving force to improve transdermal drug delivery. Alteration in the structure of skin is induced, which most likely contributes to an increase in permeability [142,177,178]. Magnetophoresis is mostly used in cancer therapy, but it has also been investigated for transdermal delivery of lipofectamine and certain genetic materials [179,180].

3.4.2.5. Pressure Waves

Pressure waves are generated by intense laser radiation and are only applied for a very short time (i.e. microseconds to milliseconds). It is hypothesised that the pressure waves form a continuous or hydrophilic pathway across skin due to the development of lacunae domains in the SC. Adequate permeation of the SC is possible with only a single pressure wave, which allows the transport of peptides and proteins into the dermis and epidermis. Additionally, drugs can also pass into the vasculature and yield a systemic effect [142,177,181]. Insulin delivered across the skin by means of pressure waves reduced blood glucose concentrations over several hours [142,181].

3.5. Buccal Delivery

The mucosa of the oral cavity offers an opportunity for systemic drug delivery since it is highly vascularized with relatively low enzyme activity and avoids first pass metabolism. However, the limited absorption surface area combined with the barrier functions of the mucosa constitutes challenges against effective drug delivery. Permeation of protein and peptide drugs is specifically limited by their high molecular weight and hydrophilic nature [54,182].

The term "buccal" refers to the lining of the cheek and the lips, which only represents about one third of the total surface area of the oral cavity. The lining of the buccal mucosa consists of non-keratinised, multilayered squamous epithelium supported by the underlying lamina propria [183].

Different approaches have been used to improve drug permeation across the buccal mucosa such as incorporation of chemical permeation enhancers, enzyme inhibitors and mucoadhesive polymers to retain the drug in close contact with the site of delivery for a prolonged period.

3.5.1. Absorption Enhancers

Buccal delivery of several protein and peptide drugs with different types of permeation enhancers have been investigated in different *in vitro* and *in vivo* models, which include insulin, octreotide acetate, recombinant human interferon alpha B/D hybrid, gonadotropin releasing hormone, buserelin, luteinising hormone-releasing hormone and glucagon-like-peptide 1 [184].

When transforming growth-factor β was incorporated into a 2% w/v chitosan gel, a marked increase in the amount that moved across the different strata of the buccal mucosa was observed in comparison with when the drug was applied alone. The improved permeability of the drug caused by the

Table 1. Examples of non-invasive peptide drug delivery products under clinical investigation or available on the market.

Name	Company	Active ingredient	Status	Reference
Oral route of administration				
Peptelligence®	This platform is the proprietary of Unigene Laboratories, licenced to other companies for product development	Salmon calcitonin	Phase III clinical trial completed	[187, 188]
Eligen®	This platform is the proprietary of Emisphere, licenced to other companies for product development	Semaglutide (GPL-1 agonist), insulin, calcitonin	Under clinical investigation	[187, 189]
IN-105	Biocon (taken over from Nobex)	Insulin analogue based on HIM2	Under clinical investigation	[190]
Capsulin™	Diabetology	Insulin	Under clinical investigation	[190]
HDV-I	Diasome	Insulin linked to a hepatic targeting molecule	Under clinical investigation	[190]
Pulmonary route of administration				
Exubera®	Pfizer	Insulin	Discontinued in 2007	[78]
Technosphere®	This platform is the proprietary of MannKind Corp, licenced to other companies for product development	Insulin (AFREZZA™)	Comparative trials	[191]
Nasal route of administration				
µCO™ system in Fitlizer™ devices	SNBL Ltd	Insulin, Parathyroid hormone, calcitonin	Pre-clinical studies in non-human primates	[192]
Miacalcin®	Novartis	Salmon calcitonin	Marketed	[78, 192]
Minirin®	Ferring Pharmaceuticals	Desmopressin	Marketed	[78, 192]
Synarel®	Pharmacia	Nafarelin	Marketed	[78, 192]
Transedrmal route of administration				
PassPort™	Proprietary of Altea Therapeutics Corporation licenced to other companies for product development	e.g., KAI Pharmaceuticals Proprietary peptides, insulin	Under clinical investigation	[193]
ViaDor™	TransPharma Medical Ltd	hPTH, GLP-1, calcitonin	Under clinical investigation (Phase Ib completed for GLP-1)	[193]
P.L.E.A.S.E. (precise laser epidermal system)	Pantec Biosolutions	Therapeutic proteins, e.g., FSH	Under clinical investigation	[193]
Buccal route of administration				
Oral-lyn™	Generex	Insulin	Marketed	[194]

chitosan gel was explained by a potential interference of the polymer with the lipid organisation in the superficial layers of the buccal epithelium combined with a mucoadhesive interaction with the tissue [185]. This permeation enhancing effect of chitosan across the buccal mucosal epithelium was confirmed with statistically significantly increased permeation of hydrophilic and macromolecular model compounds across an *in vitro* buccal cell culture model [182].

3.5.2. Oral Spray Device

Oral-lyn® is a product that delivers insulin systemically through the buccal mucosa and is administered with a spraying device (i.e. Rapidmist®). One spray from the Rapidmist® device contains 10 insulin units and with an absorption of 10% of the total dose, one insulin unit is therefore delivered to the systemic circulation with each spray. The insulin reaches the blood within 5 min, peaks at 30 min and returns back to baseline after 2 h. A clinical trial in Type 1 diabetes mellitus patients showed a very high degree of reproducible insulin delivery in the blood when administered weekly over a three week period. A two year safety study in dogs with four applications daily indicated no adverse effects or pathological changes in the buccal epithelium [186].

4. CONCLUSION

In recent years, there has been a renewed interest in the quest for the non-invasive delivery of peptide and protein drugs. Different routes of drug administration have been investigated for this purpose, including the oral, pulmonary, nasal, transdermal and buccal routes. Although the number of successes in terms of commercialised products does not correlate with the research efforts so far, promising technologies and devices have been developed to serve as platforms for further investigations. Certain approaches and technologies have resulted in products that are in different stages of clinical testing. However, it is important to note that factors such as production cost, difficulty of use, acceptance by clinicians as well as patients, and safety need to be carefully taken into consideration to ensure the marketing potential of a product. Despite all the obstacles, recent progress has highlighted the possibility of non-invasive delivery of biotechnology based drugs.

A summary of some products that are under clinical investigation or commercially available for non-invasive protein and peptide drug delivery via different routes of administration is given in Table **1**.

CONFLICT OF INTEREST

The authors confirm that this article content has no conflict of interest.

ACKNOWLEDGEMENTS

Declared none.

REFERENCES

[1] Banga, A.K. Therapeutic peptides and proteins: Formulation, processing and delivery systems, 2nd ed.; Taylor and Francis, **2005.**

[2] Van der Walle, C.F.; Olejnik, O.An overview of the field of peptide and protein delivery. In: Peptide and protein delivery; Van der Walle, Ed.; Elsevier: Amsterdam, **2011**; pp. 1-23.

[3] Lee, H.J. Protein drug oral delivery: The recent progress. *Arch. Pharm. Res.*, **2002**, *25*, 572-584.

[4] Rekha, M.R.; Sharma, C.P. Oral delivery of therapeutic protein/peptide for diabetes – Future perspectives. *Int. J. Pharm.*, **2013**, *440*, 48-62.

[5] Brown, L.R. Commercial challenges of protein drug delivery. *Expert Opin. Drug Deliv.*, **2005**, *2*, 29-42.

[6] Al-Tabakha, M.M.; Arida, A.I. Recent challenges in insulin delivery systems: A review. *Indian J. Pharm. Sci.*, **2008**, *70*, 278-286.

[7] Roach, P. New insulin analogues and routes of drug delivery-Pharmacodynamic and clinical considerations. *Clin. Pharmacokinet.*, **2008**, *47*, 595-610.

[8] Grant, M.; Leone-Bay, A. Peptide therapeutics: it's all in the delivery. *Ther. Deliv.*, **2012**, *3*, 981-996.

[9] Brandt, D.; Boss, A. The next generation insulin therapy. http://www.ondrugdelivery.com/publications/diabetes.pdf (Accessed June 21 **2013**).

[10] Brayden, D.J.; Maher, S. Oral absorption enhancement : taking the next steps in therapeutic delivery. *Ther. Deliv.*, **2010**, *1*, 5-9.

[11] Moeller, E.H.; Jorgensen, L. Alternative routes of administration for systemic delivery of protein pharmaceuticals. *Drug Discov. Today Technol.*, **2008**, *5*, e89-e94.

[12] Pauletti, G.; Gangwar, S.; Siahaan, T.; Aubé, J.; Borchardt, R. Improvement of oral peptide bioavailability: peptidomimetics and prodrug strategies. *Adv. Drug Deliv. Rev.*, **1997**, *27*, 235-256.

[13] Renukuntla, J.; Vadlapudi, A.; Patel, A.; Boddu, S.; Mitra, A. Approaches for enhancing oral bioavailability of peptides and proteins. *Int. J. Pharm.*, **2013**, *447*, 75-93.

[14] Cheng, W.; Lim, L.-Y. Synthesis, characterization, and in vivo activity of salmon calcitonin coconjugated with lipid and polyethylene glycol. *J. Pharm. Sci.*, **2009**, *98*, 1438-1451.

[15] Jabarian, L.; Rouini, M.; Atayabi, F.; Foroumadi, A.; Nassiri, S.; Dinarvand, R. In vitro and in vivo evaluation of an in situ gel forming system for the delivery of PEGylated octreotide. *Eur. J. Pharm. Sci.*, **2013**, *48*, 87-96.

[16] Brown, L. Commercial challenges of protein drug delivery. *Expert Opin. Drug Deliv.*, **2005**, *2*, 29-42.

[17] Roberts, M.; Bentley, M.; Harris, J. Chemistry for peptide and protein PEGylation. *Adv. Drug Deliv. Rev.*, **2002**, *54*, 459-476.

[18] Veronese, F.; Pasut, G. PEGylation, successful approach to drug delivery. *Drug Discov. Today*, **2005**, *10*, 1451-1458.

[19] Hinds, K.; Kim, S. Effects of PEG conjugation on insulin properties. *Adv. Drug Deliv. Rev.*, **2002**, *54*, 505-530.

[20] Knipes, M.; Dandona, P.; Tripathy, D.; Still, G.; Kosutic, G. Control of postprandial plasma glucose by an oral insulin product (HIM2) in patients with type 2 diabetes. *Diabetes Care*, **2003**, *26*, 421-426.

[21] Shen, W.-C. Oral peptide and protein delivery: unfilfilled promises? *Drug Discov. Today*, **2003**, *8*, 607-608.

[22] Sharma, A.; Arora, S. Commercial challenges and emerging trends in oral delivery of peptide and protein drugs: a review. *Res. J. Pharm. Biol. Chem. Sci.*, **2011**, *2*, 778-790.

[23] Biocon: Active Drug Discovery Programs - Oral Insulin & Rheumatoid Arthritis. http://www.biocon.com/biocon_researc_ discovery.asp (Accessed September *19*, **2013**.)

[24] Ekrami, H.; A.R.; K.; Shen, W. Water-soluble fatty acid derivatives as acylating agents for reversible lipidization of polypeptides. *FEBS Lett.*, **1995**, *371*, 283-286.

[25] Wang, J.; Chow, D.; Heiati, H.; Shen, W.-C. Reversible lipidization for the oral delivery of salmon calcitonin. *J. Control. Release*, **2003**, *88*, 369-380.

[26] Cheng, W.; Satyanarayanajois, S.; Lim, L.-Y. Aqueous-soluble, non-reversible, lipid conjugate of salmon calcitonin: synthesis, characterization and in vivo activity. *Pharm. Res.*, **2007**, *24*, 99-110.

[27] The Free Library: Nobex and Elan Initiate Phase I Clinical Trial of Oratonin to Treat Osteoporosis; - Calcitonin Currently Only Available as an Injectable and Nasal Spray. http://www.thefreelibrary.com/Nobex+and+Elan+Initiate+Phase+I+Clinical+Trial+of+Oratonin(TM)+to...-a085887474 (Accessed September 17 **2013**.)

[28] Mäe, M.; Langel, U. Cell-penetrating peptides as vectors for peptide, protein and oligonucleotide delivery. *Curr. Opin. Pharmacol.*, **2006**, *6*, 509-514.

[29] Khafagy, E.; Morishita, M. Oral biodrug delivery using cell-penetrating peptide. *Adv. Drug Deliv. Rev.*, **2012**, *64*, 531-539.

[30] Bechara, C.; Sagan, S. Cell-penetrating peptides: 20 years later, where do we stand? *FEBS Lett.*, **2013**, *587*, 1693-1702.

[31] Morishita, M.; Peppas, N. Advances in oral drug delivery: improved bioavailability of poorly absorbed drugs by tissue and cellular optimization. *Adv. Drug Deliv. Rev.*, **2012**, *64*, 479.

[32] Peppas, N.; Bures, P.; Leobandung, W.; Ichikawa, H. Hydrogels in pharmaceutical formulations. *Eur. J. Pharm. Biopharm.*, **2000**, *50*, 27-46.

[33] Ichikawa, H.; Peppas, N. Novel complexation hydrogels for oral peptide delivery: in vitro evaluation of their cytocompatibility and insulin-transport enhancing effects using Caco-2 cell monolayers. *J. Biomed. Mater. Res. Part A*, **2003**, *67*, 609-617.

[34] Yamagata, T.; Morishita, M.; Kavimandan, N.; Nakamura, K.; Fukuoka, Y.; Takayama, K. P. Characterization of insulin protection properties of complexation hydrogels in gastric and intestinal enzyme fluids. *J. Control. Release*, **2006**, *112*, 343-349.

[35] Dorkoosh, F.; Verhoef, J.; Borchard, G.; Rafiee-Tehrani, M.; Junginger, H. Development and characterization of a novel peroral peptide drug delivery system. *J. Control. Release*, **2001**, *71*, 307-318.

[36] Peppas, N. Devices based on intelligent biopolymers. *Int. J. Pharm.*, **2004**, *277*, 11-17.

[37] Eiamtrakarn, S.; Itoh, Y.; Kisbimoto, Y.; Yoshikawa, N.; Shibata, N.; Murakami, M. Gastrointestinal mucoadhesive patch system (GI-MAPS) for oral administration of G-CSF, a model protein. *Biomaterials*, **2002**, *23*, 145-152.

[38] Bernkop-Schnürch, A.; Krauland, A.H.; Leitner, V.M; Palmberger, T. Thiomers: potential excipients for non-invasive peptide delivery systems. *Eur. J. Pharm. Biopharm.*, **2004**, *58*, 253-263.

[39] Müller, C.; Ma, B.N.; Gust, R.; Bernkop-Schnürch, A. Thiopyrazole preactivated chitosan: Combining mucoadhesion and drug delivery. *Acta Biomaterialia*, **2013**, *9*, 6585-6593.
[40] Park, K.; Kwon, I.; Park, K. Oral protein delivery: Current status and future prospect. *React. Funct. Polym.*, **2011**, *71*, 280-287.
[41] Beg, S.; Swain, S.; Rizwan, M.; Irfanuddin, M.; Malini, D. Bioavailability enhancement strategies: basics, formulation approaches and regulatory considerations. *Curr. Drug Deliv.*, **2012**, *8*, 691-702.
[42] Sarmento, B.; Martins, B.; Ferreira, S.; Souto, E. Oral insulin delivery by means of solid lipid nanoparticles. *Int. J. Nanomedicine.*, **2007**, *2*, 743-749.
[43] Chen, M.-C.; Mi, F.-L.; Liao, Z.-X.; Hsiao, C.-W.; Sonaje, K.; Chung, M.-F. Recent advances in chitosan-based nanoparticles for oral delivery of macromolecules. *Adv. Drug Deliv. Rev.*, **2013**, *65*, 865-879.
[44] Couvreur, P. Nanoparticles in drug delivery: Past, present and future. *Adv. Drug Deliv. Rev.*, **2013**, *65*, 21-23.
[45] Chalasani, K.; Russel-Jones, G.; Yandrapu, S.; Diwan, P.; Jain, S. A novel vitamin B12-nanosphere conjugate carrier system for peroral delivery of insulin. *J. Control. Release*, **2007**, *117*, 421-429.
[46] Jin, Y.; Song, Y.; Zhu, X.; Zhou, D.; Chen, C.; Zhang, Z. Goblet cell-targeting nanoparticles for oral insulin delivery and the influence of mucus on insulin transport. *Biomaterials*, **2012**, *33*, 1573-1582.
[47] Reis, C.; Veiga, F.; Ribeiro, A.; Neufeld, R.; Damage, C. Nanoparticulate biopolymers deliver insulin orally eliciting phamacological response. *J. Pharm. Sci.*, **2008**, *97*, 5290-5305.
[48] Caminade, A.; Laurent, R.; Majoral, J. Characterization of dendrimers. *Adv. Drug Deliv. Rev.*, **2005**, *57*, 2130-2146.
[49] Klajnert, B.; Janiszewskab, J.; Urbaneczyk-Lipkowskae, Z.; Bryzewskaa, M.; Shcharbin, D.; Labieniec, M. Biological properties of low molecular mass peptide dendrimers. *Int. J. Pharm.*, **2006**, *309*, 208-217.
[50] Goldberg, D.; Vijayalakshmi, N.; Swaan, P.; Ghandehari, H. G3.5 PAMAM dendrimers enhance transepithelial transport of SN38 while minimizing gastrointestinal toxicity. *J. Control. Release*, **2011**, *150*, 318-325.
[51] Maroni, A.; Zma, L.; Del Curto, M.; Foppoli, A.; Gazzaniga, A. Oral colon delivery of insulin with the aid of functional adjuvants. *Adv. Drug Deliv. Rev.*, **2012**, *64*, 540-556.
[52] Luppi, B.; Bigucci, F.; Cerchiara, T.; Mandrioli, R.; Di Pietra, A.; Zecchi, V. New environmental sensitive system for colon-spesific delivery of peptidic drugs. *Int. J. Pharm.*, **2008**, *358*, 44-49.
[53] Katsuma, M.; Watanabe, S.; Kawai, H.; Takemura, S.; Sako, K. Effects of absorption promoters on insulin absorption through colon-targeted delivery. *Int. J. Pharm.*, **2005**, *307*, 156-162.
[54] Patel, V.F.; Liu, F.; Brown, M.B. Advances in oral transmucosal drug delivery. *J. Control. Release*, **2011**, *153*, 106-116.
[55] Lee, V.H.L. Membrane transporters. *Eur. J. Pharm. Sci.*, **2000**, *11*, S41-S50.
[56] Han, H-K.; Amidon, G.L. Targeted prodrug design to optimize drug delivery. *AAPS Pharmsci.*, **2000**, *2*, 48-58.
[57] Steffansen, B.; Nielsen, C.U.; Brodin, B.; Erikson, A.H.; Andersen, R.; Frokjaer, S. Intestinal solute carriers: an overview of trends and strategies for improving oral drug absorption. *Eur. J. Pharm. Sci.*, **2004**, *21*, 3-16.
[58] Steffansen, B.; Nielsen, C.U.; Frokjaer, S. Delivery aspects of small peptides and substrates for peptide transporters. *Eur. J. Pharm. Biopharm.*, **2005**, *60*, 241-245.
[59] Swaan, P.W.; Tukker, J.J. Molecular determinants of recognition for the intestinal peptide carrier. *J. Pharm. Sci.*, **1997**, *86*, 596-602
[60] Russel-Jones, G.J. The potential use of receptor-mediated endocytosis for oral drug delivery. *Adv. Drug Deliv. Rev.*, **2001**, *46*, 59-73.
[61] Lim, C-J.; Shen, W-C. Comparison of monomeric and oligomeric transferrin as potential carrier in oral delivery of protein drugs. *J. Control. Release*, **2005**, *106*, 273-286.
[62] Kim, S.H.; Jeong, J.H.; Joe, C.O.; Park, T.G. Folate receptor mediated intracellular protein delivery using PLL-PEG-FOL conjugate. *J. Control. Release*, **2005**, *103*, 625-634
[63] Zheng, Y.; Song, X.; Darby, M.; Liang, Y.; He, L.; Cai, Z.; Chen, Q.; Bi, Y.; Yang, X.; Xu, J.; Li, Y.; Sun, Y.; Lee, R.J.; Hou, S. Preparation and characterization of folate-poly(ethylene glycol)-grafted-trimethylchitosan for intracellular transport of protein through folate receptor-mediated endocytosis. *J. Biotechnol.*, **2010**, *145*, 47-53.
[64] Friden, P.M. Utilization of an endogenous cellular transport system for the delivery of therapeutics across the blood-brain barrier. *J. Control. Release*, **1996**, *46*, 117-128.
[65] Amet, N.; Wang, W.; Shen, W-C. Human growth hormone-transferrin fusion protein for oral delivery in hypophysectomized rats. *J. Control. Release*, **2010**, *141*, 177-182.
[66] Tewes, F.; Tajber, L.; Corrigan, O.I.; Ehrhardt, C.; Healy, A.M. Development and characterisation of soluble polymeric particles for pulmonary peptide delivery. *Eur. J. Pharm. Sci.*, **2010**, *41*, 337-352.
[67] Merkel, O.M.; Kissel, T.; Beck-Broichsitter, M. Controlled pulmonary drug and gene delivery using polymeric nano-carriers. *J. Control. Release*, **2012**, *161*, 214-224.
[68] Oya Alpara, H.; Somavarapua, S.; Atuahb, K.N.; Bramwella, V.W. Biodegradable mucoadhesive particulates for nasal and pulmonary antigen and DNA delivery. *Adv. Drug Deliv. Rev.*, **2005**, *57*, 411-430.
[69] Bernkop-Schnürch, A.; Dünnhaupt, S. Chitosan-based drug delivery systems. *Eur. J. Pharm. Biopharma.*, **2012**, *81*, 463-469.
[70] Dombu, C.Y.; Betbeder, D. Airway delivery of peptides and proteins using nanoparticles. *Biomaterials*, **2013**, *34*, 516-525.
[71] Al-Qadi, S.; Grenha, A.; Carrión-Recio, D.; Seijo, B.; Remuñán-López, C. Microencapsulated chitosan nanoparticles for pulmonary protein delivery: In vivo evaluation of insulin-loaded formulations. *J. Control. Release*, **2012**, *157*, 383-390.
[72] Beck-Broichsitter, M.; Schweiger, C.; Schmehl, T.; Gessler, T.; Seeger, W.; Kissel, T. Characterization of novel spray-dried polymeric particles for controlled pulmonary drug delivery. *J. Control. Release*, **2012**, *158*, 329-335.
[73] Jani, P.; Manseta, P.; Patel, S. Pharmaceutical approaches related to systemic delivery of protein and peptide drugs: an overview. *Int. J. Pharm. Sci. Rev. Res.*, **2012**, *12*, 42-52.
[74] Yamamoto, A.; Umemori, S.; Muranishi, S. Absorption enhancement of intra-pulmonary administered insulin by various absorption enhancers and protease inhibitors in rats. *J. Pharm. Pharmacol.*, **1994**, *46*, 14-18.
[75] Illum, L. Nasal Drug delivery-recent developments and future aspects. *J. Control. Release*, **2012**, *161*, 254-263.
[76] Na, L.; Mao, S.; Wang, J.; Sun, W. Comparison of different absorption enhancers on the intranasal absorption of isosorbide dinitrate in rats. *Int. J. Pharm.*, **2010**, *397*, 59-66.
[77] Siekmeier, R.; Scheuch, G. Inhaled insulin – does it become reality? *J. Physiol. Pharmacol.*, **2008**, *6*, 81-113.
[78] McCrudden, M.T.C.; Singh, T.R.R.; Migalska, K.; Donnelly, R.F. Strategies for enhanced peptide and protein delivery. *Ther. Deliv.*, **2013**, *5*, 593-614.
[79] Islam, N.; Cleary, M.J. Developing an efficient and reliable dry powder inhaler for pulmonary drug delivery – a review for multidisciplinary researchers. *Med. Eng. Phys.*, **2012**, *34*, 409-427.
[80] Leone-Bay, A.; Grant M. Technosphere technology: A platform for inhaled protein therapeutics. http://www.ondrugdelivery.com (Accessed August 27 **2013**).
[81] Sarala, N.; Bengalorkar, G.; Bhuvana, K. Technosphere: new drug delivery system for inhaled insulin. *Future Prescriber*, **2012**, *13*, 14-16.
[82] Claus, S.; Weiler, C.; Schiewe, J.; Friess W. Optimization of the fine particle fraction of a lyophilized lysozyme formulation for dry powder inhalantion. *Pharm. Res.*, **2013**, *30*, 1698-1713.
[83] Costantino, H.R.; Illum, L.; Brand, G.; Johnson, P.; Quay, S.C. Intranasal delivery: physicochemical and therapeutic aspects. *Int. J. Pharm.*, **2007**, *337*, 1-24.
[84] Illum, L. Nasal drug delivery: new developments and strategies. *Drug Discov. Today*, **2002**, *7*, 1184-1189.
[85] Irwin, W.J.; Dwivedi, A.K.; Holbrook, P.A.; Dey, M.J. The Effect of cyclodextrins on the stability of peptides in nasal enzymic systems. *Pharm. Res.*, **1994**, *11*, 1698-1703.
[86] Morita, T.; Yamahara, H. Encyclopedia of Pharmaceutical Technology, 3rd ed.; Swarbrick, Ed.; Informa Healthcare: London, **2007**; Vol. 4.
[87] Romeo, V.D.; deMeireles, J.C.; Gries, W.J.; Xia, W.J.; Sileno, A.P.; Pimplaskar, H.K.; Behl, C.R. Optimization of systemic nasal drug delivery with pharmaceutical excipients. *Adv. Drug Deliv. Rev.*, **1998**, *29*, 117-133.
[88] Davis, S.S.; Illum, L. Absorption enhancers for nasal drug delivery. *Clin. Pharmacokinet.*, **2003**, *42*, 1107-1128.

[89] Mitra, R.; Pezron, I.; Chu, W.A.; Mitra, A.K. Lipid emulsions as vehicles for enhanced nasal delivery of insulin. *Int. J. Pharm.*, **2000**, *205*, 127-134.
[90] Kumar, M.; Pathak, K.; Misra, A. Formulation and characterization of nanoemulsion-based drug delivery system of risperidone. *Drug Dev. Ind. Pharm.*, **2009**, *35*, 387-395.
[91] Gungor, S.; Okyar, A.; Erturk-Toker, S.; Baktir, G.; Ozsoy, Y. Ondansetron-loaded biodegradable microspheres as a nasal sustained delivery system: *In vitro/in vivo* studies. *Pharm. Dev. Tech.*, **2009**, *15*, 258-265.
[92] Stote, R.M.; Marbury, T.; Shi, L.; Miller, M.; Strange, P. Comparison pharmacokinetics of two concentrations (0.7% and 1.0%) of Nasulin TM, an ultra-rapid-acting intra-nasal insulin formuation. *J. Diabetes Sci. Tech.*, **2010**, *4*, 603-609.
[93] Ahsan, F.; Arnold, J.; Meezan, E.; Pillion, D.J. Enhanced bioavailability of calcitonin formulated with alkylglycosides following nasal and ocular administration in rats. *Pharm. Res.*, **2001**, *18*, 1742-1746.
[94] Pillion, D.J.; Ahsan, F.; Arnold, J.J.; Balusubramanian, B.M.; Piraner, O.; Meezan, E. Synthetic long chain alkyl maltosides and alkyl sucrose esters as enhancers of nasal insulin absorption. *J. Pharm. Sci.*, **2002**, *91*, 1456-1462.
[95] Maggio, E.T. Intravail®: highly effective intranasal delivery of peptide and protein drugs. *Expert Opin. Drug Deliv.*, **2006**, *3*, 529-539.
[96] Arnold, J.J.; Ahsan, F.; Meezan, E.; Pillion, D.J. Correlation of tetradecylmaltoside in-duced increases in nasal peptide drug delivery with morphological changes in nasal epithelial cells. *J. Pharm. Sci.*, **2004**, *93*, 2205-2213.
[97] Eddy, P.; Krause, D.; Merutka, G.; MacDonald, B. Intranasal (IN) Pharmacokinetics and Bioavailability of ZT-031, A Novel Parathyroid Hormone (PTH) Analog.www.aegisthera.com (Accessed 28 September **2013**).
[98] Lewis, A.L.; Jordan, F.M.; Illum, L.Evaluation of a novel absorption promoter for nasal delivery,Abstract, CRS Annual Meeting and Exposition: Copenhagen, Denmark, **2009**; pp. 19-22.
[99] Illum, L.; Jordan, F.; Lewis, A.L. Nasal delivery of peptides and proteins - are we there yet? Abstract, CRS Annual Meeting and Exposition: Portland, Oregon, USA, **2010**; pp. 10-14.
[100] Illum, L.; Jordan, F.; Lewis, A.L. A novel efficient nasal delivery system for human growth hormone. *J. Control. Release*, **2012**, *162*, 194-200.
[101] Brayden, D.J.; Bzik, V.; Lewis, A.; Illum, L. Promotes Permeation of Flux Markers across Rat Colonic Mucosae and Caco-2 Cell Monolayers. *Pharm. Res.*, **2012**, *29*, 2543-2554.
[102] Agnihotri, S.A.; Mallikarjuna, N.N.; Aminabhavi, T.M. Recent advances on chitosan-based micro- and nanoparticles in drug delivery. *J. Control. Release*, **2004**, *100*, 5-28.
[103] Van der Lubben, I.M.; Verhoef, J.C.; Borchard, G.; Junginger, H.E. Chitosan and its derivatives in mucosal drug and vaccine delivery. *Eur. J. Pharm. Sci.*, **2001**, *14*, 201-207.
[104] Wong, T.W. Chitosan and its use in design of insulin delivery system. *Recent Pat. Drug Deliv. Formul.*, **2009**, *3*, 8-25.
[105] Soane, R.J.; Hinchcliffe, M.; Davis, S.S.; Illum, L. Clearance characteristics of chitosan based formulations in the sheep nasal cavity. *Int. J. Pharm.*, **2001**, *217*, 183-191.
[106] Illum, L.; Watts, P.; Fisher, A.N.; Jabbal Gill, I.; Davis S.S. Novel chitosan-based delivery systems for the nasal administration of a LHRH-analogue. *STP Pharm. Sci.*, **2000**, *10*, 89-94
[107] Leitner, V.M.; Guggi, D.; Krauland, A.H.; Bernkop-Schnürch, A. Nasal Delivery of human growth hormone: In vitro and in vivo evaluation of a thiomer/glutathione microparticulate delivery system. *J. Control. Release*, **2004**,100, 87-95.
[108] Gratieri, T.; Alberti, I.; Lapteva, M.; Kalia, Y.N. Next generation intra- and transdermal therapeutic systems: Using non- and minimally-invasive technologies to increase drug delivery into and across the skin. *Eur. J. Pharm. Sci.*, **2013** 50(5), 609-22.
[109] Guy, R.H.; Hadgraft, J. Transdermal Drug Delivery: Developmental Issues And Research Initiatives; Marcel Dekker: New York, **1989**.
[110] Mitragotri, S. Synergistic effect of enhancers for transdermal drug delivery. *Pharm. Res.*, **2000**, *17*, 1354-1357.
[111] Thomas, B.J.; Finnin, B.C. The transdermal revolution. *Drug Discov. Today Res. Focus Rev.*, **2004**, *9*, 697-703.
[112] Joshi, S.C.; Jasuja N.D. Enhancement of transdermal delivery system and antidiabetic approach: An overview. *Int. J. Pharmacy.*, **2012**, *2*, 129-141.
[113] Schuetz, Y.B.; Naik, A.; Guy, R.H.; Kalia, Y.N. Emerging strategies for the transdermal delivery of peptide and protein drugs. *Expert Opin. Drug Deliv.*, **2005**, *2*, 533-548.
[114] Dua, K.; Sharma, V.K.; Sara, U.V.S.; Agrawal, D.K.; Ramana, M.V. Penetration enhancers for TDDS: a tale of the under skin travellers. *Adv. Nat. Appl. Sci.*, **2009**, *3*, 95-101.
[115] Kalluri, H.; Banga, A.K. Transdermal delivery of proteins. *Pharm. Sci. Technol.*, **2011**, *12*, 431-41.
[116] Walters, K.A. Penetration enhancers and their use in transdermal therapeutic systems. In:Transdermal Drug Delivery Developmental Issues And Research Initiatives;Hadgraft; Guy, Eds.; **1989**, pp. 197-246.
[117] Lashmar, U.T.;Hadgraft, J.; Thomas, N. Topical application of penetration enhancers to the skin of nude mice: a histopathological study. *J. Pharm. Pharmacol.*, **1989**, *41*, 118-22.
[118] Prausnitz, M.R.; Mitragotri, S.; Langer, R. Current status and future potential of transdermal drug delivery. *Nat. Rev.*, **2004**, *3*, 115-124.
[119] Nair, V.B.; Panchagnula, R. Effects of iontophoresis and fatty acids on permeation of arginine vasopressin through rat skin. *Pharmacol. Res.*, **2003b**, *47*, 563-569.
[120] Pillai, O.; Panchagnula, R. Transdermal delivery of insulin from poloxamer gel: ex vivo and in vivo skin permeation studies in rat using iontophoresis and chemical enhancers. *J. Control. Release*, **2003**, *89*, 127-140.
[121] Lu, MY.; Lee, D.; Rao, G.S. Percutaneous absorption enhancement of leuprolide. *Pharm. Res.*, **1992**, *9*, 1575-1579.
[122] Sintov, A.C.; Wormser, U. Topical iodine facilitates transdermal delivery of insulin. *J. Control. Release*, **2007**, *118*, 185-188.
[123] Srinivasan, V.; Su, M.H.; Higuchi W.; Behl, C.R. Iontophoresis of polypeptides: effect of ethanol pretreatment of human skin. *J. Pharm. Sci.*, **1990**, *79*, 588-591.
[124] Romanenko, I.; Araviski, R. Comparative levels of amphotericin B in the skin and subcutaneous fatty tissue after cutaneous application of amphotericin ointment by phonophoresis and with preliminary treatment by dimethyl sulfoxides. *Antibiotiki I Khimioterapiia*, **1991**, *36*, 29.
[125] Escobar-Chávez, J.J.; Días-Torres, R.; Rodríguez-Cruz, I.M.; Domínguez-Delgado, C.L.; Morales, R.S.; Angeles-Anguiano, E.;Melgoza-Contreras, L.M. Nanocarriers for transdermal drug delivery. *Res. Report Transdermal Drug Deliv.*, **2012**, *1*, 3-17.
[126] Prausnitz, M.R.; Langer, R. Transdermal drug delivery. *Nat. Biotechnol.*, **2008**, *26*, 1261-1268.
[127] Cui, Z.; Han, S.; Padinjarae, D.; Huang, L. Immunostimulation mechanism of LPD nanoparticles as a vaccine carrier. *Mol. Pharmaceut.*, **2005**, *2*, 22-28.
[128] Dubey, V.; Mishra, D.; Asthana, A.; Jain, N.K. Transdermal delivery of a pineal hormone: melatonin via elastic liposomes. *Biomaterials*, **2006**, *27*, 3491-3496.
[129] Gupta, P.N.; Mishra, V.; Rawat, A.; Dubey, P.; Mahor, S.;Jain, S.; Chatterji, D.P.; Vyas, S.P. Non-invasive vaccine delivery in transfersomes, niosomes and liposomes: a comparative study. *Int. J. Pharm.*, **2005a**, *293*, 73-82.
[130] Gupta, P.N.; Mishra, V.; Singh, P.; Rawat, A.; Dubey, P.;Mahor, S.; Vyas, S.P. Tetanus toxoid-loaded transfersomes for topical immunization. *J. Pharm. Pharmacol.*, **2005b**, *57*, 295-301.
[131] Javin, S.; Jain, P.; Umamaheshwari, R.B.; Jain, N.K. Transfersomes - a novel vesicular carrier for enhanced transdermal delivery: development, characterization, and performance evaluation. *Drug Dev. Ind. Pharm.*, **2003**, *29*, 1013-1026.
[132] Cevc, G. Transdermal drug delivery of insulin with ultradeformable carriers. *Clin. Pharmacokinet.*, **2003**, *42*, 461-474.
[133] Cevc, G.; Sch~itzlein, A.; Gebauer D.; Blume, G. Ultra-high efficiency of drug and peptide transfer through the intact skin by means of novel drug-carriers, Transfersomes. In: Prediction of Percutaneous Penetration; Bain; Hadgkraft; James; Water, Eds.; STS Publishing: Cardiff, **1993**; Vol. 3b, pp. 226-234.
[134] Rathbone, M.J.; Hadgraft, J.; Roberts, M.S. Modified release drug delivery technology, Marcel Dekker Inc: New York, **2004**.
[135] Goswami, S.; Bajpai, J.; Bajpai, A.K. Designing gelatin nanocarriers as a swellable system for controlled release of insulin: an in-vitro kinetic study. *J. Macromol. Sci.*, **2010**, *47*, 119-130.
[136] Huang, Y.; Yu, F.; Park, Y.S.; Wang, J.; Shin, M.C.; Chung, H.S.; Yang, V.C. Co-administration of protein drugs with gold nanopar-

TR146 cell culture model – an in vitro model of the buccal epithelium. *Pharm. Res.*, **2002**, *19*, 169-174.

[183] Rossi, S.; Sandri, G.; Caramella, C.M. Buccal drug delivery: A challenge already won. *Drug Discov. Today Technol.*, **2005**, *2*, 59-65.

[184] Senel, S.; Hincal, A.A. Drug permeation enhancement via buccal route: possibilities and limitations. *J. Control. Release*, **2001**, *72*, 133-144.

[185] Senel, S.; Kremer, M.J.; Kas, S.; Werts, P.W.; Hincal, A.A.; Squier, C.A. Enhancing effect of chitosan on peptide drug delivery across buccal mucosa. *Biomaterials*, **2000**, *21*, 2067-2071.

[186] Bernstein, G. Delivery of insulin to the buccal mucosa utilising the RapidMist™ system. *Expert. Opin. Drug Deliv.*, **2008**, *5*, 1047-1055.

[187] Maher, S.; Breyden, D.J. Overcoming poor permeability: translating permeation enhancers for oral peptide delivery. *Drug Discov. Today Technol.*, **2012**, *9*, e113-e119.

Received: October 1, 2013 Revised: January 15, 2014 Accepted: July 22, 2014

[188] Stern, W.; Mehta, N.; Carl, S. Oral delivery of peptides by Peptelligence™ technology. *Drug Dev. Deliv.*, **2013**, *13*, 36-42.

[189] Park, K.; Kwon, I.C.; Park, K. Oral protein delivery: Current status and future prospect. *React. Funct. Polym.*, **2011**, *71*, 280-287.

[190] Heinemann, L.; Jacques, Y. Oral insulin and buccal insulin: A critical reappraisal. *J. Diabetes Sci. Technol.*, **2009**, *3*, 568-584.

[191] Neumiller, J.J.; Campbell, R.K. Technosphere® Insulin an inhaled prandial insulin product. *Biodrugs*, **2010**, *24*, 165-172.

[192] Haruta, S. A nasal delivery solution to the challenges in biotherapeutic delivery. *OnDrugDeliv.*, **2012**, 14-16.

[193] Herwadkar, A.; Banga, A.K. Peptide and protein transdermal drug delivery. *Drug Discov. Today Technol.*, **2012**, *9*, e147-e154.

[194] Kumria, R.; Goomber, G. Emerging trends in insulin delivery: Buccal route. *J. Diabetol.*, **2011**, *2*, 1-9.

ticles to enable percutaneous delivery. *Biomaterials*, **2010**, *31*, 9086-9091.

[137] Li, G.P.; Liu, Z.G.; Liao, B.; Zhong, N.S. Induction of Th1-type immune response by chitosan nanoparticles containing plasmid DNA encoding house dust mite allergen Der p 2 for oral vaccination in mice. *Cell Mol. Immunol.*, **2009**, *6*, 45-50.

[138] Yoo, H.S.; Lee, J.E.; Chung, H.; Kwon, I.C.; Jeong, S.Y. Self-assembled nanoparticles containing hydrophobically modified glycol chitosan for gene delivery. *J. Control. Release*, **2005**,103, 235-243.

[139] Huang, X.; Du, Y.; Yuan, H.; Hu, F. Preparation and pharmacodynamics of low molecular-weight chitosan nanoparticles containing insulin. *Carbohydr. Polym.*, **2009**, *76*, 368-373.

[140] Ugazio, E.; Cavalli, R.; Gasco, M.R. Incorporation of cyclosporin A in solid lipid nanoparticles (SLN). *Int. J. Pharm.*, **2002**, *241*, 341-344.

[141] Wagner, V.; Dullaart, A.; Bock, A.K.; Zweck, A. The emerging nanomedicine land-scape. *Nat. Biotechnol.*, **2006**, *24*, 1211-1217.

[142] Mbah, C.J.; Uzor, P.F.; Omeje, E.O. Perspectives on Transdermal Drug Delivery. *J. Chem. Pharm. Res.*, **2011**, *3*, 680-700.

[143] Shakeel, F.; Ramadan, W. Transdermal delivery of anticancer drug caffeine from water-in-oil nanoemulsions. *Colloids Surf. B Biointerfaces*, **2010**, *75*, 356-362.

[144] Sonneville-Aubrun, O.; Simonnet, J.T.; L'Alloret, F. Nanoemulsions: a new vehicle for skincare products. *Adv. Colloid. Interface Sci.*, **2004**, 108-109, 145-149.

[145] Díaz-Torres, R. Transdermal nanocarriers. In Current Technologies to Increase the Transdermal Delivery of Drugs; Escobar-Chávez; Merino, Eds.; Bentham Science: Bussum, **2010**, pp. 120-140.

[146] Sun, H.; Liu, K.; Liu, W.; Wang, W.; Guo, C.; Tang, B.; Gu, J.; Zhang, J.; Li, H.; Mao, X.; Zou, Q.; Zeng, H.Development and characterization of a novel nanoemulsion drug-delivery system for potential application in oral delivery of protein drugs. *Int. J. Nanomed.*, **2012**, *7*, 5529-5543.

[147] Chen, Y.; Shen, Y.; Guo, X.; Zhang, C.;Yang, W.; Ma, M.; Liu, S.; Zhang, M.; Wen, L-P. Transdermal protein delivery by a coadministered peptide identified via phage display. *Nat. Biotechnol.*, **2006**, *24*, 455-460.

[148] Zhang, T.; Qu, H.; Li, X.; Zhao, B.; Zhou, J.; Li, Q.; Sun, M. Transmembrane delivery and biological effect of human growth hormone via a phage displayed peptide *in vivo* and *in vitro*. *J. Pharm. Sci.*, **2010**, *99*, 4880-4891.

[149] Ruan, R.; Wang, S.; Wang, C.; Zhang, L.; Zhang, Y.; Zhou, W.; Ding, W.; Jin, P.; Wei, P.; Man, N.; Wen, L. Transdermal delivery of human epidermal growth factor facilitated by a peptide chaperon. *Eur. J. Med. Chem.*, **2013**, *62*, 405-409.

[150] Kim, Y.C.; Ludovice, P.J.; Prausnitz, M.R. Transdermal delivery enhanced by magainin pore-forming peptide. *J. Control. Release*, **2007**, *122*, 375-383.

[151] Caccetta, R.; Blanchfield, J.T.; Harrison, J.; Toth, I.; Benson, H.A.E. Epidermal penetration of a therapeutic peptide by lipid conjugation; stereo-selective peptide availability of a topical distereomeric lipopeptide. *Int. J. Pept. Res. Ther.*, **2006**, *12*, 327-333.

[152] Foldvari, M.; Baca-Estrada, M.E.; He, Z.; Hu, J.; Attah-Poku, S.; King, M. Dermal and transdermal delivery of protein pharmaceuticals: lipid-based delivery systems for interferon alpha. *Biotechnol. Appl. Biochem.*, **1999**, *30*, 129-137.

[153] Rothbard, J.B.; Garlington, S.; Lin, Q.; Kirschberg, T.; Kreider, E.; McGrane, P.L.; Wender, P.A.; Khavari, P.A. Conjugation of arginine oligomers to cyclosporin facilitates topical delivery and inhibition of inflammation. *Nat. Med.*, **2006**, *6*, 1253-1257.

[154] Arora, A.; Prausnitz, M.R.; Mitragotri, S. Micro-scale devices for transdermal drug delivery. *Int. J. Pharm.*, **2008**, *364*, 227-236.

[155] Tokumoto, S.; Higo, N.; Sugibayashi, K. Effect of electroporation and pH on the iontophoretic transdermal delivery of human insulin. *Int. J. Pharm.*, **2006**, *326*, 13-19.

[156] Chang, L.C.; Hofmann, G.A.; Zhang, L.; Deftos, L.J.; Banga, A.K. The effect of electroporation on iontophoretic transdermal delivery of calcium regulating hormones. *J. Control. Release*, **2000a**, *66*, 127-133.

[157] Chang, S.L.; Hofmann, G.A.; Zhang, L.; Deftos, L.J.; Banga, A.K. Transdermal iontophoretic delivery of salmon calcitonin. *Int. J. Pharm.*, **2000b**, *200*, 107-113.

[158] Alexander, A.; Dwivedi, S.; Ajazuddin, Giri, T.K.; Saraf, S.; Saraf, S.; Tripathi, D.K. Approaches for breaking the barriers of drug permeation through transdermal drug delivery. *J. Control. Release*, **2012**, *164*, 26-40.

[159] Brown, M.B.; Traynor, M.J.; Martin, G.P.; Akomeah, F.K. Transdermal Drug Delivery Systems: Skin Perturbation Devices. In: Drug Delivery Systems: Methods in Molecular Biology; Jain, Ed.; Humana Press, USA, **2008**; Vol. 437,pp. 119-139.

[160] Herwadkar, A.; Banga, A.K. Peptide and protein transdermal drug delivery. *Drug Discov. Today Technol.*, **2012**, *9*, 147-154.

[161] Green, P.G. Iontophoretic delivery of peptide drugs. *J. Control. Release*, **1996**, *41*, 33-48.

[162] Henchoz, Y.; Abla, N.; Venthey, J.L.; Carrupt, P.A. A fast screening strategy for characterizing peptide delivery by transdermal iontophoresis. *J. Control. Release*, **2009**, *137*, 123-129.

[163] Kalia, Y.N.; Naika, A.; Garrisone, J.; Guy, R.H. Iontophoretic drug delivery. *Adv. Drug Deliv. Rev.*, **2004**, *56*, 619-658.

[164] Subramony, J.A. Needle free parenteral drug delivery: Leveraging active transdermal technologies for paediatric use. *Int. J. Pharm.*, **2013**, *455*(1-2), 14-8.

[165] Chaturvedula, A.; Joshi, D.P.; Anderson, C.; Morris, R.L.; Sembrowich, W.L.; Banga, A.K. In vivo iontophoretic delivery and pharmacokinetics of salmon calcitonin. *Int. J. Pharm.*, **2005**, *297*, 190-196.

[166] Suzuki, Y.; Iga, K.; Yanai, S.; Matsumoto, Y.; Kawase, M.; Fukuda, T.; Adachi, H.; Higo, N.; Ogawa, Y. Iontophoretic pulsatile transdermal delivery of human parathyroid hormone (1–34). *J. Pharm. Pharmacol.*, **2001**, *53*, 1227-1234.

[167] Suzuki, Y.; Nagase, Y.; Iga, K.; Kawase, M.; Oka, M.; Yanai, S.; Matsumoto, Y.; Nakagawa, S.; Fukuda, T.; Adachi, H.; Higo, N.; Ogawa, Y. Prevention of bone loss in ovariectomized rats by pulsatile transdermal iontophoretic administration of human PTH (1-34). *J. Pharm. Sci.*, **2002**, *91*, 350-361.

[168] Banga, A.K.; Katakam M.; Mitra, R. Transdermal iontophoretic delivery and degradation of vasopressin across human cadaver skin. *Int. J. Pharm.*, **1995**, *116*, 211-216.

[169] Scott, E.R.; Phipps, J.B.; Gyory, J.R.; Padmanabhan, R.V. Electrotransport system for transdermal delivery: a practical implementation of iontophoresis. In: Handbook of Pharmaceutical Controlled Release Technology; Wise, Ed.; Marcel Dekker: New York, **2000**, pp. 617-659.

[170] Heit, M.C.; Monteiro-Riviere, N.A.; Jayes, F.L.; Riviere, J.E. Transdermal iontophoretic delivery of luteinizing hormone releasing hormone (LHRH): effect of repeated administration. *Pharm. Res.*, **2004**, *11*, 1000-1003.

[171] Nanada, A.; Nanda, S.; Khan Ghilzai, N.M. Current developments using emerging transdermal technologies in physical enhancement methods. *Curr. Drug Deliv.*, **2006**, *3*, 233-242.

[172] Subramony, J.A.; Sharma, A.; Phipps, J.B. Microprocessor controlled transdermal drug delivery. *Int. J. Pharm.*, **2006**, *317*, 1-6.

[173] Schoellhammer, C.M.; Polat, B.E.; Mendenhall, J.; Maa, R.; Jones, R.; Hart, D.P.; Langer, R.; Blankschtein, D. Rapid skin permeabilization by the simultaneous application of dual-frequency, high-intensity ultrasound. *J. Control. Release*, **2012**, *163*, 154-160.

[174] Mitragotri, S.; Blankschtein, D.; Langer, R. Ultrasound-mediated transdermal protein delivery. *Science*, **1995a**, *269*, 850-853.

[175] Mitragotri, S.; Edwards, D.A.; Blankschtein, D.; Langer. R. A mechanistic study of ultrasonically-enhanced transdermal drug delivery. *J. Pharm. Sci.*, **1995b**, *84*, 697-706.

[176] Tezel, A.; Mitragotri, S. Interactions of inertial cavitation bubbles with stratum corneum lipid bilayers during low-frequency sonophoresis. *Biophys. J.*, **2003**, *85*, 3502-3512

[177] Doukas, A.G.; Kollias, N. Transdermal drug delivery with a pressure wave. *Adv. Drug Deliv. Rev.*, **2004**, *56*, 559-579.

[178] Murthy, S.N. Magnetophoresis: An approach to enhance transdermal drug diffusion. *Pharmazie*, **1999**, *54*, 377-379.

[179] Scherer, F.; Anton, M.; Schillinger, U.; Bergemann, C.; Krüger, A.K.; Gänsbacher, B.; Plank, C. Magnetofection: enhancing and targeting gene delivery by magnetic force in vitro and in vivo. *Gene Ther.*, **2002**, *9*, 102-109.

[180] Bharkatiya, M.; Nema, R.K. Skin penetration enhancement techniques. *Pharmaceutics*, **2009**, *1*, 110-115.

[181] Lee, S.; McAuliffe, D.J.; Mulholland, S.E.; Doukas, A.G. Photomechanical transdermal delivery of insulin in vivo. *Lasers Surg. Med.*, **2001**, *73*, 282-285.

[182] Portero, A.; Remuñán-López, C.; Nielsen H.M. The potential of chitosan in enhancing peptide and protein absorption across the

TR146 cell culture model – an in vitro model of the buccal epithelium. *Pharm. Res.*, **2002**, *19*, 169-174.

[183] Rossi, S.; Sandri, G.; Caramella, C.M. Buccal drug delivery: A challenge already won. *Drug Discov. Today Technol.*, **2005**, *2*, 59-65.

[184] Senel, S.; Hincal, A.A. Drug permeation enhancement via buccal route: possibilities and limitations. *J. Control. Release*, **2001**, *72*, 133-144.

[185] Senel, S.; Kremer, M.J.; Kas, S.; Werts, P.W.; Hincal, A.A.; Squier, C.A. Enhancing effect of chitosan on peptide drug delivery across buccal mucosa. *Biomaterials*, **2000**, *21*, 2067-2071.

[186] Bernstein, G. Delivery of insulin to the buccal mucosa utilising the RapidMist™ system. *Expert. Opin. Drug Deliv.*, **2008**, *5*, 1047-1055.

[187] Maher, S.; Breyden, D.J. Overcoming poor permeability: translating permeation enhancers for oral peptide delivery. *Drug Discov. Today Technol.*, **2012**, *9*, e113-e119.

Received: October 1, 2013 **Revised: January 15, 2014** **Accepted: July 22, 2014**

[188] Stern, W.; Mehta, N.; Carl, S. Oral delivery of peptides by Peptelligence™ technology. *Drug Dev. Deliv.*, **2013**, *13*, 36-42.

[189] Park, K.; Kwon, I.C.; Park, K. Oral protein delivery: Current status and future prospect. *React. Funct. Polym.*, **2011**, *71*, 280-287.

[190] Heinemann, L.; Jacques, Y. Oral insulin and buccal insulin: A critical reappraisal. *J. Diabetes Sci. Technol.*, **2009**, *3*, 568-584.

[191] Neumiller, J.J.; Campbell, R.K. Technosphere® Insulin an inhaled prandial insulin product. *Biodrugs*, **2010**, *24*, 165-172.

[192] Haruta, S. A nasal delivery solution to the challenges in biotherapeutic delivery. *OnDrugDeliv.*, **2012**, 14-16.

[193] Herwadkar, A.; Banga, A.K. Peptide and protein transdermal drug delivery. *Drug Discov. Today Technol.*, **2012**, *9*, e147-e154.

[194] Kumria, R.; Goomber, G. Emerging trends in insulin delivery: Buccal route. *J. Diabetol.*, **2011**, *2*, 1-9.

ANNEXURE B: DISSOLUTION DATA

ANNEXURE B: DISSOLUTION DATA

Table B1.1: Dissolution data for the optimum bead formulation containing *Aloe ferox* gel

Time (min)	% dissolution	% dissolution	% dissolution	Average% dissolution	Standard deviation
0	0	0	0	0	
15	52.24	82.54	68.10	67.63	15.15
30	78.34	94.43	97.74	90.17	10.38
60	83.14	96.87	101.18	93.73	9.42
90	85.98	95.29	93.47	91.58	4.94
120	81.30	94.88	86.82	87.67	6.83
150	83.16	95.28	97.82	92.09	7.84
180	71.91	88.13	43.81	67.95	22.43

Table B1.2: Dissolution data for the optimum bead formulation containing *Aloe marlothii* gel

Time (min)	% dissolution	% dissolution	% dissolution	Average % dissolution	Standard deviation
0	0.00	0.00	0.00	0.00	0.00
15	53.16	53.15	46.83	51.05	3.65
30	99.48	48.17	95.87	81.18	28.64
60	102.80	96.62	100.04	99.82	3.10
90	102.81	93.93	100.46	99.07	4.60
120	100.94	98.68	100.46	100.03	1.19
150	98.14	98.13	95.53	97.27	1.51
180	100.00	79.95	65.12	81.69	17.51

Table B1.3: Dissolution data for the optimum bead formulation containing *Aloe vera* gel

Time (min)	% dissolution	% dissolution	% dissolution	Average % dissolution	Standard deviation
0	0.00	0.00	0.00	0.00	0.00
15	53.04	53.04	69.47	58.51	7.74
30	99.42	48.22	95.42	81.02	23.25
60	102.80	96.52	99.67	99.66	2.57
90	102.82	93.94	100.10	98.95	3.71
120	100.96	98.67	100.10	99.91	0.94
150	98.16	98.14	95.14	97.14	1.42
180	97.68	79.99	64.52	80.73	13.55

Table B 1.4: Dissolution data for the optimum bead formulation containing Insulin

Time (min)	% dissolution	% dissolution	% dissolution	Average % dissolution	Standard deviation
0	0.00	0.00	0.00	0.00	0.00
15	7.33	6.40	4.48	6.07	1.18
30	12.25	46.90	7.75	22.30	17.49
60	28.83	61.36	40.82	43.67	13.43
90	51.60	84.65	58.58	64.94	14.22
120	54.35	95.27	59.33	69.65	18.23
150	73.44	85.10	75.81	78.12	5.03
180	82.21	98.14	88.60	89.65	6.55

ANNEXURE C: TRANSPORT DATA

ANNEXURE C: TRANSPORT DATA

Table C1.1: Percentage transport for the optimum bead formulation containing *Aloe ferox* gel

Time (min)	% Transport	% Transport	% Transport	Average% Transport	Standard deviation
0	0	0	0	0	0
20	2.72	1.69	1.65	2.02	0.50
40	2.36	2.92	2.80	2.69	0.24
60	2.02	2.53	3.19	2.58	0.48
80	2.65	2.74	3.83	3.07	0.54
100	2.61	3.38	1.94	2.64	0.59
120	3.16	3.71	3.51	3.46	0.23

Table C1.2: Percentage transport for the optimum bead formulation containing *Aloe marlothii* gel

Time (min)	% Transport	% Transport	% Transport	Average% Transport	Standard deviation
0	0	0	0	0	0
20	8.28	3.58	12.74	8.20	3.74
40	7.54	4.16	15.55	9.08	4.78
60	7.31	4.78	15.16	9.08	4.42
80	7.14	6.21	15.07	9.48	3.98
100	7.56	6.52	15.23	9.77	3.88
120	8.03	6.95	14.49	9.82	3.33

Table C1.3: Percentage transport for the optimum bead formulation containing *Aloe vera* gel

Time (min)	% Transport	% Transport	% Transport	Average% Transport	Standard Deviation
0	0	0	0	0	0
20	10.07	12.15	16.46	12.89	2.66
40	12.20	16.09	20.75	16.35	3.49
60	10.52	19.60	23.65	17.92	5.49
80	17.32	22.30	25.67	21.76	3.43
100	19.40	24.01	28.41	23.94	3.68
120	20.78	20.68	27.16	22.87	3.03

Table C1.4: Percentage transport for the optimum bead formulation containing Insulin

Time (min)	% Transport	% Transport	% Transport	Average% Transport	Standard deviation
0	0	0	0	0	0
20	5.24	3.66	3.12	4.01	0.90
40	3.37	4.27	2.43	3.36	0.75
60	14.73	5.02	3.32	7.69	5.02
80	4.59	6.39	3.44	4.81	1.21
100	4.82	6.10	3.77	4.90	0.96
120	4.34	7.28	4.88	5.50	1.28

ANNEXURE D: TEER DATA

ANNEXURE D: TEER DATA

Table D.1: TEER values of Caco-2 cell monolayers treated with *Aloe ferox* bead formulations

Formulations	**-20 min**	**0 min**	**20 min**	**40 min**	**60 min**	**80 min**	**100 min**	**120 min**
Aloe ferox gel 10%	2450 2660 3030	2570 2730 3010	215 315 372	199 236 255	185 231 230	184 215 208	166 188 182	166 205 194
Aloe ferox gel 10%, Ac-di-sol® 3%	730 2280 2720	685 2570 2660	252 473 243	198 440 186	187 506 171	174 362 167	177 339 160	170 325 163
Aloe ferox gel 5%	588 2850 2370	560 2810 2200	289 236 139	300 209 149	221 198 155	195 190 150	180 183 143	171 170 154
Aloe ferox gel 10%, Ac-di-sol® 1.5%	2790 2610 3010	2720 2620 2870	252 287 306	186 279 294	174 207 277	169 190 213	169 162 240	178 173 217
Aloe ferox gel 5%, Ac-di-sol® 3%	3080 2750 2650	3060 2790 2690	285 338 313	219 252 273	184 201 197	184 209 187	170 201 191	178 167 183
Aloe ferox gel 5%, Ac-di-sol® 1.5%	2640 2700 2860	2610 2670 2830	272 268 290	206 224 259	180 176 218	181 167 210	185 160 191	171 158 176
Aloe ferox gel 5%, Ac-di-sol® 1.5%	1067 2550 2620	1090 2500 2740	229 249 269	209 219 212	164 170 169	140 170 154	163 175 167	162 172 151
Aloe ferox gel 5%, Ac-di-sol® 1.5%	2660 *2830* 595	2650 *2810* 603	263 *266* 251	211 *200* 229	173 *166* 160	177 *165* 170	171 *161* 166	165 *151* 144

Table D.2: TEER values, normalised for surface area of Transwell® 24 well plates, of Caco-2 cell monolayers treated with *Aloe ferox* bead formulations

Formulations	**-20 min**	**0 min**	**20 min**	**40 min**	**60 min**	**80 min**	**100 min**	**120 min**
Aloe ferox gel 10%	808.50 877.80 999.90	848.10 900.90 993.30	70.95 103.95 122.76	65.67 77.88 84.15	61.05 76.23 75.90	60.72 70.95 68.64	54.78 62.04 60.06	54.78 67.65 64.02
Aloe ferox gel 10%, Ac-di-sol® 3%	240.90 752.40 897.60	226.05 848.10 877.80	83.16 156.09 80.19	65.34 145.20 61.38	61.71 166.98 56.43	57.42 119.46 55.11	58.41 111.87 52.80	56.10 107.25 53.79
Aloe ferox gel 5%	194.04 940.50 782.10	184.80 927.30 726.00	95.37 77.88 45.87	99.00 68.97 49.17	72.93 65.34 51.15	64.35 62.70 49.50	59.40 60.39 47.19	56.43 56.10 50.82
Aloe ferox gel 10%, Ac-di-sol® 1.5%	920.70 861.30 993.30	897.60 864.60 947.10	83.16 94.71 100.98	61.38 92.07 97.02	57.42 68.31 91.41	55.77 62.70 70.29	55.77 53.46 79.20	58.74 57.09 71.61
Aloe ferox gel 5%, Ac-di-sol® 3%	1016.40 907.50 874.50	1009.80 920.70 887.70	94.05 111.54 103.29	72.27 83.16 90.09	60.72 66.33 65.01	60.72 68.97 61.71	56.10 66.33 63.03	58.74 55.11 60.39
Aloe ferox gel 5%, Ac-di-sol® 1.5%	871.20 891.00 943.80	861.30 881.10 933.90	89.76 88.44 95.70	67.98 73.92 85.47	59.40 58.08 71.94	59.73 55.11 69.30	61.05 52.80 63.03	56.43 52.14 58.08
Aloe ferox gel 5%, Ac-di-sol® 1.5%	352.11 841.50 864.60	359.70 825.00 904.20	75.57 82.17 88.77	68.97 72.27 69.96	54.12 56.10 55.77	46.20 56.10 50.82	53.79 57.75 55.11	53.46 56.76 49.83
Aloe ferox gel 5%, Ac-di-sol® 1.5%	877.80 933.90 196.35	874.50 927.30 198.99	86.79 87.78 82.83	69.63 66.00 75.57	57.09 54.78 52.80	58.41 54.45 56.10	56.43 53.13 54.78	54.45 49.83 47.52

Table D.3: Percentage TEER values of Caco-2 cell monolayers treated with *Aloe ferox* bead formulations

Formulations	-20 min	0 min	20 min	40 min	60 min	80 min	100 min	120 min
Aloe ferox gel 10%	95.33 97.44 100.66	100.00 100.00 100.00	8.37 11.54 12.36	7.74 8.64 8.47	7.20 8.46 7.64	7.16 7.88 6.91	6.46 6.89 6.05	6.46 7.51 6.45
Aloe ferox gel 10%, Ac-di-sol® 3%	106.57 88.72 102.26	100.00 100.00 100.00	36.79 18.40 9.14	28.91 17.12 6.99	27.30 19.69 6.43	25.40 14.09 6.28	25.84 13.19 6.02	24.82 12.65 6.13
Aloe ferox gel 5%	105.00 101.42 107.73	100.00 100.00 100.00	51.61 8.40 6.32	53.57 7.44 6.77	39.46 7.05 7.05	34.82 6.76 6.82	32.14 6.51 6.50	30.54 6.05 7.00
Aloe ferox gel 10%, Ac-di-sol® 1.5%	102.57 99.62 104.88	100.00 100.00 100.00	9.26 10.95 10.66	6.84 10.65 10.24	6.40 7.90 9.65	6.21 7.25 7.42	6.21 6.18 8.36	6.54 6.60 7.56
Aloe ferox gel 5%, Ac-di-sol® 3%	100.65 98.57 98.51	100.00 100.00 100.00	9.31 12.11 11.64	7.16 9.03 10.15	6.01 7.20 7.32	6.01 7.49 6.95	5.56 7.20 7.10	5.82 5.99 6.80
Aloe ferox gel 5%, Ac-di-sol® 1.5%	101.15 101.12 101.06	100.00 100.00 100.00	10.42 10.04 10.25	7.89 8.39 9.15	6.90 6.59 7.70	6.93 6.25 7.42	7.09 5.99 6.75	6.55 5.92 6.22
Aloe ferox gel 5%, Ac-di-sol® 1.5%	97.89 102.00 95.62	100.00 100.00 100.00	21.01 9.96 9.82	19.17 8.76 7.74	15.05 6.80 6.17	12.84 6.80 5.62	14.95 7.00 6.09	14.86 6.88 5.51
Aloe ferox gel 5%, Ac-di-sol® 1.5%	100.38 100.71 98.67	100.00 100.00 100.00	9.92 9.47 41.63	7.96 7.12 37.98	6.53 5.91 26.53	6.68 5.87 28.19	6.45 5.73 27.53	6.23 5.37 23.88

Table D.4: Average percentage TEER values of Caco-2 cell monolayers treated with *Aloe ferox* bead formulations

Formulations	**-20 min**	**0 min**	**20 min**	**40 min**	**60 min**	**80 min**	**100 min**	**120 min**
Aloe ferox gel 10%	97.81	100.00	10.75	8.29	7.77	7.32	6.46	6.80
Aloe ferox gel 10%, Ac-di-sol® 3%	99.18	100.00	21.44	17.67	17.81	15.26	15.02	14.53
Aloe ferox gel 5%	104.72	100.00	22.11	22.59	17.85	16.13	15.05	14.53
Aloe ferox gel 10%, Ac-di-sol® 1.5%	102.36	100.00	10.29	9.24	7.98	6.96	6.92	6.90
Aloe ferox gel 5%, Ac-di-sol® 3%	99.24	100.00	11.02	8.78	6.85	6.82	6.62	6.20
Aloe ferox gel 5%, Ac-di-sol® 1.5%	101.11	100.00	10.24	8.48	7.06	6.87	6.61	6.23
Aloe ferox gel 5%, Ac-di-sol® 1.5%	98.50	100.00	13.60	11.89	9.34	8.42	9.35	9.08
Aloe ferox gel 5%, Ac-di-sol® 1.5%	99.92	100.00	20.34	17.69	12.99	13.58	13.24	11.83

Table D.5: Standard deviation of average percentage TEER values of Caco-2 cell treated with *Aloe ferox* bead formulations

Formulations	**-20 min**	**0 min**	**20 min**	**40 min**	**60 min**	**80 min**	**100 min**	**120 min**
Aloe ferox gel 10%	1.90	0.00	1.49	0.34	0.45	0.35	0.30	0.43
Aloe ferox gel 10%, Ac-di-sol® 3%	7.61	0.00	11.49	8.95	8.62	7.85	8.20	7.75
Aloe ferox gel 5%	2.58	0.00	20.88	21.91	15.28	13.21	12.09	11.33
Aloe ferox gel 10%, Ac-di-sol® 1.5%	2.15	0.00	0.74	1.71	1.33	0.53	1.02	0.47
Aloe ferox gel 5%, Ac-di-sol® 3%	1.00	0.00	1.22	1.23	0.59	0.61	0.75	0.43
Aloe ferox gel 5%, Ac-di-sol® 1.5%	0.04	0.00	0.16	0.52	0.47	0.48	0.46	0.26
Aloe ferox gel 5%, Ac-di-sol® 1.5%	2.64	0.00	5.24	5.17	4.04	3.16	3.98	4.12
Aloe ferox gel 5%, Ac-di-sol® 1.5%	0.89	0.00	15.05	14.35	9.58	10.34	10.11	8.53

Table D.6: TEER values of Caco-2 cell monolayers treated with *Aloe marlothii* bead formulations

Formulations	**-20 min**	**0 min**	**20 min**	**40 min**	**60 min**	**80 min**	**100 min**	**120 min**
Aloe marlothii gel 10%	2340 2430 1930	2480 2570 2080	206 252 216	162 160 134	146 198 198	150 155 133	163 182 191	175 196 186
Aloe marlothii gel 10%, Ac-di-sol® 3%	2750 2980 2230	2720 2980 2110	237 291 306	175 212 205	174 191 192	173 186 177	140 151 154	140 146 145
Aloe marlothii gel 5%	2180 2190 2340	2350 2330 2470	407 452 400	256 262 274	295 259 310	251 283 327	318 339 559	325 327 347
Aloe marlothii gel 10%, Ac-di-sol® 1.5%	2860 3030 3120	2800 2960 2900	188 258 213	166 203 178	170 145 175	155 173 151	138 154 147	145 150 139
Aloe marlothii gel 5%, Ac-di-sol® 3%	1946 1646 1356	782 2160 1650	266 194 220	200 172 179	182 160 174	151 133 144	141 131 137	126 128 131
Aloe marlothii gel 5%, Ac-di-sol® 1.5%	1834 1472 1736	2120 740 2330	189 186 227	158 170 162	155 144 146	134 123 134	128 113 129	127 110 129
Aloe marlothii gel 5%, Ac-di-sol® 1.5%	2870 490 2680	2980 506 2740	239 276 240	211 235 236	205 195 233	196 188 206	192 175 192	168 180 186
Aloe marlothii gel 5%, Ac-di-sol® 1.5%	2620 2930 2870	2660 3030 3020	176 224 258	162 186 245	163 187 209	146 179 186	152 176 173	160 181 174

Table D.7: TEER values, normalised for surface area of Transwell® 24 well plates, of Caco-2 cell monolayers treated with *Aloe marlothii* bead formulations

Formulations	-20 min	0 min	20 min	40 min	60 min	80 min	100 min	120 min
Aloe marlothii gel 10%	772.20 801.90 636.90	818.40 848.10 686.40	67.98 83.16 71.28	53.46 52.80 44.22	48.18 65.34 65.34	49.50 51.15 43.89	53.79 60.06 63.03	57.75 64.68 61.38
Aloe marlothii gel 10%, Ac-di-sol® 3%	907.50 983.40 735.90	897.60 983.40 696.30	78.21 96.03 100.98	57.75 69.96 67.65	57.42 63.03 63.36	57.09 61.38 58.41	46.20 49.83 50.82	46.20 48.18 47.85
Aloe marlothii gel 5%	719.40 722.70 772.20	775.50 768.90 815.10	134.31 149.16 132.00	84.48 86.46 90.42	97.35 85.47 102.30	82.83 93.39 107.91	104.94 111.87 184.47	107.25 107.91 114.51
Aloe marlothii gel 10%, Ac-di-sol® 1.5%	943.80 999.90 1029.60	924.00 976.80 957.00	62.04 85.14 70.29	54.78 66.99 58.74	56.10 47.85 57.75	51.15 57.09 49.83	45.54 50.82 48.51	47.85 49.50 45.87
Aloe marlothii gel 5%, Ac-di-sol® 3%	642.18 543.18 447.48	258.06 712.80 544.50	87.78 64.02 72.60	66.00 56.76 59.07	60.06 52.80 57.42	49.83 43.89 47.52	46.53 43.23 45.21	41.58 42.24 43.23
Aloe marlothii gel 5%, Ac-di-sol® 1.5%	605.22 485.76 572.88	699.60 244.20 768.90	62.37 61.38 74.91	52.14 56.10 53.46	51.15 47.52 48.18	44.22 40.59 44.22	42.24 37.29 42.57	41.91 36.30 42.57
Aloe marlothii gel 5%, Ac-di-sol® 1.5%	947.10 161.70 884.40	983.40 166.98 904.20	78.87 91.08 79.20	69.63 77.55 77.88	67.65 64.35 76.89	64.68 62.04 67.98	63.36 57.75 63.36	55.44 59.40 61.38
Aloe marlothii gel 5%, Ac-di-sol® 1.5%	864.60 966.90 947.10	877.80 999.90 996.60	58.08 73.92 85.14	53.46 61.38 80.85	53.79 61.71 68.97	48.18 59.07 61.38	50.16 58.08 57.09	52.80 59.73 57.42

Table D.8: Percentage TEER values of Caco-2 cell monolayers treated with *Aloe marlothii* bead formulations

Formulations	**-20 min**	**0 min**	**20 min**	**40 min**	**60 min**	**80 min**	**100 min**	**120 min**
Aloe marlothii gel 10%	94.35 94.55 92.79	100.00 100.00 100.00	8.31 9.81 10.38	6.53 6.23 6.44	5.89 7.70 9.52	6.05 6.03 6.39	6.57 7.08 9.18	7.06 7.63 8.94
Aloe marlothii gel 10%, Ac-di-sol® 3%	101.10 100.00 105.69	100.00 100.00 100.00	8.71 9.77 14.50	6.43 7.11 9.72	6.40 6.41 9.10	6.36 6.24 8.39	5.15 5.07 7.30	5.15 4.90 6.87
Aloe marlothii gel 5%	92.77 93.99 94.74	100.00 100.00 100.00	17.32 19.40 16.19	10.89 11.24 11.09	12.55 11.12 12.55	10.68 12.15 13.24	13.53 14.55 22.63	13.83 14.03 14.05
Aloe marlothii gel 10%, Ac-di-sol® 1.5%	102.14 102.36 107.59	100.00 100.00 100.00	6.71 8.72 7.34	5.93 6.86 6.14	6.07 4.90 6.03	5.54 5.84 5.21	4.93 5.20 5.07	5.18 5.07 4.79
Aloe marlothii gel 5%, Ac-di-sol®3%	248.85 76.20 82.18	100.00 100.00 100.00	34.02 8.98 13.33	25.58 7.96 10.85	23.27 7.41 10.55	19.31 6.16 8.73	18.03 6.06 8.30	16.11 5.93 7.94
Aloe marlothii gel 5%, Ac-di-sol®1.5%	86.51 198.92 74.51	100.00 100.00 100.00	8.92 25.14 9.74	7.45 22.97 6.95	7.31 19.46 6.27	6.32 16.62 5.75	6.04 15.27 5.54	5.99 14.86 5.54
Aloe marlothii gel 5%, Ac-di-sol®1.5%	96.31 96.84 97.81	100.00 100.00 100.00	8.02 54.55 8.76	7.08 46.44 8.61	6.88 38.54 8.50	6.58 37.15 7.52	6.44 34.58 7.01	5.64 35.57 6.79
Aloe marlothii gel 5%, Ac-di-sol® 1.5%	98.50 96.70 95.03	100.00 100.00 100.00	6.62 7.39 8.54	6.09 6.14 8.11	6.13 6.17 6.92	5.49 5.91 6.16	5.71 5.81 5.73	6.02 5.97 5.76

Table D.9: Average percentage TEER values of Caco-2 cell monolayers treated with *Aloe marlothii* bead formulations.

Formulations	**-20 min**	**0 min**	**20 min**	**40 min**	**60 min**	**80 min**	**100 min**	**120 min**
Aloe marlothii gel 10%	93.90	100.00	9.50	6.40	7.70	6.16	7.61	7.88
Aloe marlothii gel 10%, Ac-di-sol® 3%	102.26	100.00	10.99	7.75	7.30	7.00	5.84	5.64
Aloe marlothii gel 5%	93.83	100.00	17.64	11.08	12.07	12.02	16.90	13.97
Aloe marlothii gel 10%, Ac-di-sol® 1.5%	104.03	100.00	7.59	6.31	5.67	5.53	5.07	5.01
Aloe marlothii gel 5%, Ac-di-sol® 3%	135.74	100.00	18.78	14.80	13.74	11.40	10.80	9.99
Aloe marlothii gel 5%, Ac-di-sol® 1.5%	119.98	100.00	14.60	12.46	11.01	9.56	8.95	8.80
Aloe marlothii gel 5%, Ac-di-sol® 1.5%	96.99	100.00	23.77	20.71	17.97	17.08	16.01	16.00
Aloe marlothii gel 5%, Ac-di-sol® 1.5%	96.74	100.00	7.52	6.78	6.41	5.85	5.75	5.92

Table D.10: Standard deviation of average percentage TEER values of Caco-2 cell treated with *Aloe marlothii* bead formulations

Formulations	**-20 min**	**0 min**	**20 min**	**40 min**	**60 min**	**80 min**	**100 min**	**120 min**
Aloe marlothii gel 10%	0.68	0.00	0.76	0.11	1.28	0.14	0.98	0.68
Aloe marlothii gel 10%, Ac-di-sol® 3%	2.46	0.00	2.52	1.41	1.27	0.99	1.03	0.88
Aloe marlothii gel 5%	0.81	0.00	1.33	0.14	0.68	1.05	4.07	0.10
Aloe marlothii gel 10%, Ac-di-sol® 1.5%	2.52	0.00	0.84	0.40	0.54	0.26	0.11	0.16
Aloe marlothii gel 5%, Ac-di-sol® 3%	80.01	0.00	10.92	7.71	6.86	5.69	5.19	4.40
Aloe marlothii gel 5%, Ac-di-sol® 1.5%	56.03	0.00	7.46	7.44	5.99	5.00	4.48	4.29
Aloe marlothii gel 5%, Ac-di-sol® 1.5%	0.62	0.00	21.76	18.21	14.56	14.20	13.14	13.85
Aloe marlothii gel 5%, Ac-di-sol® 1.5%	1.41	0.00	0.79	0.94	0.36	0.28	0.04	0.11

Table D.11: TEER measurements of Caco-2 cell monolayers with *Aloe vera* bead formulations.

Formulations	**-20 min**	**0 min**	**20 min**	**40 min**	**60 min**	**80 min**	**100 min**	**120 min**
Aloe vera gel 10%	3090 2950 3030	2840 2730 2740	861 868 454	455 599 367	338 542 363	276 451 347	284 497 360	272 503 385
Aloe vera gel 10%, Ac-di-sol® 3 %	2820 2940 2830	2710 2840 2690	393 335 352	356 208 258	298 194 218	181 213 327	169 161 172	166 162 151
Aloe vera gel 5%	3120 2960 2420	2940 2810 2350	778 690 609	380 365 532	359 278 428	245 310 316	281 346 348	324 403 378
Aloe vera gel 10%, Ac-di-sol® 1.5%	2650 476 2230	2660 489 2310	490 282 299	294 273 226	325 232 194	256 217 188	244 201 167	195 174 165
Aloe vera gel 10%, Ac-di-sol® 1.5%	2300 2520 2550	2440 2630 2570	232 248 271	195 223 213	208 216 190	200 213 184	185 153 166	177 162 151
Aloe vera gel 5%, Ac-di-sol® 1.5%	3310 2550 632	3100 2290 656	253 333 368	197 258 283	185 206 261	183 190 260	175 188 236	165 177 215
Aloe vera gel 5%, Ac-di-sol® 1.5%	3040 367 563	3000 381 413	238 258 201	236 250 192	237 221 181	220 196 176	177 192 161	176 181 155
Aloe vera gel 5%, Ac-di-sol® 1.5%	3080 2510 2880	3050 2530 3000	374 272 292	317 219 227	311 211 201	303 180 193	300 181 176	266 167 165

Table D.12: TEER values, normalised for surface area of Transwell® 24 well plates, of Caco-2 cell monolayers treated with *Aloe vera* bead formulations

Formulations	**-20 min**	**0 min**	**20 min**	**40 min**	**60 min**	**80 min**	**100 min**	**120 min**
Aloe vera gel 10%	1019.7 973.5 999.9	937.2 900.9 904.2	284.13 286.44 149.82	150.15 197.67 121.11	111.54 178.86 119.79	91.08 148.83 114.51	93.72 164.01 118.8	89.76 165.99 127.05
Aloe vera gel 10%, Ac-di-sol® 3%	930.6 970.2 933.9	894.3 937.2 887.7	129.69 110.55 116.16	117.48 68.64 85.14	98.34 64.02 71.94	59.73 70.29 107.91	55.77 53.13 56.76	54.78 53.46 49.83
Aloe vera gel 5%	1029.6 976.8 798.6	970.2 927.3 775.5	256.74 227.7 200.97	125.4 120.45 175.56	118.47 91.74 141.24	80.85 102.3 104.28	92.73 114.18 114.84	106.92 132.99 124.74
Aloe vera gel 10%, Ac-di-sol® 1.5%	874.5 157.08 735.9	877.8 161.37 762.3	161.7 93.06 98.67	97.02 90.09 74.58	107.25 76.56 64.02	84.48 71.61 62.04	80.52 66.33 55.11	64.35 57.42 54.45
Aloe vera gel 10%, Ac-di-sol® 1.5%	759 831.6 841.5	805.2 867.9 848.1	76.56 81.84 89.43	64.35 73.59 70.29	68.64 71.28 62.7	66 70.29 60.72	61.05 50.49 54.78	58.41 53.46 49.83
Aloe vera gel 5%, Ac-di-sol® 1.5%	1092.3 841.5 208.56	1023 755.7 216.48	83.49 109.89 121.44	65.01 85.14 93.39	61.05 67.98 86.13	60.39 62.7 85.8	57.75 62.04 77.88	54.45 58.41 70.95
Aloe vera gel 5%, Ac-di-sol® 1.5%	1003.2 121.11 185.79	990 125.73 136.29	78.54 85.14 66.33	77.88 82.5 63.36	78.21 72.93 59.73	72.6 64.68 58.08	58.41 63.36 53.13	58.08 59.73 51.15
Aloe vera gel 5%, Ac-di-sol® 1.5%	1016.4 828.3 950.4	1006.5 834.9 990	123.42 89.76 96.36	104.61 72.27 74.91	102.63 69.63 66.33	99.99 59.4 63.69	99 59.73 58.08	87.78 55.11 54.45

Table D.13: Percentage TEER values of Caco-2 cell monolayers treated with *Aloe marlothii* bead formulations

Formulations	**-20 min**	**0 min**	**20 min**	**40 min**	**60 min**	**80 min**	**100 min**	**120 min**
Aloe vera gel 10%	108.80	100.00	30.32	16.02	11.90	9.72	10.00	9.58
	108.06	100.00	31.79	21.94	19.85	16.52	18.21	18.42
	110.58	100.00	16.57	13.39	13.25	12.66	13.14	14.05
Aloe vera gel 10%, Ac-di-sol® 3%	104.06	100.00	14.50	13.14	11.00	6.68	6.24	6.13
	103.52	100.00	11.80	7.32	6.83	7.50	5.67	5.70
	105.20	100.00	13.09	9.59	8.10	12.16	6.39	5.61
Aloe vera gel 5%	106.12	100.00	26.46	12.93	12.21	8.33	9.56	11.02
	105.34	100.00	24.56	12.99	9.89	11.03	12.31	14.34
	102.98	100.00	25.91	22.64	18.21	13.45	14.81	16.09
Aloe vera gel 10%, Ac-di-sol® 1.5%	99.62	100.00	18.42	11.05	12.22	9.62	9.17	7.33
	97.34	100.00	57.67	55.83	47.44	44.38	41.10	35.58
	96.54	100.00	12.94	9.78	8.40	8.14	7.23	7.14
Aloe vera gel 10%, Ac-di-sol® 1.5%	94.26	100.00	9.51	7.99	8.52	8.20	7.58	7.25
	95.82	100.00	9.43	8.48	8.21	8.10	5.82	6.16
	99.22	100.00	10.54	8.29	7.39	7.16	6.46	5.88
Aloe vera gel 5%, Ac-di-sol® 1.5%	106.77	100.00	8.16	6.35	5.97	5.90	5.65	5.32
	111.35	100.00	14.54	11.27	9.00	8.30	8.21	7.73
	96.34	100.00	56.10	43.14	39.79	39.63	35.98	32.77
Aloe vera gel 5%, Ac-di-sol® 1.5%	101.33	100.00	7.93	7.87	7.90	7.33	5.90	5.87
	96.33	100.00	67.72	65.62	58.01	51.44	50.39	47.51
	136.32	100.00	48.67	46.49	43.83	42.62	38.98	37.53
Aloe vera gel 5%, Ac-di-sol® 1.5%	100.98	100.00	12.26	10.39	10.20	9.93	9.84	8.72
	99.21	100.00	10.75	8.66	8.34	7.11	7.15	6.60
	96.00	100.00	9.73	7.57	6.70	6.43	5.87	5.50

Table D.14: Average percentage TEER values of Caco-2 cell monolayers treated with *Aloe vera* bead formulations

Formulations	**-20 min**	**0 min**	**20 min**	**40 min**	**60 min**	**80 min**	**100 min**	**120 min**
Aloe vera gel 10%	109.15	100.00	26.23	17.12	15.00	12.97	13.78	14.02
Aloe vera gel 10%, Ac-di-sol® 3%	104.26	100.00	13.13	10.02	8.64	8.78	6.10	5.81
Aloe vera gel 5%	104.81	100.00	25.64	16.18	13.44	10.94	12.23	13.82
Aloe vera gel 10%, Ac-di-sol® 1.5%	97.83	100.00	29.68	25.55	22.69	20.71	19.17	16.69
Aloe vera gel 5%, Ac-di-sol® 3%	96.43	100.00	9.83	8.25	8.04	7.82	6.62	6.43
Aloe vera gel 5%, Ac-di-sol® 1.5%	109.06	100.00	11.35	8.81	7.48	7.10	6.93	6.53
Aloe vera gel 5%, Ac-di-sol® 1.5%	101.33	100.00	7.93	7.87	7.90	7.33	5.90	5.87
Aloe vera gel 5%, Ac-di-sol® 1.5%	98.73	100.00	10.92	8.87	8.41	7.83	7.62	6.94

Table D.15: Standard deviation of average percentage TEER values of Caco-2 cell treated with *Aloe vera* bead formulations

Formulations	**-20 min**	**0 min**	**20 min**	**40 min**	**60 min**	**80 min**	**100 min**	**120 min**
Aloe vera gel 10%	1.06	0.00	6.86	3.57	3.47	2.79	3.38	3.61
Aloe vera gel 10%, Ac-di-sol® 3%	0.70	0.00	1.11	2.39	1.74	2.41	0.31	0.22
Aloe vera gel 5%	1.34	0.00	0.80	4.56	3.51	2.09	2.14	2.10
Aloe vera gel 10%, Ac-di-sol® 1.5%	1.31	0.00	19.92	21.41	17.58	16.74	15.53	13.36
Aloe vera gel 5%, Ac-di-sol® 3%	2.07	0.00	0.51	0.20	0.48	0.47	0.73	0.59
Aloe vera gel 5%, Ac-di-sol® 1.5%	6.28	0.00	21.25	16.31	15.28	15.37	13.73	12.41
Aloe vera gel 5%, Ac-di-sol® 1.5%	17.79	0.00	24.94	24.02	21.09	19.06	18.87	17.75
Aloe vera gel 5%, Ac-di-sol® 1.5%	2.06	0.00	1.04	1.16	1.43	1.52	1.65	1.34

Table D.16: TEER measurements of Caco-2 cell monolayers with MCC 100%, Ac-di-sol® 1.5%, Ac-di-sol® 3%, SLS 0.02% bead formulations and DMEM

Formulations	**-20 min**	**0 min**	**20 min**	**40 min**	**60 min**	**80 min**	**100 min**	**120 min**
MCC 100%	2680 3140 2920	2460 2770 2600	2380 1220 2330	2450 1010 766	1270 405 653	1210 1070 583	434 1080 543	403 739 540
Ac-di-sol® 1.5%	3180 2630 2750	2990 2500 2630	599 633 1670	645 352 440	280 248 464	295 238 276	364 263 251	364 311 247
Ac-di-sol® 3%	2830 2750 2520	2670 2620 2390	712 505 598	378 412 368	270 302 315	245 318 282	252 311 259	227 343 230
SLS 0.2%	2710 3050 3310	2780 3260 3200	182 178 213	161 181 190	165 180 165	159 167 172	154 167 160	149 164 156
DMEM	2800 3510 3450	2480 3070 3020	2200 2800 2800	2280 2820 2650	2420 3010 2810	2410 3100 2880	2360 2980 2750	2350 2980 2850

Table D.17: TEER values, normalised for surface area of Transwell® 24 well plates, of Caco-2 cell monolayers treated with MCC 100%, Ac-di-sol® 1.5%, Ac-di-sol® 3%, SLS 0.2% bead formulations and DMEM

Formulations	**-20 min**	**0 min**	**20 min**	**40 min**	**60 min**	**80 min**	**100 min**	**120 min**
MCC 100%	884.4 1036.2 963.6	811.8 914.1 858	785.4 402.6 768.9	808.5 333.3 252.78	419.1 133.65 215.49	399.3 353.1 192.39	143.22 356.4 179.19	132.99 243.87 178.2
Ac-di-sol® 1.5%	1049.4 867.9 907.5	986.7 825 867.9	197.67 208.89 551.1	212.85 116.16 145.2	92.4 81.84 153.12	97.35 78.54 91.08	120.12 86.79 82.83	120.12 102.63 81.51
Ac-di-sol® 3%	907.5 178.2 831.6	864.6 174.9 788.7	166.65 168.3 197.34	135.96 146.19 121.44	99.66 115.17 103.95	104.94 95.04 93.06	102.63 86.46 85.47	113.19 77.88 75.9
SLS 0.2%	894.3 1006.5 1092.3	917.4 1075.8 1056	60.06 58.74 70.29	53.13 59.73 62.7	54.45 59.4 54.45	52.47 55.11 56.76	50.82 55.11 52.8	49.17 54.12 51.48
DMEM	924 1158.3 1138.5	818.4 1013.1 996.6	726 924 924	752.4 930.6 874.5	798.6 993.3 927.3	795.3 1023 950.4	778.8 983.4 907.5	775.5 983.4 940.5

Table D.18: Percentage TEER values of Caco-2 cell monolayers treated with MCC 100%, Ac-di-sol® 1.5%, Ac-di-sol® 3%, SLS 0.2% bead formulations and DMEM

Formulations	-20 min	0 min	20 min	40 min	60 min	80 min	100 min	120 min
MCC 100%	108.94	100.00	96.75	99.59	51.63	49.19	17.64	16.38
	113.36	100.00	44.04	36.46	14.62	38.63	38.99	26.68
	112.31	100.00	89.62	29.46	25.12	22.42	20.88	20.77
Ac-di-sol® 1.5%	106.35	100.00	20.03	21.57	9.36	9.87	12.17	12.17
	105.20	100.00	25.32	14.08	9.92	9.52	10.52	12.44
	104.56	100.00	63.50	16.73	17.64	10.49	9.54	9.39
Ac-di-sol® 3%	104.96	100.00	19.27	15.73	11.53	12.14	11.87	13.09
	101.89	100.00	96.23	83.58	65.85	54.34	49.43	44.53
	105.44	100.00	25.02	15.40	13.18	11.80	10.84	9.62
SLS 0.2%	97.48	100.00	6.55	5.79	5.94	5.72	5.54	5.36
	93.56	100.00	5.46	5.55	5.52	5.12	5.12	5.03
	103.44	100.00	6.66	5.94	5.16	5.38	5.00	4.88
DMEM	112.90	100.00	88.71	91.94	97.58	97.18	95.16	94.76
	114.33	100.00	91.21	91.86	98.05	100.98	97.07	97.07
	114.24	100.00	92.72	87.75	93.05	95.36	91.06	94.37

Table D.19: Average percentage TEER values of Caco-2 cell monolayers treated with MCC 100%, Ac-di-sol® 1.5%, Ac-di-sol® 3%, SLS 0.2% bead formulations and DMEM

Formulations	**-20 min**	**0 min**	**20 min**	**40 min**	**60 min**	**80 min**	**100 min**	**120 min**
MCC 100%	111.54	100.00	76.80	55.17	30.45	36.75	25.84	21.28
Ac-di-sol® 1.5%	105.37	100.00	36.28	17.46	12.31	9.96	10.75	11.34
Ac-di-sol® 3%	104.10	100.00	46.84	38.24	30.19	26.09	24.05	22.41
SLS 0.2%	98.16	100.00	6.22	5.76	5.54	5.41	5.22	5.09
DMEM	113.82	100.00	90.88	90.51	96.22	97.84	94.43	95.40

Table D.20: Standard deviation of average TEER percentage of Caco-2 cell monolayers with MCC 100%, Ac-di-sol® 1.5%, Ac-di-sol® 3%, SLS 0.2% bead formulations and DMEM.

Formulations	**-20 min**	**0 min**	**20 min**	**40 min**	**60 min**	**80 min**	**100 min**	**120 min**
MCC 100%	1.88	0.00	23.35	31.54	15.57	11.01	9.39	4.22
Ac-di-sol® 1.5%	0.74	0.00	19.36	3.10	3.78	0.40	1.09	1.38
Ac-di-sol® 3%	1.57	0.00	35.00	32.07	25.23	19.97	17.96	15.70
SLS 0.2%	4.1	0.0	0.5	0.2	0.3	0.2	0.2	0.2
DMEM	0.65	0.00	1.65	1.96	2.26	2.34	2.51	1.19

ANNEXURE E: LANGUAGE EDITING CERTIFICATE

Gill Smithies

Proofreading & Language Editing Services

59, Lewis Drive, Amanzimtoti, 4126, Kwazulu Natal

Cell: 071 352 5410 E-mail: moramist@vodamail.co.za

Work Certificate

To	Elmarie Kleynhans
Address	Dept of Pharmaceuticals, North West University, Potchefstroom
Date	17/11/2014
Subject	Masters: Chapters 1 to 5 and Abstract, by Elmarie Kleynhans.
Ref	GS/EK /01

I, Gill Smithies, certify that I have proofed and language edited:

Masters: Chapters 1 to 5 and Abstract, by Elmarie Kleynhans,

to the standard as required by NWU, Potchefstroom Campus.

Gill Smithies

17/11/2014